UNIVERSIDADE D
COIMBRA

Carolina Marques dos Santos

Can the extracellular vesicles released by Müller glial cells provide neuroprotection to retinal ganglion cells?

Dissertação no âmbito do Mestrado em Investigação Biomédica, com especialização em Ciências da Visão, orientada pela Professora Doutora Ana Raquel Sarabando Santiago e coorientada pelo Investigador Doutor António Francisco Rosa Gomes Ambrósio e apresentada à Faculdade de Medicina da Universidade de Coimbra.

Outubro de 2021

Faculdade de Medicina da Universidade de Coimbra

CAN THE EXTRACELLULAR VESICLES RELEASED BY MÜLLER GLIAL CELLS PROVIDE NEUROPROTECTION TO RETINAL GANGLION CELLS?

Carolina Marques dos Santos

Dissertação no âmbito do Mestrado em Investigação Biomédica, com especialização em Ciências da Visão, orientada pela Professora Doutora Ana Raquel Sarabando Santiago e coorientada pelo Investigador Doutor António Francisco Rosa Gomes Ambrósio e apresentada à Faculdade de Medicina da Universidade de Coimbra.

Outubro 2021

1 2 9 0

UNIVERSIDADE D
COIMBRA

Dissertação para obtenção do grau de Mestre em Investigação Biomédica apresentada à Faculdade de Medicina da Universidade de Coimbra, Portugal. O trabalho experimental descrito nesta dissertação foi realizado no Instituto de Investigação Clínica e Biomédica de Coimbra, no grupo "Retinal Dysfunction & Neuroinflammation Group", sob a orientação científica da Doutora Ana Raquel Sarabando Santiago e do Doutor António Francisco Rosa Gomes Ambrósio. Este trabalho foi financiado pela Fundação para a Ciência e a Tecnologia (FCT), Portugal (UID/NEU/04539/2019, UIDB/04539/2020 e UIDP/04539/2020), COMPETE-FEDER (FCOMP-01-0124-FEDER-028417; e POCI-01-0145-FEDER-007440), Programa Operacional Regional do Centro - Centro 2020 (CENTRO-01-0145-FEDER-000008: BRAINHEALTH 2020).

Dissertation for the attribution of the Master degree in Biomedical Research submitted to the Faculty of Medicine of the University of Coimbra, Portugal. The experimental work described in this dissertation was performed at Coimbra Institute for Clinical and Biomedical Research (iCBR), in Retinal Dysfunction & Neuroinflammation Group, under the supervision of Doctor Ana Raquel Sarabando Santiago and Doctor António Francisco Rosa Gomes Ambrósio. This work was funded by Fundação para a Ciência e a Tecnologia (FCT), Portugal (UID/NEU/04539/2019, UIDB/04539/2020 and UIDP/04539/2020), COMPETE-FEDER (FCOMP-01-0124-FEDER-028417; and POCI-01-0145-FEDER-007440), Centro 2020 Regional Operational Programme (CENTRO-01-0145-FEDER-000008: BRAINHEALTH 2020).

Agradecimentos

A quem permitiu que tudo acontecesse, agradeço começando pela minha orientadora Doutora Ana Raquel Santiago que sempre esteve presente. Acompanhou-me e ensinou-me desde o início da minha atividade científica. Dando-me a conhecer o mundo da ciência ainda eu não tinha concluído a licenciatura em Bioquímica, e que até hoje nunca me abandonou.

Ao Doutor Francisco Ambrósio, líder do grupo Retinal Dysfunction and Neuroinflammation Lab, agradeço a oportunidade que me deu de fazer parte deste grupo desde 2017 proporcionando-me as condições necessárias para o desenvolvimento do meu trabalho.

À minha mini chefe Raquel Boia que me permitiu "colocar as mãos na massa" desde o primeiro minuto. Confiou no meu trabalho, motivou-me para crescer e ajudou a desenvolver as minhas capacidades, acompanhando-me sempre de perto, até hoje. Obrigada por todo o apoio e preocupação e quanto a esta tese, obrigada pelos longos dias de ERG e OCT, por não desistires quando nos deparamos com tantas adversidades no modelo animal e também por fazeres com que esta tese ganhasse forma.

À Inês Aires quero também agradecer muito pelo quanto me ensinou e acompanhou ao longo destes anos. Sem esquecer a Magda neste último ano que, além de me passar o legado das células MIO-M1, também esteve presente com uma palavra amiga e pronta a ajudar, obrigada.

Ao restante grupo FA Lab quero também deixar o meu sincero obrigado: à Rita, à Fi, à Elisa, à Neves, à Sara N., à Hélène e ao Henrique. Todos sempre dispostos a ajudar, a tirar dúvidas de última hora e a dar uma palavra amiga de apoio e incentivo diário. Ao "Cool Gab Lab", constituído pela Joana M. e pela Sara O., que tantas conversas, risos e crises existenciais acompanharam de perto neste ano repleto de altos e baixos, obrigada por tudo.

Agradeço ao Doutor Henrique Girão, coordenador do Mestrado em Investigação Biomédica, por todo o apoio e disponibilidade demonstrados ao longo destes dois anos. Não posso deixar de agradecer ao seu grupo de investigação: os companheiros do grupo "do lado" - os GUICs. Ao Steve, à Teresa e à Mónica que acompanharam o meu trabalho de uma forma mais direta, ajudando-me a obter resultados e estando disponíveis para transfetar células, prestar apoio técnico nos microscópios e no medonho NTA, e a encontrar EVs bonitas no TEM, respetivamente. À Carla Marques, à Neuza, ao Jorge, à Dani e à Tânia, obrigada pelas conversas, boa disposição e ajuda no dia-a-dia do laboratório.

Por fim quero agradecer à Xandra, a minha espanhola favorita. Começámos em inglês, mas logo percebemos que o "Portunhol" seria o melhor e hoje entendemo-nos quase na perfeição. Agradeço-lhe o que me ensinou no laboratório e o tanto que contribuiu para esta tese, sempre com muita paciência. Obrigada pelo companheirismo, amizade e apoio constante.

Aos meus Martins: Xana, Drika, João Luís, Dri, Guidinha, Ana, Victor, Parracheira, Governo, Daniela e Bubas. Obrigada por não se esquecerem de mim. O que Bioquímica uniu ninguém separa!

Agradeço à minha Xana, a amiga das chamadas telefónicas infinitas, dos desabafos, dos bailados, das boleias de perder a conta, das mini panquecas, dos ataques de riso e dos olhares tão facilmente compreendidos. Que esta amizade seja até ao fim dos tempos.

À Drika e ao João Luís, os meus amigos do peito. Donos de um coração gigante, sempre prontos para dar a mão e para ajudar. Obrigada pelas conversas e enorme amizade.

À Jéssica e ao Leitão, os amigos da terrinha. Não importa quanto tempo passa, a amizade não desvanece. Obrigada pelos bons momentos de descontração.

Ao Joel, o meu companheiro dos dias sim e dos dias não, que tem uma paciência infinita para a minha teimosia e que continua presente mesmo nos meus piores dias. Obrigada por me acompanhares e acreditares em mim, sempre.

E seria impossível esquecer-me de agradecer ao meu Zequinha e à querida Mª João. Obrigada ao Zequinha, que se preocupa comigo como se de um irmão mais velho se tratasse. Obrigada pelo carinho imensurável, por aquele abraço apertado sempre que nos vemos e por me dizeres de forma incansável que eu consigo tudo. E já agora… obrigada pelo computador!

Esta tese é de quem nunca me largou a mão desde que me propus a iniciar este percurso. É dos meus pais, da minha Nana e do meu Babá. A eles devo tudo o que sou hoje, no que me tornei. Nunca vos conseguirei retribuir nem agradecer o suficiente. Obrigada por todos os sacrifícios que os quatro fizeram ao longo destes 24 anos, por estarem aqui no bom e no menos bom, por acreditarem sempre que eu sou capaz de tudo, e principalmente por nunca me largarem a mão quando mais preciso. É por vocês que eu estou aqui. Esta tese é vossa.

List of contents

List of figures

List of tables

Abbreviations

α -SMA - α-smooth muscle actin
AQP4 - aquaporin-4
AREG - amphiregulin
ARF6 - ADP-ribosylation factor 6
ARRDC1 - arrestin domain-containing protein 1
ARVO - Association for Research in Vision and Ophthalmology

BDNF - brain derived neurotrophic factor
BCA - bicinchoninic acid
bFGF - basic fibroblast growth factor
BRB - blood retinal barrier
Brn3a - transcription factor of the Brn3 family

Ca^{2+} - calcium
CM - conditioned medium
CM MIO-M1 - conditioned medium from MIO-M1 cells
CM Müller - conditioned medium from primary Müller cells
CNS - central nervous system
CNTF - ciliary neurotrophic factor
CRALBP - cellular retinaldehyde–binding protein
Cryo-TEM - cryo transmission electron microscopy

DAPI - 4',6-diamidino-2-phenylindole
DIV - day *in vitro*
DNA - deoxyribonucleic acid

EAA1 - glutamate-aspartate transporter
ECF - enhanced chemifluorescence
ECL - enhanced chemiluminescence
EGF-R - retinaldehyde-binding protein
EHP - elevated hydrostatic pressure
ERG - electroretinography
ESCRT - endosomal sorting complex required for transport
EVs - extracellular vesicles
EXOs - exosomes
Exo-free FBS - FBS depleted of vesicles

FBS - fetal bovine serum

GCL - ganglion cell layer
GDNF - glial cell line-derived neurotrophic factor
GFAP - glial fibrillary acidic protein
GLAST - glutamate-aspartate transporter
GPMNB - glycoprotein nonmetastatic melanoma protein B
GS - glutamine synthetase

HATMSC1 - human immortalized mesenchymal stem cells

Iba1 - ionized calcium-binding adapter molecule 1
ILM - inner limiting membrane
ILVs - intraluminal vesicles
INL - inner nuclear layer
IPL - inner plexiform laye
IOP - intraocular pressure
I-R - ischemia reperfusion
IS - inner segment

K^+ - potassium

LGN - lateral geniculate nucleus

mESEVs - mouse embryonic stem cells EVs
MHC-II - major histocompatibility complex II
MIO-M1 - human Müller cell line
miRNA - micro RNA
mRNA - messenger RNA
MSCs - mesenchymal stem cells
MVBs - multivesicular bodies
MVs - microvesicles
MVs MIO-M1 - microvesicles isolated from MIO-M1 cells
MVs Müller - microvesicles isolated from primary Müller cells

NFL - nerve fiber layer
nSTR - negative scotopic threshold response

NTA - nanoparticle tracking analysis

OCT - optical coherence tomography
ONL - outer nuclear layer
OPL - outer plexiform layer
OS - outer segment
OS/IS - outer and inner segments

p75^{NTR} - pan-neurotrophin receptor
PBS - phosphate-buffered saline
PDGF - platelet derived growth factor
PEDF - pigment epithelium derived factor
PFA - paraformaldehyde
pSTR - positive scotopic threshold response
PVDF - poly(vinylidene difluoride)

RBPMS - RNA binding protein
RGCs - retinal ganglion cells
RIPA - radioimmunoprecipitation assay
RNA - ribonucleic acid
RPE - retinal pigment epithelium

SEM - standard error of the mean
SDS-PAGE - sodium dodecyl sulphate-poly(acrylamide) gel electrophoresis
SPP1 - osteoponin
STR - scotopic threshold response

TBS-T - tris-buffered saline with Tween-20
TEM - transmission electron microscopy
TrkB - tropomyosin related kinase receptor
TRPV1 - transient receptor potential vanilloid 1
TUNEL - terminal deoxynucleotidyl transferase (TdT)-mediated dUTP nick end labelling

Resumo

As vesículas extracelulares têm um papel importante na comunicação intercelular e incluem exosomas, microvesículas e corpos apoptóticos. As vesículas extracelulares são produzidas por vários tipos de células.

O glaucoma é uma neuropatia ótica caracterizada pela perda de células ganglionares da retina (CGRs) e degeneração do nervo ótico (axónios das CGRs) que origina a perda de campos visuais, culminando eventualmente em cegueira. A terapêutica atual foca-se na redução da pressão intraocular, o principal fator de risco, mas a doença progride em muitos doentes. Desta forma, novas abordagens terapêuticas direcionadas à proteção das CGRs são necessárias para abrandar a progressão da doença.

As células de Müller são as principais células da glia da retina e desempenham funções importantes na regulação da homeostasia. Estas células participam na proteção das CGRs, seja por contacto físico seja através de fatores libertados. Um estudo anterior demonstrou que as células de Müller libertam vesículas extracelulares. Devido às propriedades neuroprotetoras das células de Müller, este trabalho pretendeu elucidar o papel do meio condicionado e das microvesículas libertadas pelas células de Müller na sobrevivência das CGRs num contexto de pressão elevada.

Culturas primárias de células de Müller e de CGRs, e células MIO-M1 (linha celular) foram expostas a pressão hidrostática elevada (PHE), para mimetizar o aumento da pressão intraocular. Culturas primárias de células de Müller e culturas de células MIO-M1 foram incubadas à pressão atmosférica (controlo) para recolha do meio condicionado. O efeito dos meios condicionados na sobrevivência celular foi observado incubando culturas primárias de CGRs e co-culturas de CGRs e células de Müller expostas a PHE com os meios condicionados. As microvesículas derivadas de células MIO-M1 (MVs MIO-M1) e de células de Müller primárias foram isoladas por ultracentrifugação de baixa velocidade e caracterizadas em tamanho, morfologia e concentração por análise de rastreio de nanopartículas, microscopia eletrónica de transmissão e pela presença de proteínas por Western Blot. As culturas de células MIO-M1 e as culturas primárias de CGRs foram incubadas sob PHE com microvesículas, e a sobrevivência celular foi analisada. Adicionalmente, os efeitos das MVs MIO-M1 na retina foram avaliados 7 dias após a injeção no vítreo de ratos Wistar Han.

Em condições de PHE observou-se uma diminuição da sobrevivência das CGRs após 24h, em culturas primárias de CGRs. A sobrevivência das células de Müller em culturas primárias diminuiu significativamente quando as células foram expostas a PHE durante 48h e 72h. Contudo, quando em co-cultura, as CGRs apresentaram uma diminuição significativa da sua sobrevivência apenas às 72h sob PHE e a sobrevivência das células de Müller foi afetada apenas às 72h de exposição. A sobrevivência de células MIO-M1 não foi afetada pela exposição a PHE nos tempos avaliados. A exposição das células de Müller primárias ou das células MIO-M1 a PHE não alterou a proliferação celular.

Ambos os meios condicionados promoveram a sobrevivência de CGRs quando expostas a PHE. Em co-culturas este efeito não foi tão pronunciado. MVs MIO-M1 aumentaram a sobrevivência das CGRs e não afetaram a proliferação de células MIO-M1 sob PHE. Os resultados revelaram que ambos os meios condicionados e que MVs MIO-M1 promoveram a sobrevivência de CGRs *in vitro*.

A injeção intravítrea de solução tampão fosfato-salino (PBS, do inglês Phosphate-buffered saline) 1h antes da indução da isquémia e reperfusão da retina causou alterações estruturais na mesma, um efeito aparentemente causado pela ação sinergística do insulto e do PBS. Os olhos contralaterais não apresentaram alterações na estrutura da retina. Portanto, avaliou-se o efeito da injeção intravítrea das MVs MIO-M1 em retinas contralaterais. A injeção intravítrea de MVs MIO-M1 ou PBS não evidenciaram alterações na função ou estrutura da retina. Contudo, por tomografia de coerência ótica foram observados pontos brilhantes no vítreo, sugerindo a presença de células. Sete dias após a injeção, avaliou-se o efeito das MVs MIO-M1 na morte celular da retina, sobrevivência das CGRs, número de células da microglia e de microglia reativa e imunorreatividade de GFAP. A injeção intravítrea de MVs MIO-M1 aumentou a reatividade de células de Müller e da microglia, sem alterações significativas na morte celular e sobrevivência das CGR.

Resumindo, os resultados demonstram que o meio condicionado de diferentes tipos de células de Müller protegem CGRs expostas a PHE. As células de Müller libertam microvesículas que promovem a sobrevivência de CGRs. Além disso, MVs MIO-M1 não causam alterações na estrutura e função da retina, mas aumentam a reatividade das células da glia. Mais experiências são necessárias para compreender melhor as propriedades das MVs derivadas de células de Müller num contexto de neuroproteção em glaucoma.

Palavras-chave: Células de Müller; vesículas extracelulares; glaucoma; proteção; retina

Abstract

Extracellular vesicles (EVs) play an important role in intercellular communication and include exosomes (EXOs), microvesicles (MVs) and apoptotic bodies. EVs are produced by many cell types.

Glaucoma is an optic neuropathy, characterized by retinal ganglion cell (RGC) loss and degeneration of optic nerve (RGC axons) that leads to loss of visual fields, culminating in blindness. The current therapeutics are focused in lowering intraocular pressure (IOP), the main risk factor, but the disease progresses in a large number of patients. Therefore, novel and effective therapeutic strategies targeting RGC neuroprotection are needed to halt disease progression.

Müller cells, the main glial cell type of the retina, have important functions in the regulation of homeostasis of the retina. Müller cells have the ability to protect RGCs either by physical contact or by secreted factors. A previous study demonstrated that Müller cells release EVs. Due to the neuroprotective properties of Müller cells, this study aimed to elucidate the role of the conditioned medium (CM) and MVs from Müller cells in the survival of RGCs in the context of elevated pressure.

Primary cultures of Müller cells and RGCs and cultures of MIO-M1 cells were exposed to elevated hydrostatic pressure (EHP) to mimic the elevated IOP. Primary Müller cell cultures and MIO-M1 cell line were incubated in atmospheric (control) pressure and CM were collected. The effect of CM in cell survival was assessed incubating primary RGC cultures and co-cultures of RGCs and Müller cells exposed to EHP with CM. MVs from MIO-M1 cells (MVs MIO-M1) and from primary Müller cells (MVs Müller) were isolated by low-speed ultracentrifugation and characterized in size, morphology and concentration by nanoparticle tracking analysis, transmission electron microscopy, and by the presence of proteins by Western Blot. MIO-M1 cultures and primary cultures of RGCs were incubated under EHP with MVs and cell survival was analysed. Additionally, the effect of MVs MIO-M1 in the retina were determined 7 days after intravitreal injection of MVs MIO-M1.

Under EHP conditions, RGCs had a significant decrease in cell survival at 24h in pure RGC cultures. The exposure of Müller cells to EHP for 48h and 72h significantly decreased cell survival. However, when in co-culture, RGCs only presented a significant decrease in cell survival at 72h under EHP and Müller cells showed a tendency to a decrease in cell survival at 72h under EHP. MIO-M1 cells survival was not affected by exposure to EHP for 24h or 48h. The exposure of primary Müller cells or MIO-M1 cells to EHP did not cause alterations in cell proliferation. CM from both Müller cell cultures promoted the survival of RGC cultures exposed to EHP. In co-cultures, this effect was not so pronounced. MVs MIO-M1 increased RGC survival and did not affect MIO-M1 cells proliferation in EHP conditions. The results showed that both CMs and MVs MIO-M1 could increase RGCs survival *in vitro*.

Additionally, we observed that the intravitreal injection of phosphate-buffered saline (PBS) 1h before I-R caused alterations in the retinal structure, an effect apparently caused by the synergistic action of I-R injury and PBS. The contralateral eyes of the I-R eyes did not present changes in retinal structure. Therefore, we evaluated the effect of intravitreal injection of MVs MIO-M1 only in contralateral retinas. The intravitreal injection of MVs MIO-M1 or PBS did not seem to change retinal function or structure. However, by optical coherence tomography bright spots were observed in the vitreous, suggesting the presence of cells infiltrates. Seven days after injection, retinal cell death, RGCs survival, number of microglia, reactive microglia and glial fibrillary acidic protein immunoreactivity were assessed. Intravitreal injection of MVs MIO-M1 increased the reactivity of Müller cells and microglia, but did not change cell death or the number of RGCs.

In summary, the results demonstrate that CM from different types of Müller cells can protect RGCs exposed to EHP. Also, Müller cells release MVs that promote the survival of RGCs. Moreover, MVs from MIO-M1 cells do not cause alterations in the structure and function of the retina, but cause glial reactivity. Further experiments are needed to understand the protective properties of MVs from Müller cells in the context of glaucoma neuroprotection.

Keywords: Müller cells; extracellular vesicles; glaucoma; protection; retina

Chapter 1

Introduction

1.1. Extracellular vesicles

Extracellular vesicles (EVs) can be considered masters of intercellular communication, being able to deliver their cargo into nearby cells as well as over long distances via the blood stream. EVs are the collective term for secreted vesicles and include exosomes (EXOs), microvesicles (MVs), and apoptotic bodies (Doyle and Wang 2019). The presence of mitochondrial material was interpreted as EXOs bearing mitochondrial proteins, lipids, and mitochondrial DNA (Haraszti et al. 2016; Guescini et al. 2010), but a new subtype of EVs of mitochondrial origin was proposed, referred as mitovesicles that sediment with EXOs (D'Acunzo et al. 2021).

EVs have distinct biogenesis pathways and are often distinguished by their size, surface proteins and internal cargo (Thery et al. 2018). EVs are formed by a lipidic bilayer membrane and are known to carry proteins, mRNA, miRNA, and lipids that can be delivered to recipient cells changing, for example, the translation of new proteins and modulation of gene expression (Ratajczak et al. 2006; Skog et al. 2008; Mead and Tomarev 2020). It was demonstrated that over 100 proteins are more abundant in EVs than in the cell, suggesting that the loading of EVs is active and specific (Eirin et al. 2016). To differentiate the EVs subtypes, various techniques need to be combined, as microscopy and biochemical techniques. However, since the nomenclature of EVs is difficult and not always consensual among the scientific community, in this study, EVs isolated from high-speed ultracentrifugation will be referred as EXOs, and EVs isolated from low-speed ultracentrifugation will be referred as MVs. The characterization and identification of the several types of EVs is of crucial importance, but it is still not possible to propose specific and universal markers of each type of EVs. Therefore, the characterization of the EVs solely by the presence of molecular markers is not recommended (Thery et al. 2018). Yet, there are surface proteins more associated with one type of EVs than others even knowing that in recent years most of the proteins could be found in all the subtypes (Thery et al. 2018; Kowal et al. 2016).

EXOs are vesicles with a size range of 30 to 150 nm, shed continually by almost every cell type to the extracellular space and are present in body fluids (as tears, aqueous humour, vitreous humour, blood, urine, breast milk, saliva, etc) (Colombo, Raposo, and Thery 2014). The term “exosome” was first used in the early 1980s to describe small vesicles of endosomal origin released during the maturation of sheep reticulocytes (Pan et al. 1985; Johnstone et al. 1987). The biosynthesis of EXOs is an endosomal-dependent process. Early endosomes mature into late endosomes and during this process they accumulate intraluminal vesicles (ILVs) in their lumen. These are called multivesicular bodies (MVBs) and its main outcome is to fuse with lysosomes ensuring the degradation of their content or they can be released into the extracellular space, via fusion with the plasma membrane (Figure 1) (Colombo, Raposo, and Thery 2014). The best-described mechanism for formation of MVBs and ILVs is driven by the endosomal sorting complex required for transport (ESCRT), which comprises four complexes that facilitate receptor

sorting into the lumen of MVBs. ESCRT-0 and ESCRT-I subunits cluster ubiquitylated transmembrane cargoes on microdomains of MVBs. Then, ESCRT-II and ESCRT-III perform budding and fission of this microdomain, finally forming the ILVs (Colombo, Raposo, and Thery 2014; van Niel, D'Angelo, and Raposo 2018). Nevertheless, EXOs can also be formed in an ESCRT-independent manner, where MVBs, featuring ILVs loaded with CD63, are still formed upon depletion of components of the four ESCRT complexes (Stuffers et al. 2009). Some proteins were already found to regulate ESCRT-independent endosomal sorting, like CD63, tetraspanins CD81, CD82 and CD9 (Gauthier et al. 2017; Buschow et al. 2009; van Niel, D'Angelo, and Raposo 2018). Both ESCRT-dependent and ESCRT-independent mechanisms are involved differently in the biogenesis of EXOs depending on the cargo which recruits them and the type of cell (Stuffers et al. 2009; van Niel, D'Angelo, and Raposo 2018).

In 1967, Peter Wolf described MVs as "platelet dust", subcellular material originating

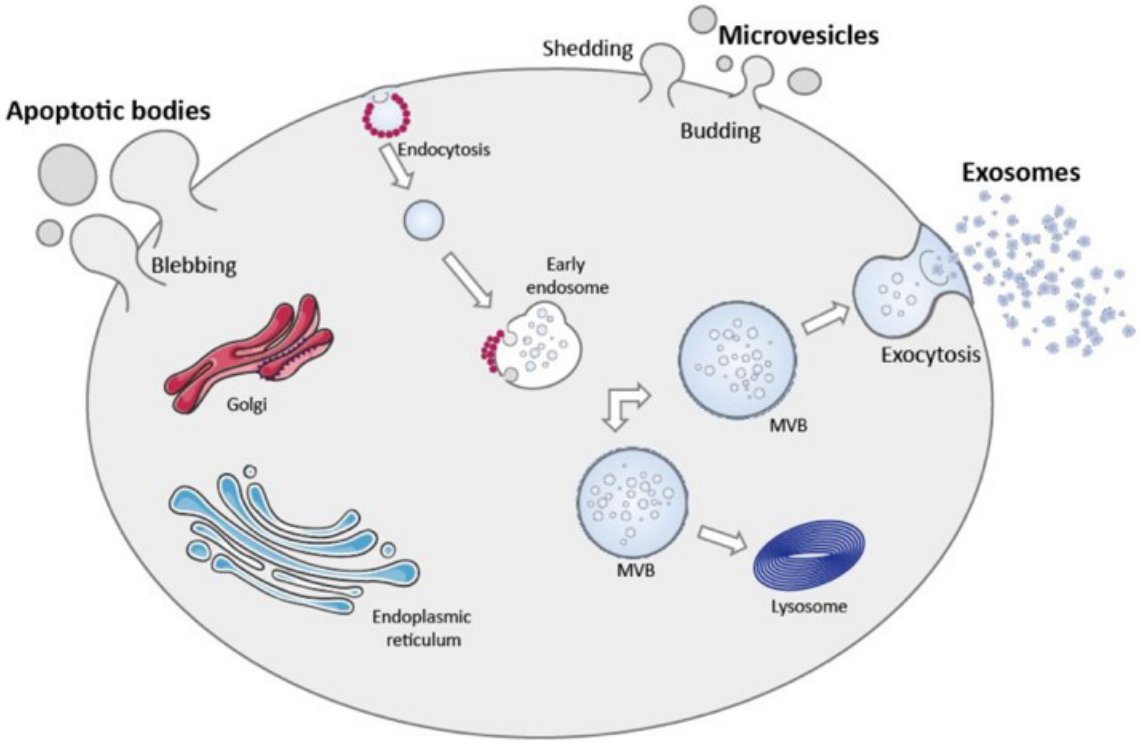

Figure 1: Schematic representation of the mechanisms involved in EVs biogenesis and release. The biosynthesis of EXOs is an endosomal-dependent process, where early endosomes mature and forming MVBs. Its main outcome is to fuse with lysosomes ensuring the degradation of their content or they can be released to the extracellular space, via fusion with the plasma membrane. MVs are produced through the shedding of the plasma membrane. Apoptotic bodies are released by dying cells and are formed after the disassembly of an apoptotic cell into subcellular fragments. Image from Aires et al. 2021.

from platelets in normal plasma and serum (Wolf 1967). MVs range in size from 50 to 1000 nm. They are produced through the shedding of the plasma membrane, and released into the extracellular space (Figure 1) (van Niel, D'Angelo, and Raposo 2018). For the release of MVs from the cell, the plasma membrane needs to be not only rearranged at lipid and protein composition but also requires alterations in the Ca^{2+} levels. The formation of MVs is dependent on the translocation of the phospholipid phosphatidylserine from the inner leaflet of the plasma membrane to the outer leaflet, which is carried out by aminophospholipid translocases (flippases and floppases). Then ADP-ribosylation factor 6 (ARF6) initiates the contraction of cytoskeletal components, with rearrangement of actin protein, causing a curvature in the membrane (Muralidharan-Chari et al. 2009). The ESCRT-1 complex also plays a role in MVs formation. The arrestin domain-containing protein 1 (ARRDC1) recruits the ESCRT-I accessory protein TSG101 to the cell membrane mediating the formation of MVs (Nabhan et al. 2012; J.M. Gudbergsson 2017). For the reason that MVs are formed by an outward budding of the cell's plasma membrane, it is easily understood that MVs are enriched in cytosolic and plasma membrane associated proteins, especially proteins known to cluster at the plasma membrane surface, such as tetraspanins. MVs also carry other proteins as cytoskeletal proteins, heat shock proteins and integrins (Doyle and Wang 2019).

Apoptotic bodies are released by dying cells, ranging from 500 to 2000 nm and are formed after the disassembly of an apoptotic cell into subcellular fragments (Figure 1) being phagocytosed by other cells (macrophages). The process of formation of apoptotic bodies is considered a hallmark of apoptosis (Ihara et al. 1998; Ravichandran 2010). Apoptotic bodies are quite variable in size and content, as they can contain a wide variety of cellular components as cytosol portions, degraded proteins, DNA fragments, etc, and even intact organelles (Poon et al. 2014).

1.1.1. Isolation and characterization methods of extracellular vesicles

There are several methods for EVs isolation: differential ultracentrifugation, density gradient ultracentrifugation, ultrafiltration, precipitation with polymers and size-exclusive chromatography. Other option is combining isolation methods to increase purification, as for example, ultrafiltration can be an additional step in ultracentrifugation protocols (Campoy et al. 2016; Aires et al. 2020). A mixed population of vesicles is obtained in most studies of EVs for all used isolation methods since every method has limitations (Konoshenko et al. 2018). These constraints lead to a necessity of characterize EVs population samples.

The characterization of EVs is achieved by the combination of EVs size distribution, morphology and protein composition. For the size distribution analysis, nanoparticle tracking analysis (NTA) can be used. It combines the properties of both laser light scattering microscopy and Brownian motion in order to obtain size distributions of

particles in a liquid suspension, however it does not discriminate different subpopulations of EVs or contaminants in the sample (Vestad et al. 2017). Transmission electron microscopy (TEM) and cryo transmission electron microscopy (cryo-TEM) have been the most used electron microscopy techniques used for morphological analysis of EVs. The sample preparation for these two techniques is different, with TEM needing the EVs to be fixed and contrasted which might affect their size and change their morphology (Cizmar and Yuana 2017). Finally, EVs surface membrane composition and EVs cargo requires great attention and can be investigated by proteomic analysis, RNA/DNA sequencing, flow cytometry, mass spectrometry and Western Blot (Ji et al. 2014; Pitt, Kroemer, and Zitvogel 2016; Thery et al. 2018). Western Blot is the most common technique used to confirm EVs presence in samples by showing the presence or absence of certain proteins known to be expressed in determined EVs subtypes. Nevertheless, as already explained before in this chapter, many proteins are not exclusive of a certain type of EVs what makes this kind of characterization difficult and in the need of support with other techniques to confirm the EVs subtype (Thery et al. 2018). Not only proteins but also lipids from the EVs membrane can be used to characterize the EVs sample (Haraszti et al. 2016; Ramirez et al. 2018). EVs content is wide and diverse, given their significant presence in most if not all body fluids, which makes them easily and noninvasively accessible. The deep understanding of their cargo identification and quantification is of great importance as it can emerge as new biomarkers for diseases (Lane et al. 2018; Ramirez et al. 2018).

1.2. The eye

Animals use vision to explore different environments being vision one of the most deeply studied senses, in part motivated by the dominance of sight in our own sensory experience. The visual cortex occupies approximately 55 % of the entire cortical area of the primate brain, suggesting that over 50 % of brain capacity storage can be related to vision (Felleman and Van Essen 1991; Prasad and Galetta 2011). Vision is guaranteed not only by the brain but also by the eyes, which receive light from the exterior transforming it into electrochemical signals. These are sent to the brain to be processed and perceived as images.

The globe is protected by the eyelids and lubrication of the ocular surface. The eye itself is divided in two distinct parts: anterior and posterior segments. Cornea, aqueous humour, iris and lens form the anterior segment of the eye, while vitreous, retina, choroid and the sclera constitute the posterior segment of the eye (Figure 2). The cornea is transparent and avascular, being the primary infectious and structural barrier of the eye. Aqueous humour is a fluid that supplies nutrients and some oxygen to the ocular avascular tissue, namely cornea and lens, filling the anterior chamber. The iris is the colourful part of the eye, a muscle localized between cornea and lens that controls the diameter of the pupil, expanding or contracting depending on the amount

of light on the exterior. The lens is attached to ciliary muscles and is responsible for the focus at different object distances, changing its shape depending on the distance. Vitreous is a gelatinous and transparent substance that keeps the eye in its shape. Next to the vitreous is the retina that receives direct stimulation from light and images from the outside world and transports the information to the brain through electrochemical signals. Adjacent to the most external part of the retina is the Bruch's membrane (which mediates interactions between the retinal pigment epithelium (RPE) and blood flow from the choroid) and then the choroid, enriched in a complex network of blood fenestrated capillaries that provides nutrients and oxygen to the photoreceptors. The most external part of the eye is the sclera, a white layer constituted by conjunctive tissue, which in the front of the eye becomes transparent creating the cornea (Lammert 2014; DelMonte and Kim 2011).

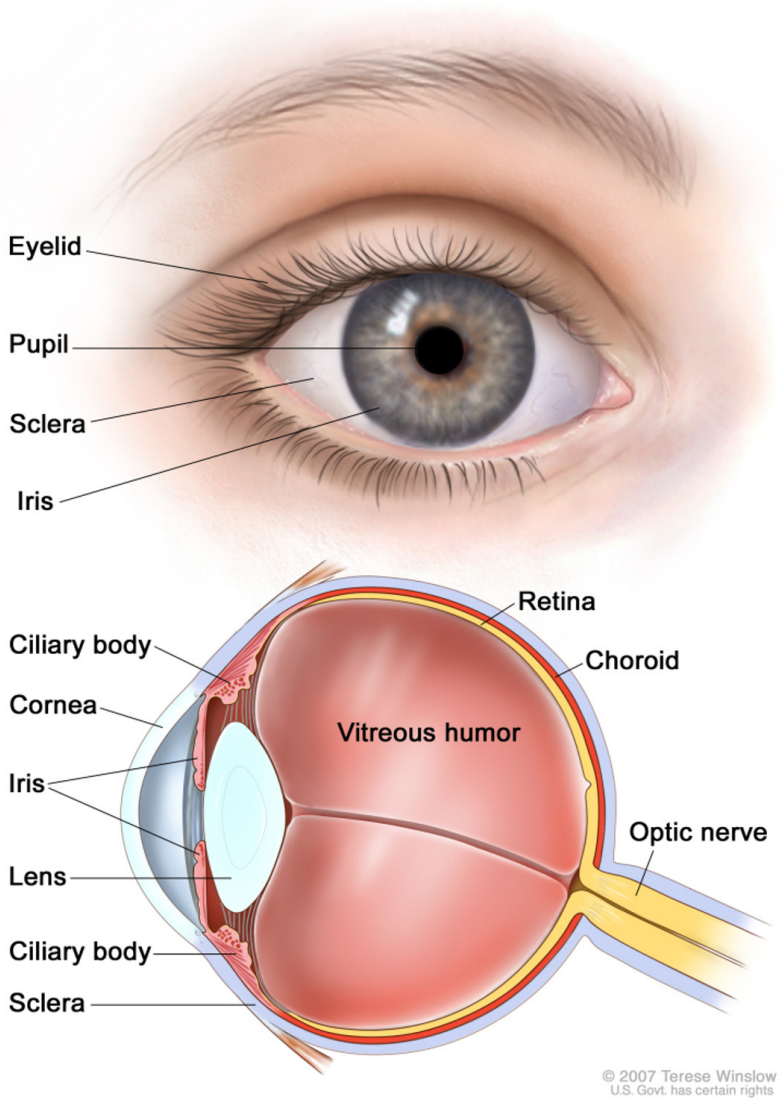

Figure 2: Anatomy of the human eye, showing the outside and inside of the eye. Illustration of the eye structure, including the cornea, iris, ciliary body, lens, vitreous humour, pupil, retina, sclera, choroid and the optic nerve. Image from NationalCancerInstituteUS 2021.

1.3. The retina: structure and function

The retina is a tissue sensible to light and it is part of the central nervous system (CNS). It converts photons into neuroelectrical impulses, and the information reaches the brain through the optic nerve. The inner part of the retina is in contact with the vitreous and its outermost part with the choroid. Retinas from vertebrates are characterized by layers of cells bodies – nuclear layers - interspersed with layers of cellular processes – plexiform layers. From the inner part of the retina, the first retinal layer, near the vitreous, is the inner limiting membrane (ILM) constituted by astrocytes and the end feet of Müller cells. Next is the nerve fiber layer (NFL) composed by the retinal ganglion cells (RGCs) axons. RGCs have their nuclei located in the ganglion cell layer (GCL) where astrocytes are also present. In the inner plexiform layer (IPL), amacrine and bipolar cells synapse with RGCs, since their cellular bodies together with horizontal cells and Müller cells and some microglia cells are in the next retinal layer, the inner nuclear layer (INL). In the outer plexiform layer (OPL), bipolar and horizontal cells communicate with photoreceptors (rods and cones), and it is followed by the outer nuclear layer (ONL) where the cell bodies of photoreceptors are located. Outer and inner segments (OS/IS) of photoreceptors are located right before the most external layer of the retina, the RPE, a monolayer of epithelial cells (Figure 3) (Lammert 2014; Madeira et al. 2015a; Vecino et al. 2016).

1.3.1. Retinal neuronal cells

There are five types of neurons in the retina: photoreceptors, bipolar cells, RGCs, horizontal cells, and amacrine cells.

For the passage of information in the retina there are two different pathways: vertical and lateral visual pathways. The vertical pathway involves the passage of information from the photoreceptors to bipolar cells and from bipolar cells to RGCs, whereas lateral pathway relies on local feedback circuits from horizontal cells back to photoreceptors and from amacrine cells back to bipolar cells (Byzov 1977; Kaneko and Tachibana 1987; Tachibana and Kaneko 1987).

Neuronal signals need to be passed through the different type of retinal neurons, from the photoreceptors until RGCs that finally transmits the information until the lateral geniculate nucleus (LGN) in the thalamus and the superior colliculus in the midbrain (London, Benhar, and Schwartz 2013). The primate and rodent visual systems are not identical. In primates around half of the optic nerve fibers cross the optic chiasm and project in the contralateral hemisphere (Kupfer, Chumbley, and Downer 1967). In contrast, in rodents, more than 90 % of optic nerve fibers project to the contralateral hemisphere after reaching the optic chiasm (Forrester and Peters 1967). The superior colliculus receives projections from more than 96 % of RGCs axons in rat (Salinas-Navarro et al. 2009). Also, axons of RGCs that project in the superior colliculus also pass through the LGN (Ellis et al. 2016).

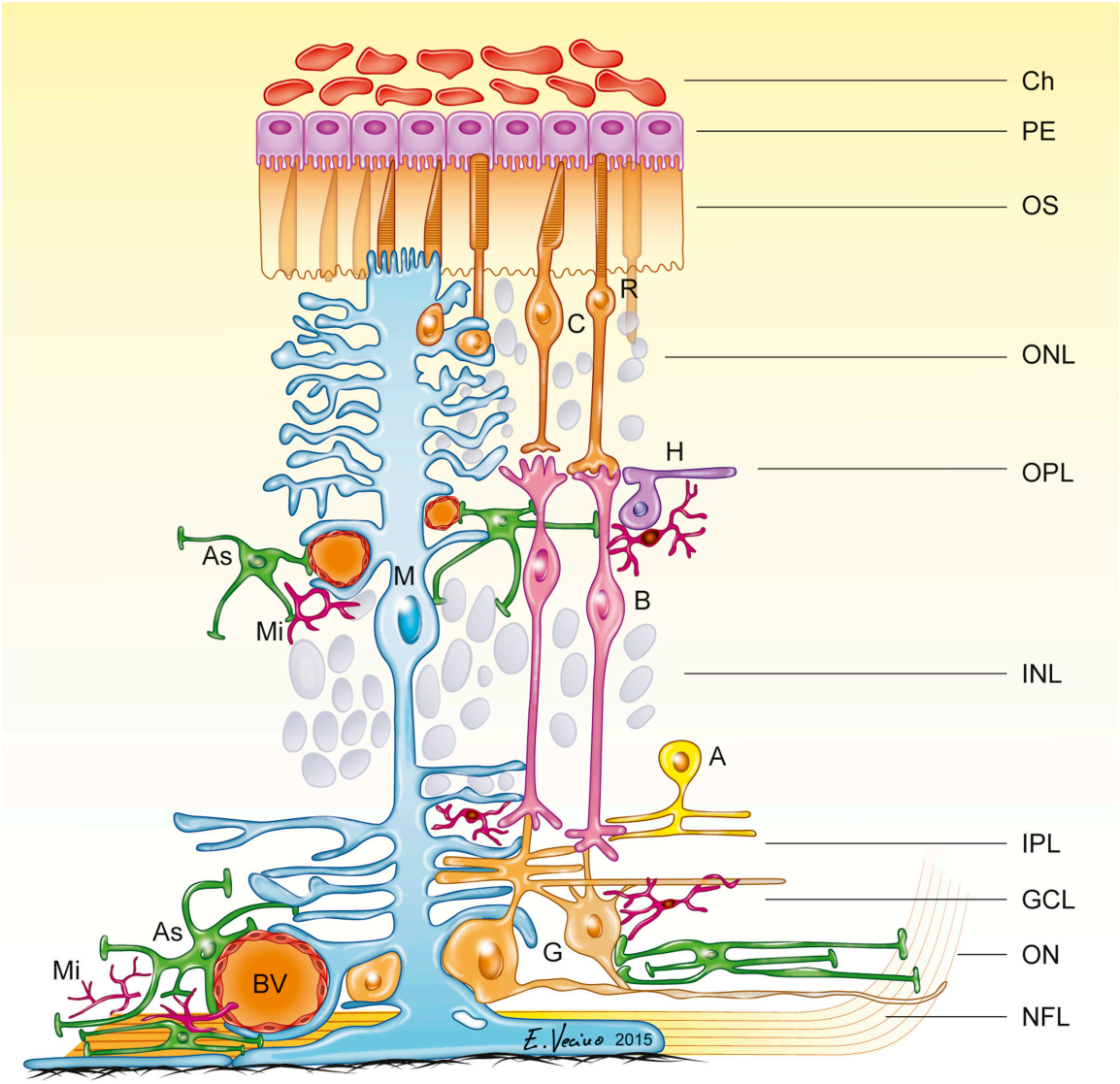

Figure 3: Schematic drawing of cells in the mammalian retina. Note the interactions between the cells and blood vessels (BV). Amacrine cells (A), astrocytes (AS), bipolar cells (B), cones (C), ganglion cells (G), horizontal cells (H), Müller cells (M), microglia (Mi), rods (R). Retinal layers (from the most internal to the outer layers): optic nerve (ON), nerve fibre layer (NFL), ganglion cell layer (GCL), inner plexiform layer (IPL), inner nuclear layer (INL), outer plexiform layer (OPL), outer nuclear layer (ONL), outer segment layer (OS), pigment epithelium (PE), choroid (Ch). Image from Vecino et al. 2016.

1.3.1.1. Photoreceptors

Mammals have two classes of photoreceptors: rods and cones (Peichl 2005). Rods and cones have an outer segment (OS) and an inner segment (IS). The OS contains photopigment, being next to the RPE, while the IS contains the nucleus, mitochondria and the synaptic terminals where occurs the neurotransmission to horizontal or bipolar cells.

The photopigment is responsible for the light absorption, leading to alterations in the

membrane potential of the photoreceptor which in the end allows the communication to the next cells in contact. Rods are sufficiently sensitive to low light levels, being responsible for the scotopic vision. Cones are responsible for photopic vision, under higher light levels (Purves D 2001; Wassle 2004).

1.3.1.2. Bipolar cells

Bipolar cells receive stimuli from photoreceptors and transmit them to the dendrites of amacrine and RGCs. Bipolar cells can receive neurotransmission signals from cones and rods. There is one type of rod-bipolar cells and at least nine types of cone-bipolar cells. In terms of function, bipolar cells can be subdivided, according to their light responses, into ON and OFF bipolar cells (Wassle 2004). Glutamate is the neurotransmitter released by photoreceptors: in the dark cones are depolarized and glutamate release increases, in light conditions cones are hyperpolarized and the release of glutamate decreases. A bipolar cell that reacts by excitation to glutamate will be depolarized in the dark (OFF bipolar cells) and a bipolar cell that respond to glutamate by hyperpolarization will be hyperpolarized in the dark (ON bipolar cells) (Feher 2012).

1.3.1.3. Horizontal cells

Horizontal cells are GABAergic interneurons with dendrites that connect with photoreceptors (both cones and rods) modulating their signal output (Chapot, Euler, and Schubert 2017). They provide lateral feedback inhibition at the photoreceptor synaptic terminal keeping the visual system sensitivity to luminance supporting contrast enhancement (Wassle 2004).

1.3.1.4. Amacrine cells

Amacrine cells are interneurons that mediate lateral interactions between bipolar cells terminals and the dendrites of RGCs. The majority of amacrine cells are in the INL, however there are also some displaced amacrine cells at the GCL. These neurons sharply respond to light contrast changes as well as light movement through the retina (Lagnado 1998).

1.3.1.5. Retinal ganglion cells

Retinal ganglion cells soma are present in the GCL. They are the neurons responsible for carrying electrical messages from the retina (collecting information from bipolar cells and amacrine cells) to the brain through the optic nerve. The optic nerve is a bundle of all RGC axons (more than a million fibers in humans) that in mammals target specific brain sections to process the information: the LGN and the superior colliculus (Kolb 2003; Wassle and Boycott 1991). There are several subtypes of RGCs, distinct in morphology, brain region targeted and also if they are photosensitive. A small percentage of RGCs are photosensitive, as they express melanopsin and are involved in circadian

rhythm maintenance, pupillary light reflex and in sleep (Schmidt, Chen, and Hattar 2011). The large extension of their axons leads to an increased susceptibility to injuries (Chidlow and Osborne 2003; Boia et al. 2020). Moreover, the regenerative capacity of these cells is reduced after synaptic connections have been established shortly after birth (Goldberg et al. 2002; Curcio and Bradke 2018).

1.3.2. Retinal glial cells

Glial cells were described in the late 1800s. Glial cells are crucial for the maintenance of normal retinal function and structure but they also participate in pathological processes during noxious conditions. In the retina there are three types of glial cells: astrocytes, microglia and Müller cells.

1.3.2.1. Astrocytes

In the retina, astrocytes are star shaped glial cells mostly present in the NFL and GCL, the inner layers of the retina. Astrocytes are important for neurotrophic support, enhanced mechanical support for degenerating axons and maintenance of the integrity of the blood-retinal barrier (BRB), a physiologic barrier that regulates ion, protein, and water flux into and out of the retina (Vecino et al. 2016; Cunha-Vaz, Bernardes, and Lobo 2011).

1.3.2.2. Microglia

Microglia cells are responsible for the immune response of the retina. They can be found in the retina in the OPL, ONL, IPL and also in the GCL in healthy retinas, but depending on their activation state, microglia show different morphologies: a ramified appearance (in their resting state) or an ameboid appearance (in the activated state) (Kettenmann et al. 2011; Santiago et al. 2014). Retinal microglia keep the retina under surveillance by moving their processes (Okunuki et al. 2019). Microglial cells are implicated in many functions essential for the proper development of the CNS, from neurogenesis to synaptic pruning, the process of synapse elimination (Bilimoria and Stevens 2015). They are also involved in programmed cell death in the developing retina (Ashwell et al. 1989).

Under pathological conditions, microglia became active and migrate to the injury site (Lee et al. 2008). Microglia was also already described as being involved in several retinal degenerative diseases such as glaucoma (Madeira et al. 2015a). Our group showed that EXOs derived from microglia cells exposed to EHP could be an important link between microglia activation and the loss of RGCs (Aires et al. 2020). This makes EXOs from microglia cells a potential player in glaucomatous damage, showing that EVs are becoming established signalling mediators between cells, including in the eye.

1.3.2.3. Müller cells

The Müller cell represents 90 % of the retinal glia and highlight themselves by their unique radial morphology from the ILM until the ONL (the somata are located in the INL), which allows interactions with all types of retinal cells, including neurons, being responsible for their functional, structural and metabolic support (Newman and Reichenbach 1996; Vecino et al. 2016). Müller cells were observed to enfold retinal neurons and becoming gliotic (activated) after nearly every pathological challenge in the retina (Hernandez et al. 2010; Wang et al. 2002; Bringmann et al. 2009). They participate in the establishment of the BRB, equilibrate ions and balance water transport through specialized water channels as aquaporin-4 (AQP4) (Cunha-Vaz, Bernardes, and Lobo 2011; Bringmann et al. 2005). The fast removal of glutamate from the synaptic clefts during neurotransmission is performed by the glutamate/aspartate transporter (GLAST), present in Müller cells, protecting neurons from glutamate excitotoxicity (Bringmann et al. 2013). These cells produce and secrete neurotrophic factors, growth factors and cytokines vital for neuronal survival (Del Rio et al. 2011; Cao et al. 1997; Harada et al. 2000). Moreover, it was described diverse subtypes of Müller cells that react differently to an injury possibly due to their different spatial proximities to dying cells (Roesch, Stadler, and Cepko 2012).

Aside the important role in keeping the retinal homeostasis, Müller cells are responsible for the light path guidance trough the retina, acting as "optical fibers" that reliably transfer light with low scattering from the retinal surface to the photoreceptor cell layer (Franze et al. 2007).

Although microglia cells are the principal glial cells responsible for the immune response in the retina, it is known that Müller cells also play a role (Kumar et al. 2013).

The MIO-M1 cell line is a spontaneously immortalized human Müller cell line obtained from human retina (Limb et al. 2002). This cell line expresses cellular retinaldehyde–binding protein (CRALBP), epidermal growth factor receptor (EGF-R), GS, □-smooth muscle actin (□-SMA) and GFAP. MIO-M1 cell line was considered to retain the phenotype and functional characteristics of Müller cells *in vitro* (Limb et al. 2002). However, studies using this cell line should be interpretated with caution since these cells can express proteins that are not common in primary Müller cells, like opsins, for example (Hollborn et al. 2011).

Müller cells release extracellular vesicles *in vitro* (DB Lamb 2018). Moreover, Müller cells are able to uptake EVs and it has been demonstrated that the exposure of human Müller cells to mouse embryonic stem cells EVs (mESEVs) induces morphological and transcriptome changes in these cells. MVs from mESEVs transfer mRNAs to Müller cells that are involved in the maintenance of pluripotency, including OCT4 and SOX2, but also induce up-regulation of the basal levels of endogenous human OCT4 mRNA in Müller cells (Katsman et al. 2012). Müller cells similarly internalize MVs and EXOs from human embryonic stem cells in a time-dependent process. However, only MVs

induce an increase in OCT4 and a decrease in SOX2 mRNAs and proteins, suggesting that mRNA transfer into Müller cells by MVs and EXOs primarily depends on the content of the EV (Peng et al. 2018).

1.4. Glaucoma

Glaucoma is a group of ocular disorders, an optic neuropathy, characterized by RGC loss (with degeneration of RGCs axons) and loss of visual fields that can culminate in blindness (Schwartz 2005; Pardue and Allen 2018). High intraocular pressure (IOP) is the primary risk factor for glaucoma onset and progression (Walland et al. 2006). Older age, genetics and vascular dysregulation have also been associated with glaucoma (Yamamoto and Kitazawa 1998; Pardue and Allen 2018). Because it may be asymptomatic until a relatively late stage, diagnosis is frequently delayed. Nowadays, glaucoma treatment relies in lowering IOP, either by surgical procedures, laser treatment or by topical application of pharmaceuticals. Nevertheless, in a significant number of patients with controlled IOP the disease still progresses (Walland et al. 2006) and subjects with normal IOP values develop glaucoma (normal tension glaucoma), indicating that other pathological mechanisms may be involved in the disease.

1.4.1. Neuroprotection in glaucoma

Glaucoma is considered to be a progressive neurodegenerative disease. In glaucoma, as in other optic neuropathies, neuroprotective treatments aim to preserve vision preventing retinal neuronal death, specially improving the survival of RGCs or regenerating the optic nerve fibers (Fu et al. 2019). However, until now, there is no therapeutic strategy directed to promote axonal regeneration of RGCs or RGCs survival as a therapeutic approach for glaucoma, since current therapies rely in lowering IOP, the principal risk factor of the disease.

Numerous neuroprotective strategies have been investigated for optic neuropathies as integrating transplanted RGCs in the diseased retina, peripheral nerve grafting, pharmacological agents, and also neurotrophic factors due to their important role in keeping neuronal homeostasis. The failure to regenerate RGCs has already been attributed not only but also to an environment poor in growth-promoting trophic factors (Su et al. 2009). Indeed, in glaucoma, the increased IOP affects anterograde and retrograde axonal transports that lead to deprivation of RGCs of neurotrophic factors produced by brain targets (Quigley, Guy, and Anderson 1979; Quigley et al. 2000).

However, none of the attempts described above have been successfully translated to clinical practice (Shruthi et al. 2017; Cen and Ng 2018; Allen et al. 2013; Fu et al. 2019). The limitations in translating these experimental therapies to clinical practice are especially due to the difficulty in using an animal model that fully replicates the human disease. Furthermore, experimental endpoints differ greatly between animal models and human clinical trials, with visual acuity, contrast sensitivity, and visual

field being difficult to assess in animals (Fu et al. 2019; Boia et al. 2020).

Nevertheless, RGCs treatment remains an important field of research with enormous potential for achieving visual restoration and new targets for new therapeutic strategies need to be explored.

1.4.2. Interaction between Müller cells and RGCs

Previous studies have demonstrated that Müller cells can protect RGCs either by direct contact either by the exposure of RGCs to Müller cells conditioned medium (CM) (Garcia et al. 2002; Ruzafa et al. 2018b). Due to the neuroprotective role known of Müller cells and considering that RGCs degeneration is one of the principal causes of vision loss, understanding the interaction between these two retinal cells is of great importance. Furthermore, the communication between Müller cells and RGCs under different pathological conditions has grown exponentially in recent years due to the intrinsic properties of Müller cells in neuroprotection and their important role in many diseases. Müller cells were already reported to release a set of neurotrophic factors to the extracellular space, and the administration of different combinations of neurotrophins involved in the survival, differentiation and development of neurons in the eye has been reported to increase RGCs survival in different experimental conditions (Ruzafa et al. 2018b; Pereiro et al. 2020a). Moreover, Müller cells, astrocytes and microglia are known to synthetize neurotrophic factors and these can directly or indirectly mediate neurotrophic actions (Garcia et al. 2003; Vecino et al. 2016). Some of the most studied neurotrophic factors released by Müller cells are the ciliary neurotrophic factor (CNTF) (Ju et al. 1999), the brain derived neurotrophic factor (BDNF) (Seki et al. 2005) and the pigment epithelium derived factor (PEDF) (Unterlauft et al. 2014). The neuroprotective role of CNTF in the retina comprises several mechanisms as a direct action on photoreceptors to prevent apoptosis, the stimulation of Müller cells to produce photoreceptor survival factors, increased expression of glutamate transporters, and others (Zack 2000; Escartin et al. 2006). Also, CNTF was reported to protect RGCs in different animal models of pathology (Cao et al. 1997; Azadi et al. 2007; Fischer et al. 2004). However, the beneficial effects were determined as being dose dependent since CNTF can be harmful for the correct retinal function (Zeiss et al. 2006). BDNF is capable of protect RGCs (Seki et al. 2005; Chen and Weber 2001; Sanchez-Migallon et al. 2016). Nevertheless, in the majority of studies, the exposure of RGCs to BDNF only promoted short term beneficial effects (Guo, Nagappan, and Lu 2018). This decrease in the effect of BDNF was attributed to a decrease in the expression of the BDNF high affinity receptor tropomyosin related kinase receptor (TrkB), however the role of other BDNF receptor, the pan-neurotrophin receptor p75NTR, cannot be discarded since BDNF also binds to this low affinity neurotrophin receptor (Di Polo et al. 1998; Guo, Nagappan, and Lu 2018; Bothwell 1995). PEDF was first described as a neurotrophic factor produced only by RPE, but then it was discovered as being secreted also by

Müller cells (Becerra et al. 2012; Unterlauft et al. 2014). The upregulation of PEDF in Müller cells occurs early in gliosis and it may reflect an attempt to rescue retinal neurons (specially RGCs) from further damage (Unterlauft et al. 2012; Unterlauft et al. 2014). Osteopontin (SPP1) is a secreted glycosylated phosphoprotein that influences cell survival, inflammation, migration, and homeostasis after injury, produced by Müller cells (Ruzafa et al. 2018b). Moreover, it was found that the absence of this protein in the retina produces a reduction in the number of RGCs (Ruzafa et al. 2018a).

1.4.3. Glaucoma models

1.4.3.1. Elevated hydrostatic pressure model

With elevated IOP as one of the most prevalent features of glaucoma it is necessary to develop systems capable of reproducing this characteristic for *in vitro* experiences to understand the role of different cells in this pathology. Concerning the study of glaucoma, elevated hydrostatic pressure (EHP) has been used to mimic ocular hypertension. Glaucoma patients present IOP values between 20 to 35 mmHg. However, *in vitro* models need to mimic a chronic IOP elevation in a short period of time. This way, *in vitro* models use pressures ranging from 30 to 100 mmHg above atmospheric pressure during 10 min to 72h (Sappington, Chan, and Calkins 2006; Aires et al. 2020; Aires, Ambrosio, and Santiago 2017).

The effect of EHP in Müller cells has been described previously. Indeed, Müller cells exposed to EHP had an increased mRNA expression of Kir 2.1 and Kir 4.1 channels (the most significant mediators of K^+ buffering in Müller cells) indicating a dysregulation in ion exchanges, and also alterations in the cell surface representation of these channels (Yu et al. 2012; Fischer et al. 2019). Other study, carried out in rMC-1, a rat Müller cell line, showed that some genes are affected by EHP and that the transcriptional profile is different from the one seen in hypoxia suggesting that Müller cells response is dependent of the injury or microenvironment (Xue et al. 2011). After being challenged to EHP, the secretion of PEDF by Müller cells increase and Müller cells processes retract (Lee et al. 2015).

1.4.3.2. Animal models of glaucoma

Several animal models have been developed to model the human condition. Since elevated IOP is the main risk factor, extensive studies have been carried out to discover therapeutic targets and to develop new drugs to treat ocular hypertension using experimental models of rodents (rats and mice) and non-human primates (e.g., cynomologus, rhesus, or marmoset monkeys) (Kimura, Noro, and Harada 2020). However, other animal models non-related with IOP have been established (Johnson and Tomarev 2010). Nevertheless, rodents have become a popular model organism to study glaucoma, because of their high degree of availability, relatively low cost, short life-span, and responsiveness to experimental and genetic manipulation (Johnson and

Tomarev 2010). Between pressure-dependent models, episcleral vein cauterization (Garcia-Valenzuela et al. 1995), hypertonic saline ocular hypertension model (Morrison, Cepurna, and Johnson 2015), laser photocoagulation (Salinas-Navarro et al. 2010), microbead occlusion model (Sappington et al. 2010) and spontaneous glaucoma (DBA/2J mouse strain) (Libby et al. 2005) are some of the most used models (Johnson and Tomarev 2010).

Glaucoma is usually associated with increased IOP. Still, glaucomatous changes in the retina and optic nerve sometimes occur at normal IOP being called "normal tension glaucoma" (Walland et al. 2006). Consequently, there was a need to create pressure-independent animal models that could mimic normal tension glaucoma. These models provide perceptions of the mechanisms of RGCs degeneration despite the increased IOP, as optic nerve crush, optic nerve transection, and retinal ischemia-reperfusion (I-R) injury (Johnson and Tomarev 2010). I-R is induced through cannulation of the anterior chamber with a needle connected to an elevated sterile saline solution reservoir, allowing to increase the IOP above the ocular perfusion pressure (generally to about 110 mmHg). After the I-R exposure, the eye recovers the normal IOP values. This method involves extreme acute ocular hypertension (Johnson and Tomarev 2010). Retinal ischemia followed by reperfusion triggers apoptosis in RGCs but damage occurs throughout the various layers of the retina (Madeira et al. 2016) (Boia et al. 2017), making this model considered for global retinal degeneration.

It is reported that I-R leads to Müller cell gliosis (Hirrlinger et al. 2010) (Kim et al. 2013). Moreover, others demonstrated that Müller glia are activated at a very early stage of ischemic injury (Palmhof et al. 2019).

There is no ideal experimental model. Even more each of the existing systems have been successfully used to reveal important aspects of glaucoma pathology and might be used to develop novel therapies for the disease in the future

Aims

Glaucoma is an optic neuropathy characterized by the progressive loss of RGCs with the consequent irreversible loss of vision, being elevated IOP the principal risk factor. Müller cells have an important role in keeping retinal homeostasis, and they were already reported to protect RGCs and to promote their survival. However, how these cells communicate is still not well understood.

EVs play a significant part in intercellular communication, being able to deliver their cargo into nearby cells as well as over long distances via the blood stream. Müller cells were already reported to uptake EVs and produce them, reinforcing the importance to further explore EVs from Müller cells to understand if they could have a neuroprotective effect in the retina. Also, Müller cells release other soluble factors to the extracellular space. From this perspective, elucidating which factor or factors are determining the survival of RGCs after damage is a relevant topic in scientific research. We hypothesized that CM or EVs derived from Müller cells could promote the survival of RGCs.

The main aim of this work was to assess if CM or EVs derived from Müller cells could protect RGCs in the context of glaucoma. We started by understanding how Müller cells and RGCs react when challenged with EHP, assess if there was an autocrine function of MVs released by Müller cells and if MVs could protect RGCs from noxious environment caused by EHP. To achieve this goal, we used primary Müller cell cultures and MIO-M1 cultures to isolate and characterize EVs and to collect CM. Rat primary cultures of RGCs and Müller cells and cultures of MIO-M1 cells were exposed to EHP (+70 mmHg above atmospheric pressure), to mimic the increased IOP, for different periods to understand how their survival was affected. RGCs cultures and co-cultures were incubated under atmospheric pressure or EHP with CM from primary Müller cells and MIO-M1 cells. The effect of MVs from Müller cells and MIO-M1 cells in survival of RGC cultures and MIO-M1 cultures was assessed.

An additional objective was to evaluate the protective potential of the EVs from Müller cells against retinal degeneration using the transient retinal ischemia injury model. We assessed the effect of EVs in the eyes contralateral to the ischemic eyes because we found that the synergistic action of ischemia and an intravitreal injection of PBS harmed the retina. EVs from MIO-M1 cells were injected in the vitreous of Wistar Han rats and their effects in the retina were analysed 7 days post injection by determining retinal structure and function, retinal cell death, microglial cell activation, Müller cells reactivity and RGCs survival.

In summary, this study aimed to elucidate the role of Müller cells CM and MVs in the survival of RGCs in the context of elevated pressure.

Chapter 2

Materials and Methods

2.1. Animals

In this study, Wistar Han rats were used in agreement with the statement of the Association for Research in Vision and Ophthalmology (ARVO) for the use of animals in vision and ophthalmology research, in accordance with the European Community directive guidelines for the use of animals in laboratory (2010/63/EU) transposed to the Portuguese law (Decree-Law nº 113/2013 of August 7 and Decree-law 1/2019 of January 10). All procedures involving animals were approved by the Animal Welfare Body of the Coimbra Institute for Clinical and Biomedical Research (ORBEA nº 03/2021 and nº 03/2019).

Two to four months old Wistar Han rats (males and females) used were housed under a controlled environment (25.5 ± 0.4 °C of temperature and 41.5 ± 3.3 % of relative humidity, 12h light/dark cycle) with free access to water and food.

2.2. MIO-M1 cell line

MIO-M1 cell line (Moorfields/Institute of Ophthalmology-Müller 1) maintenance was achieved by keeping MIO-M1 cells cultured in 175 cm^2 in DMEM (Dulbecco's Modified Eagle Medium, Gibco) containing glutaMAX, high glucose (4500 mg/L), sodium pyruvate (110 mg/L) and phenol red (15 mg/L), supplemented with heat-inactivated 10 % fetal bovine serum (FBS; Gibco) and antibiotics (10000 U/mL penicillin, 10000 μg/mL streptomycin; Gibco) (culture medium) and maintained at 37 °C in a humidified atmosphere of 5 % CO2. To collect cells, after reaching approximately 80 % of confluence, cells were washed with PBS and then trypsin was added (0.05% in 0.02 mM EDTA; Sigma-Aldrich) for 3 min at 37 °C. After cells detachment, culture medium was added to stop trypsin activity. The suspension of cells was centrifuged at 450 g for 5 min at room temperature and the supernatant was discarded. Cells were resuspended in culture medium. MIO-M1 cells was used until passage 39.

For experiments, MIO-M1 cells were plated at a density of 1.32 x 10^4 cells/cm^2 in 24-well plates with coverslips (pre-coated with 0.1 mg/mL poly-L-lysine; Sigma-Aldrich) in culture medium. To collect EVs MIO-M1 cells were plated in 100 mm plates or in 24-well plates in culture medium prepared with 10 % Exo-free FBS (heat-inactivated FBS depleted of vesicles, previously prepared by ultracentrifugation at 25400 g for 16h at 4 °C). Cells were cultured at 37 °C in a humidified atmosphere of 5 % CO_2.

MIO-M1 cells were incubated at 37 °C for 24h or 48h in a custom-made pressure chamber, supplied with a pressure regulator and a gauge providing a constant hydrostatic pressure of 70 mmHg above atmospheric pressure, through injection of a mix of 95 % air 5 % CO_2 (Madeira et al. 2016; Aires et al. 2019; Rodrigues-Neves et al. 2018; Aires et al. 2020) The control cells were cultured in a standard cell incubator (atmospheric pressure).

2.3. Preparation of primary cultures

2.3.1. Tissue extraction

Wistar Han rats were sacrificed under anaesthesia (2.5 % isoflurane in 1 L/min O_2, IsoFlo; Abbott Laboratories) by cervical dislocation. Eyes were enucleated and kept in CO_2 independent medium (Gibco) until retinal dissection.

2.3.2. Primary cultures of Müller cells

Cultures of primary Müller cells, were prepared as described previously in (Pereiro et al. 2020b). The retinas were digested for 30 min in sterile Earle's Balanced Salt Solution (EBSS) containing papain (20 U/mL) and DNase (2000 U/mL; Worthington) at 37 °C. The reaction was stopped with Dulbecco's Modified Eagle Medium (DMEM; Gibco) supplemented with 10 % FBS (Gibco), 1 % L-glutamine (200 mM; Gibco) and 0.1 % gentamicin (50 mg/mL; Gibco) (culture medium) at room temperature. The retinas were mechanically dissociated using the "up and down" movement using pipette tips with different diameters starting from the biggest diameter until the smaller one. Cells were pelleted through a 270 g centrifugation for 5 min and resuspended in culture medium. All cells were plated in 12 mm coverslips in 24-well plates previously coated with 0.1 mg/mL poly-L-lysine (Sigma-Aldrich) and 10 μg/mL laminin (Sigma-Aldrich). Cells were maintained at 37 °C in a humidified atmosphere of 5 % CO_2. The medium was totally replaced by fresh culture medium on day *in vitro* (DIV) 1 since by that time Müller cells were already attached to the coverslips and other cell types and debris were eliminated by washing. After the first medium change, half of the medium was changed every 3 days. These cultures reached confluence after 7 DIV.

2.3.3. Primary cultures of RGCs

Primary cultures of RGCs were prepared based as described previously (Ruzafa and Vecino 2015; Pereiro et al. 2018). The retinas were digested for 90 min in EBSS containing papain (20 U/mL) and DNase (2000 U/mL; Worthington) at 37 °C. Then, Neurobasal-A medium (NBA; Gibco) with 2 % B27 supplement (50X, Life Technologies), 2.5 % L-glutamine (200 mM; Gibco) and 0.5 % gentamicin (50 mg/mL; Gibco) was added to stop enzyme digestion. The retinas were dissociated through a mechanical process using the "up and down" movement using pipette tips with different diameters starting from the biggest diameter until the smaller one. Cells were pelleted through a 270 g centrifugation for 5 min and resuspended in EBSS with ovomucoid inhibitor-albumin and DNase. A density gradient (ovomucoid inhibitor-albumin gradient) was used (following instructions of the Worthington kit) where more RGCs than Müller cells pass due to their smaller size, then it was centrifuged at 70 g for 6 min and the pellet was resuspended in supplemented NBA medium. All cells were plated in 12 mm coverslips in 24-well plates previously coated with poly-L-lysine (0.1 mg/mL; Sigma-

Aldrich) and laminin (10 μg/mL; Sigma-Aldrich). Cells were cultured at 37 °C in a humidified atmosphere of 5 % CO_2. To maintain the cells, half of cells culture medium was changed every 3 days.

2.3.4. Primary co-cultures of RGCs and Müller cells

The retinas were digested for 30 min in EBSS containing Papain (20 U/mL) and DNase (2000 U/mL; Worthington) at 37 °C. To stop enzyme digestion, NBA medium (Gibco) supplemented with 2% B27 (50X, Life Technologies), 10 % FBS (Gibco), 1 % L-glutamine (200 mM; Gibco) and 0.1 % gentamicin (50 mg/mL; Gibco) was added. The retinas were dissociated through a mechanical process using the "up and down" movement using pipette tips with different diameters starting from the biggest diameter until the smaller one. Cells were pelleted through a 270 g centrifugation for 5 min and resuspended in supplemented NBA medium. All cells were plated in 12 mm coverslips in 24-well plates previously coated with poly-L-lysine (0.1 mg/mL; Sigma-Aldrich) and laminin (10 μg/mL; Sigma-Aldrich). Cells were cultured at 37 °C in a humidified atmosphere of 5 % CO_2. To maintain the cells, half of cells culture medium was changed each 3 days.

2.4. Preparation of conditioned medium

Conditioned medium (CM) from primary Müller cell cultures and MIO-M1 cells was collected after confluence was reached (after 6 days in culture for primary Müller cells and 48h for MIO-M1 cells). Cells medium was changed to new culture medium without FBS for 2h to eliminate all FBS present. Then, medium was changed to new culture medium without FBS, being collected after 48h. CM was filtered with a 0.22 μm filter and frozen in aliquots at -20 °C.

2.5. Elevated hydrostatic pressure model

In the present study the elevation of pressure was assured by a customized pressurized chamber injected with a mixture of gas (95 % air and 5 % CO_2) through a pressure regulator. The pressure chamber is positioned inside a standard incubator at 37 °C and inside the pressure chamber plates with water guarantee the humidity needed for cell growing. A pressure gauge allows regulation of pressure inside the chamber (stable within ± 1 mmHg), which was kept constant in this study with 70 mm Hg above atmospheric pressure as already stablished by our group (Madeira et al. 2015b; Aires et al. 2019; Aires et al. 2020).

2.6. Isolation of extracellular vesicles

For the isolation of EVs, cells were cultured in Exo-free medium. The supernatant from MIO-M1 cells was centrifuged at 400 g for 10 min at 4 °C to pellet cells and

debris. The culture medium of primary Müller cells had an extra centrifugation at 2000 g for 10 min at 4 °C to pellet small size cell debris.

To collect EVs isolated at low-speed ultracentrifugation (from now on referred to as microvesicles, MVs), the supernatant was centrifuged at 16500 g for 20 min at 4 °C. The supernatant was gently discarded and the pellet enriched in MVs was washed with sterile PBS and centrifuged for 20 min at 16500 g at 4 °C. The pellet was resuspended in sterile PBS.

To isolate EVs at high-speed ultracentrifugation (from now on referred to as exosomes, EXOs), the supernatant discarded previously (in the MVs isolation protocol) was filtered using a 0.22 μm polyvinylidene difluoride (PVDF) syringe filter (Whatman) to remove large particles and cell debris and was centrifugated at 120000 g for 70 min. The EXOs pellet was washed with sterile PBS and centrifuged at 120000 g for 70 min. The pellet was resuspended in sterile PBS.

MVs collected from cells incubated at atmospheric pressure (control) will be referred to as MVs. MVs from primary Müller cells and from MIO-M1 cells will be referred as MVs Müller and MVs MIO-M1, respectively.

2.7. Transmission electron microscopy (TEM)

MVs and EXOs were fixed with 4 % or 2 % paraformaldehyde (PFA), respectively (Aires et al. 2020; Rodrigues 2021). Samples were adsorbed in formvard-carbon coated grids (TAAB Laboratories) for 5 min and then the grids were contrasted in 2 % uranyl acetate for 5 min. The preparations were observed in a Tecnai G2 Spirit BioTWIN electron microscope with analySIS 3.2 software (FEI).

2.8. Nanoparticle tracking analysis (NTA)

NTA was performed using a NanoSight NS300 instrument (Malvern Panalytical Limited). MVs from MIO-M1 cells and primary Müller cells, and EXOs from MIO-M1 cells were diluted in 1 mL of sterile and filtered PBS. With the camera level set at 12, 5 videos of 1 minute were recorded for each sample. The mean and estimated concentration of all size particles were obtained. All data was processed using NTA 2.2 analytical software (Malvern Panalytical Limited).

2.9. Cell treatment

2.9.1. Incubation with conditioned medium

To assess the effect of CM from primary Müller cell cultures and MIO-M1 cells in the survival of RGCs and Müller cells *in vitro*, RGC cultures and co-cultures were incubated with culture medium and CM in the proportion of 1:1 from DIV 0. Half of the medium was changed each 2 days keeping the proportion 1:1 of culture medium and CM.

2.9.2. Incubation with MVs

MVs isolated from MIO-M1 cells or from primary Müller cells were incubated with the recipient cells (MIO-M1 cells and primary RGCs) in the proportion of 1 donor cell to 1 recipient cell. Recipient MIO-M1 cells were exposed to EHP for 24h and 48h. RGCs were exposed to EHP for 24h.

2.10. Intravitreal injection

Wistar Han rats (males and females) aged 2-4 months old were anesthetized with isoflurane (2.5 % isofluorane in 1 L/min O2, IsoFlo; Abbott Laboratories). The eyes were topically anesthetised with oxybuprocaine (4 mg/mL, Anestocil; Edol) and the pupil dilated with tropicamide (10 mg/mL, Tropicil Top; Edol).

Each sample of MVs from MIO-M1 cells were isolated in the same day or the day before the intravitreal injections. MVs were collected from six 100 mm plates and the samples were equilibrated with PBS to a final volume of 100 μL. In this experiment, three conditions were analysed: naïve (non-treated animals), PBS (animals which both eyes were injected with 5 μL of the vehicle solution, PBS) and MVs (animals with both eyes injected with 5 μL of MVs). The injection was performed with a 33G needle.

2.11. Induction of retinal ischemia-reperfusion

One eye of each animal was subjected to ischemia reperfusion injury, 1h after the intravitreal injection. Animals were anesthetized with isoflurane (2.5 % isoflurane in 1 L/min O2, IsoFlo; Abbott Laboratories) and were placed on a heating blanket to maintain their body temperature. The cardiac frequency was monitored throughout the ischemic procedure. The eyes were topically anesthetised with oxybuprocaine (4 mg/mL, Anestocil; Edol) and the pupil dilated with tropicamide (10 mg/mL, Tropicil Top; Edol). Then, the anterior chamber was cannulated with a 30-gauge needle connected to an elevated reservoir infusing a sterile saline solution for 1h. To keep the cornea hydrated, a viscoelastic solution (Gel 4000; Bruschettini) was applied to both eyes during the procedure. After 1h of ischemia the needle was withdrawn to allow reperfusion. Fusidic acid (10 mg/g, Fucithalmic; Leo Pharmaceutical) was applied to the eyes at the end of the experiment to prevent infection.

2.12. Electroretinography

Electroretinography was performed 7 days after intravitreal injection to assess retinal function as described (Boia et al. 2019; Aires et al. 2020). For this, animals were dark adapted overnight before the exam. During the preparation and the procedure itself, a red light was used so that the animals remained in scotopic conditions. Rats were anaesthetized with a mixture of ketamine (75 mg/Kg, Nimatek; Dechra) and

medetomidine (0.5 mg/Kg, Sedator; Dechra) and maintained on a heating pad to keep the body temperature. The eyes received a topical anesthesia with oxybuprocaine (Anestocil, 4 mg/mL; Edol) and the pupils were dilated with tropicamide drops (Tropicil Top, 10 mg/mL; Edol). ERGs were recorded with two corneal gold wire electrodes touching the corneas (one for each eye), two reference electrodes were placed in the head and one in the tail. Carmellose sodium (Celluvisc 1 %; Allergan) was applied for the contact between the cornea and the gold ring electrode and for hydration.

Scotopic threshold responses (STR), scotopic, photopic and flicker ERG responses were recorded in response to light stimuli produced by a Ganzfeld stimulator (Roland Consult GmbH; Germany). For the STR, eyes were irradiated with light flashes of 0.000095 cd·s/m2. Under scotopic and photopic conditions (in the latter case, after light adaptation to a white background), light flashes from 0.0095 cd·s/m^2 to 9.49 cd·s/m^2 were used. For the flicker test, first and second harmonics were detected with light intensities of 0.95 cd·s/m^2 to 9.49 cd·s/m^2. The amplitudes (μV) of positive-STR (pSTR) and negative-STR (nSTR) (reflecting RGCs response); a-wave (rods response) and b-wave (bipolar cells response) in scotopic; b-wave (bipolar cells response) in photopic tests; and first and second harmonics in flicker test (pure cone response) were extracted. OFF-line digital filters were applied on the b-wave (high frequency cut-off of 50 Hz) with the RETIport software (Roland Consult GmbH, Germany) (Boia et al. 2019; Martins et al. 2011).

2.13. Optical coherence tomography (OCT)

OCT was used to evaluate retinal structure and thickness, using Phoenix Micron IV Retinal Imaging Microscope (Phoenix Technology).

Animals were anaesthetized with an intraperitoneal injection of a mixture of ketamine (75 mg/Kg, Nimatek; Dechra) and medetomidine (0.5 mg/Kg, Sedator; Dechra). The eyes were topically anesthetised with oxybuprocaine (4 mg/mL, Anestocil; Edol) and the pupil dilated with tropicamide (10 mg/mL, Tropicil Top; Edol). To prevent the eyes from drying during the examination carmellose sodium (Celluvisc 1 %; Allergan) was applied for the hydration and better contact between the eye and the lens from the equipment.

In the OCT system, the eye fundus was focused on the optic nerve zone and 4 images (2 above and 2 below the optic nerve) were analysed measuring the thickness of retinal layers from GCL to RPE using the software Insight (Phoenix Technology).

2.14. Preparation of vertical retinal sections

Animals were deeply anesthetized with an intraperitoneal injection of a mixture of ketamine (75 mg/Kg, Nimatek; Dechra) and medetomidine (0.5 mg/Kg, Sedator; Dechra) to perform a transcardiac perfusion, first with PBS and then with 4 % PFA to fix the tissue. The eye orientation was kept with a suture stitched to the upper eyelid

and the eyes were removed. The eyes were cleaned and a cut was made in the cornea under a magnifying glass, being left in a 4 % PFA solution for 1h to allow tissue to be fixed from the inside of the eye. For cryopreservation eyes were saturated with 15 % sucrose in PBS for 1h and then the solution was changed to 30 % sucrose in PBS overnight at 4 °C. To maintain the eyes preserved they were soaked in a mixed solution (1:1) of 30 % sucrose and a tissue-freezing medium (Optimal Cutting Temperature, Shandon CryomatriX, Thermo Scientific) and were stored at -80 °C until needed.

To prepare retinal cryosections, eyes were sectioned at 14 μm in a cryostat (Leica CM3050 S, Leica Biosystems) and mounted on glass slides (Superfrost Plus, Menzel-Gläser, Thermo Scientific). Retinal cryosections were kept at -20 °C.

2.15. Immunostaining

2.15.1. Immunocytochemistry

To perform the immunocytochemistry, a humidified dark chamber needed to be prepared putting on the bottom of the chamber a piece of parafilm tissue (where the coverslips were placed) and next to the walls humidified paper.

To fix the cells, coverslips were washed 3 times with PBS and then incubated for 10 min with 4 % PFA with 4 % sucrose in PBS at room temperature (MIO-M1 cells) or with methanol at -20 °C (primary cell cultures). Coverslips were washed 3 times with PBS. Cells were incubated with blocking buffer (0.25 % Triton X-100 and 3 % BSA in PBS) for 30 min at room temperature. Cells were incubated with the primary antibodies (Table 1), diluted in blocking buffer, overnight at 4 °C. Then, cells were washed 3 times with PBS and incubated with the secondary antibodies together with DAPI for 1h at room temperature, protected from light. Coverslips were washed 3 times with PBS and then mounted in slides with mounting medium (Fluorescence Mounting Medium, Dako).

2.15.2. Immunohistochemistry

Retinal sections were defrosted at room temperature overnight and fixed in acetone at -20 °C for 10 min. Cryosections were re-hydrated with PBS (twice) and then restricted with a hydrophobic pen (ImmEdge Pen; Vector Laboratories). Retinal sections were permeabilized with 0.25 % Triton X-100 in PBS for 30 min at room temperature, and the sections were then blocked with 10 % normal goat serum and 1 % BSA in PBS in a humidified chamber for 30 min. Primary and secondary antibodies (Table 2) were diluted in 1 % BSA in PBS. Retinal cryosections were incubated with primary antibodies overnight at 4 °C in a humidified chamber. Then, they were washed 3 times in PBS and incubated with secondary antibodies for 1h at room temperature in a dark and humidified chamber. Sections were washed 3 times in PBS, incubated with DAPI (1:2000) in PBS for 10 min at room temperature and washed again 3 times in

PBS. Finally, retinal cryosections were mounted using fluorescent mounting medium (Fluorescence Mounting Medium, Dako).

Table 1: List of primary and secondary antibodies used in immunocytochemistry

	Supplier, Cat #	Host	Dilution
Primary Antibodies			
Anti-Glutamine synthetase	Abcam, ab49873	rabbit	1:1000
Anti-GFAP	Millipore, ab5541	chicken	1:500
Anti-Ki67	Abcam, ab15580	rabbit	1:200
Anti-Vimentin	Abcam, ab92547	rabbit	1:200
Secondary Antibodies			
Anti-Rabbit IgG (H+L), Alexa Fluor 568	Thermo Fisher Scientific, A11036	goat	1:500
Anti-Chicken IgY (H+L), Alexa Fluor 488	Thermo Fisher Scientific, A11039	goat	1:500

Table 2: List of primary and secondary antibodies used in immunohistochemistry

	Supplier, Cat #	Host	Dilution
Primary Antibodies			
Anti-Brn3a	Sigma-Aldrich, MAB1585	rabbit	1:1000
Anti-GFAP	Millipore, ab5541	chicken	1:500
Anti-Iba1	Fujifilm Wako, 019-19741	rabbit	1:1000
Anti-MHC-II	BioRad, MCA46A647	mouse	1:500
Secondary Antibodies			
Anti-Rabbit IgG (H+L), Alexa Fluor 488	ThermoFisher Scientific, A11008	goat	1:500
Anti-Chicken IgY (H+L), Alexa Fluor 488	ThermoFisher Scientific, A11039	goat	1:500
Anti-mouse IgG1 cross-adsorbed, Alexa Fluor 568	ThermoFisher Scientific, A21124	goat	1:500
Anti-mouse IgG (H+L), Alexa Fluor 568	ThermoFisher Scientific, A11004	goat	1:500

2.16. Terminal deoxynucleotidyl transferase (TdT)-mediated dUTP nick end labelling (TUNEL) assay

Cell death was detected with DeadEndTM Fluorometric TUNEL system following the instructions provided by the manufacture (Promega). Briefly, after the incubation with the secondary antibody, cells were incubated with equilibration buffer (provided by the manufacture) at room temperature for 10 min and then coverslips were incubated with rTdT incubation buffer (equilibration buffer, nucleotide mix and rTdT enzyme) at 37 °C for 60 min, protected from light. The reaction was stopped by incubation with 20X SSC diluted 1:10, and the coverslips were washed 3 times with PBS to remove unincorporated fluorescein-12-dUTP. Cells were then incubated with DAPI (1:2000) at

room temperature for 10 min and washed 3 times with PBS. Coverslips were mounted with fluorescent mounting medium (Fluorescence Mounting Medium; Dako).

2.17. Preparation of protein extracts

Cells were washed with PBS and collected in ice-cold radioimmunoprecipitation assay (RIPA) buffer with 1 mM of dithiothreitol (DTT; Sigma-Aldrich) and complete mini protease inhibitor cocktail tablets (Roche Diagnostics). Cell lysates were then sonicated and centrifugated at 16100 g for 10 min at 4 °C. Pellets were discarded and the supernatants were immediately stored at -80 °C until used.

2.18. Bicinchoninic acid (BCA) assay

The protein quantification of cellular extracts was assessed with the BCA protein assay kit following the manufacturer instructions (Sigma-Aldrich). In a 96-well plate, samples were incubated with the provided BCA reagent for 30 min at 37 °C in the dark. The absorbance at 570 nm was read in a microplate reader (Gen5 software, Synergy HT; BioTek Instruments).

2.19. Western Blot

Protein extracts were denaturated with 6x Laemmli sample buffer (250 mM Tris-HCl, pH 6.8, 8 % sodium dodecyl sulfate, 40% glycerol, 20 % β-mercaptoethanol and 0.08 % bromophenol blue) and heated for 5 min at 95 °C. Gels were loaded with equal amounts of cellular extracts proteins, however, MVs and EXOs samples were totally loaded. Proteins were separated by 10 % sodium dodecyl sulfate-polyacrylamide gel electrophoresis (SDS-PAGE) and transferred to PVDF membranes (Millipore). Membranes were blocked with 5 % milk in Tris-buffered saline (TBS-T, 137 mM NaCl, 20 mM Tris-HCl, pH 7.6 containing 0.1 % Tween-20) for 1h at RT and then incubated overnight at 4 °C with primary antibodies (Table 3). After this incubation, membranes were washed with TBS-T and incubated with secondary antibodies (Table 3) for 1h at RT. Membranes were washed again with TBS-T and proteins were detected by enhanced chemiluminescence (ECL) (Clarity; Bio-Rad and WesternBright Sirius; Advansta) with LAS 550 equipment, or enhanced chemifluorescence (ECF) (GE Healthcare) with Thyphoon FLA 9000 equipment.

2.20. Image acquisition and cell quantification

Cells and retinal cryosections were observed with Plan-Apochromat ×20/0.8 objective in an inverted fluorescence microscope (Zeiss Axio Observer.Z1 microscope equipped with an AxioCam HRm and Zen Blue 2012 software, Carl Zeiss). Twelve images were taken of each coverslip to assess primary Müller cells survival and proliferation and

MIO-M1 cells. Total number of RGCs per coverslip was counted manually directly in the microscope, while analysis of primary Müller cells and MIO-M1 cells was measured with Fiji (ImageJ).

Cell death and the survival of RGCs in retinal cryosections were assessed by counting the number of TUNEL$^+$ cells and the number of cells immunoreactive to Brn3a (Brn3a$^+$), respectively. From each eye, two sections were used. The TUNEL$^+$ and Brn3a$^+$ cells were counted in the entire length of each section and the results were expressed as the number of cells per mm. For GFAP immunoreactivity two sections per eye were used and the entire sections were analysed. The presence of GFAP in Müller cells and astrocytes was classified, as follows: as "low" levels if present only in the GCL; "moderated" if detected from GCL until IPL; and "high" if all Müller cell body was observed. For the analysis of microglia cells number and reactivity in retinal cryosections, two sections from each eye were used and from each section 6 images were acquired. In each image, the number of Iba1$^+$ cells was normalized to the length of the section per image and the number of cells immunoreactive to both Iba1 and MHC-II (Iba1$^+$MHC-II$^+$) was counted and it was expressed in percentage of the total number of microglia (Iba1$^+$). All cell countings in retinal crysections and retinal length were measured with Fiji (ImageJ).

Table 3: List of primary and secondary antibodies used in Western Blot

	Supplier, Cat #	Host	Dilution
Primary Antibodies			
Anti-Flotillin-1	Santa Cruz, sc-74566	mouse	1:500
Anti-Glutamine synthetase	Abcam, ab49873	rabbit	1:1000
Anti-Calnexin	Sicgen, AB0041-500	goat	1:10000
Anti-EAAT1 (GLAST)	Abcam, ab416	rabbit	1:1000
Anti-TSG101	Abcam, ab83	mouse	1:200
Anti-CD63	Sicgen, AB0047-200	goat	1:5000
Secondary Antibodies			
Anti-Mouse IgG (H+L) HRP Conjugate	BioRad, 170-6516	goat	1:10000
Anti-Goat IgG (H+L) AP conjugate	ThermoFisher Scientific, 31300	rabbit	1:10000
Anti-Goat IgG (H+L) HRP Conjugate	ThermoFisher Scientific, 611620	rabbit	1:10000
Anti-Rabbit IgG (H+L) HRP Conjugate	BioRad, 170-6515	goat	1:10000
Anti-Rabbit IgG AP Conjugate	Sigma-Aldrich, A3687	goat	1:10000

AP - Alkaline phosphatase; HRP - Horseradish peroxidase

2.21. Statistical analysis

Statistical analysis was performed using the IBM SPSS Statistical software (v. 24.0). The data from the different experimental conditions were compared using an analysis of Mann-Whitney U test for comparing 2 independent medias and Kruskal-Wallis test followed by Dunn's multiple comparison test for comparing more than 2 independent medias. Differences, compared with control, were considered significant for Mann-Whitney U test at $p<0.05$ and for Kruskal-Wallis test at $p\leq0.05$. Data is presented as mean ± standard error of the mean (SEM) and the individual data plots are also shown.

Chapter 3

Results

3.1. Effect of EHP in adult primary RGCs and Müller cells survival

To mimic the elevated IOP, the main risk factor for glaucoma onset and progression, primary cultures of RGCs, the most affected cells in this disease, were subjected to EHP for 24h. RGCs were labelled with anti-βIII-Tubulin (Figure 4A) and the effect of EHP on the survival of RGCs was determined by counting the number of cells in culture. The number of RGCs in culture significantly decreased to 27.3±8.3 % ($p<0.05$) comparing with control cells (cultured in atmospheric pressure; 100.0±9.0 %) (Figure 4B).

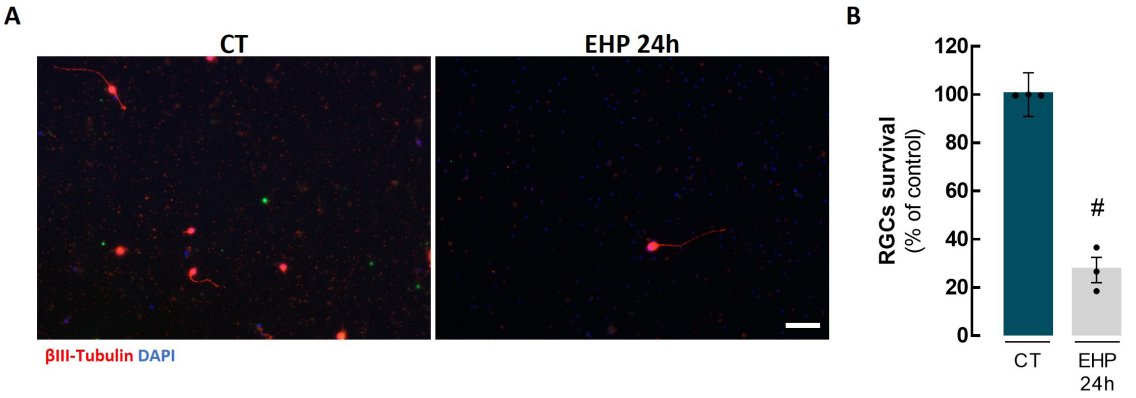

Figure 4: Effect of EHP in the survival of rat RGCs primary cultures. A. Primary cultures of RGCs were incubated in control pressure (CT) or EHP for 24h. Cells were labelled with βIII-Tubulin (red). Nuclei were stained with DAPI (blue). Representative images are depicted. **B.** The number of RGCs was counted and the results were expressed as percentage of control. Scale bar: 50 μm. #$p<0.05$, compared with CT, Mann-Whitney U test.

The effect of EHP on RGCs and Müller cells was also determined in co-cultures (Figure 5). When RGCs were cultured in the presence of Müller cells, the exposure to EHP for 24h did not cause significant alterations in the survival of RGCs (122.6±14.8 % of control), when comparing with control (100.0±17.0 %). Similar results were observed when co-cultures were challenged with EHP for 48h (94.1±12.7 % of control). However, when co-cultures were exposed to EHP for 72h there was a significant decrease in the survival of RGCs (41.7±5.7 % of control, $p\leq0.05$) (Figure 5B). The survival of Müller cells when co-cultured with RGCs was also determined (Figure 5C). The survival of Müller cells was 81.8±1.0 %, 104.7±33.3 % and 66.7±2.8 % of the control, for 24h, 48h and 72h, respectively (Figure 5C).

In addition, pure Müller cells cultures were prepared (Figure 6A) and the effect of EHP on the cell survival was assessed. The exposure of Müller cells to EHP for 24h decreased the survival of Müller cells to 63.9±1.8 % of the control. Furthermore, the survival of Müller cells was significantly compromised ($p\leq0.05$) when cells were exposed to EHP for 48h and 72h (23.4±0.4 % and 10.2%±0.8 % of the control, for 48h and 72h, respectively) (Figure 6B).

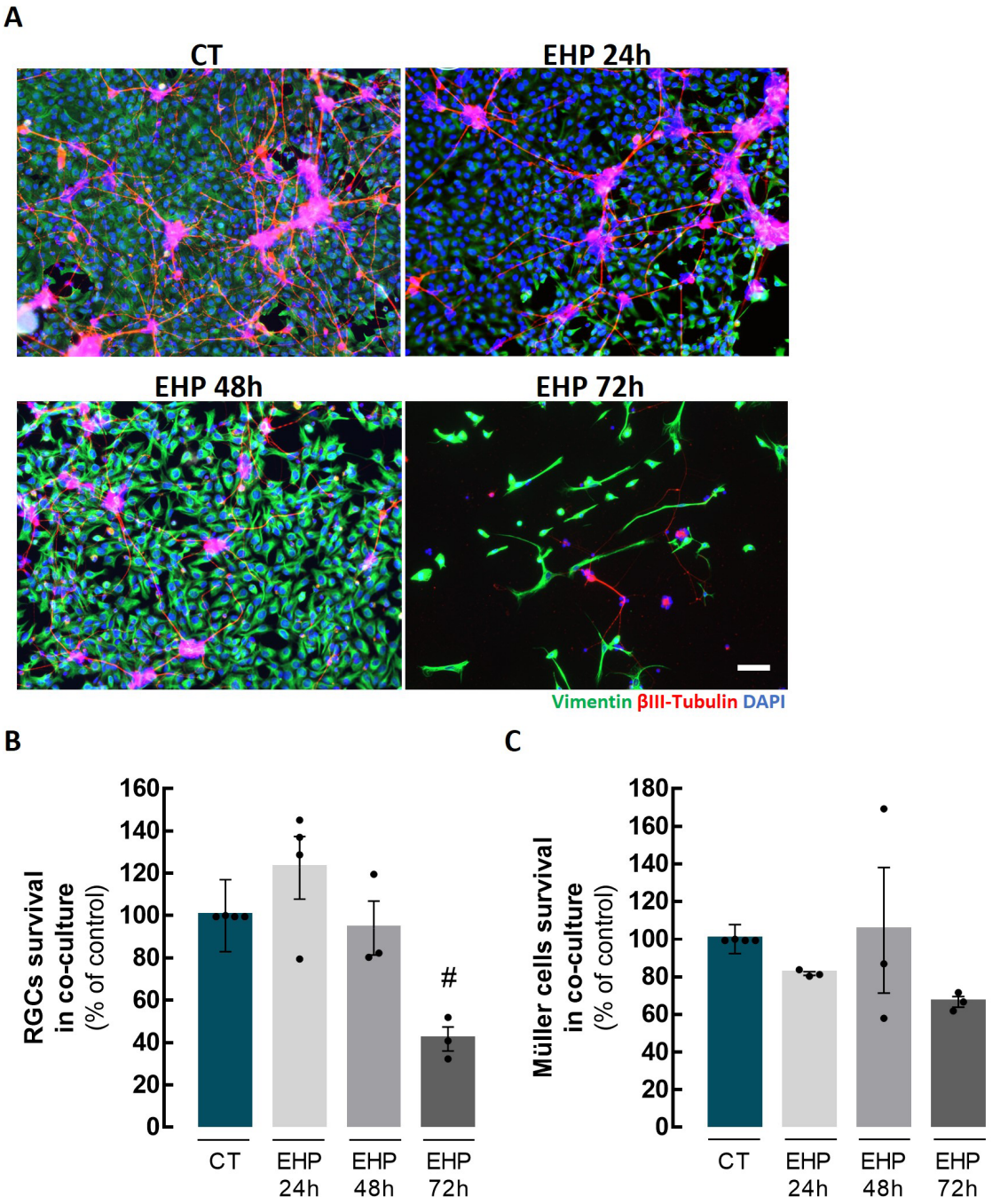

Figure 5: Effect of EHP in the survival of rat RGCs and Müller cells in co-cultures. A. Co-cultures of RGCs and Müller cells were incubated in control pressure (CT) or EHP for 24h, 48h or 72h. Cells were immunolabelled for βIII-Tubulin (red) and vimentin (green) to identify RGCs and Müller cells, respectively. Nuclei were stained with DAPI (blue). Representative images are depicted. **B.** The number of RGCs was counted and the results were expressed as percentage of control. **C.** The number of Müller cells was counted and the results were expressed as percentage of control. Scale bar: 50 μm. #p≤0.05, compared with CT, Kruskal-Wallis test followed by Dunn's multiple comparison test.

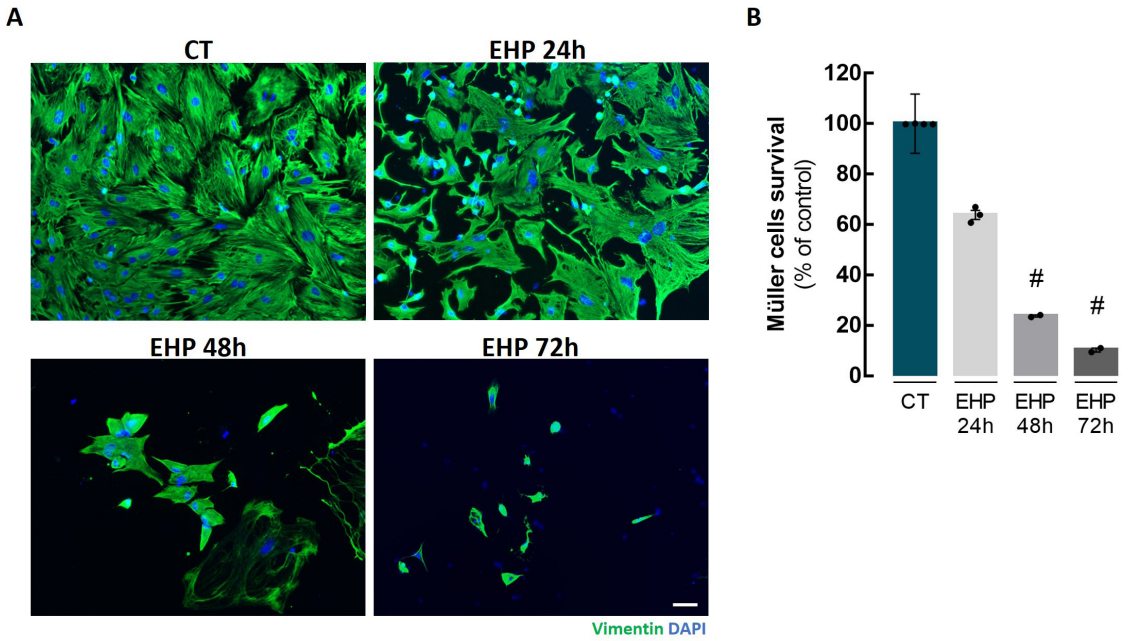

Figure 6: Effect of EHP in the survival of rat Müller cells. Primary cultures of Müller cells were incubated in control pressure (CT) or EHP for 24h, 48h or 72h. **A.** Cells were immunolabelled for vimentin (green). Nuclei were stained with DAPI (blue). Representative images are depicted. **B.** The number of Müller cells was counted and the results were expressed as percentage of control. Scale bar: 50 μm. #p≤0.05, compared with CT, Kruskal-Wallis test followed by Dunn's multiple comparison test.

These results suggested that EHP impacts differently RGCs and Müller cells and that it depends on the time-point. Therefore, to study the effect of CM and MVs from Müller cells, we chose 24h of EHP exposure for primary cultures of RGCs and 72h of EHP exposure for co-cultures of RGCs and Müller cells.

3.2. Effect of EHP in Müller cells proliferation and cell death

To assess the effect of EHP in the proliferation of Müller cells, we used primary Müller cells and MIO-M1 cells (human cell line) immunolabelled with an antibody against Ki67, a nuclear protein expressed in proliferating mammalian cells (Sun and Kaufman 2018).

As expected, more $Ki67^+$ cells were observed in the cell line than in primary cells, but the effect of EHP was similar in both cell types. The exposure of primary Müller cells to EHP for 48h did not significantly alter the number of $Ki67^+$ cells (3.9±1.2 % of total cells) when compared with control cells (5.8±3.8 % of total cells) (Figure 7). The exposure of MIO-M1 cells to EHP for 24h and 48h did not significantly change the number $Ki67^+$ cells (44.2±6.6 % and 44.6±5.3 % of total cells; for EHP 24h and 48h, respectively) comparing with control with 53.1±10.2 % of total cells (Figure 8).

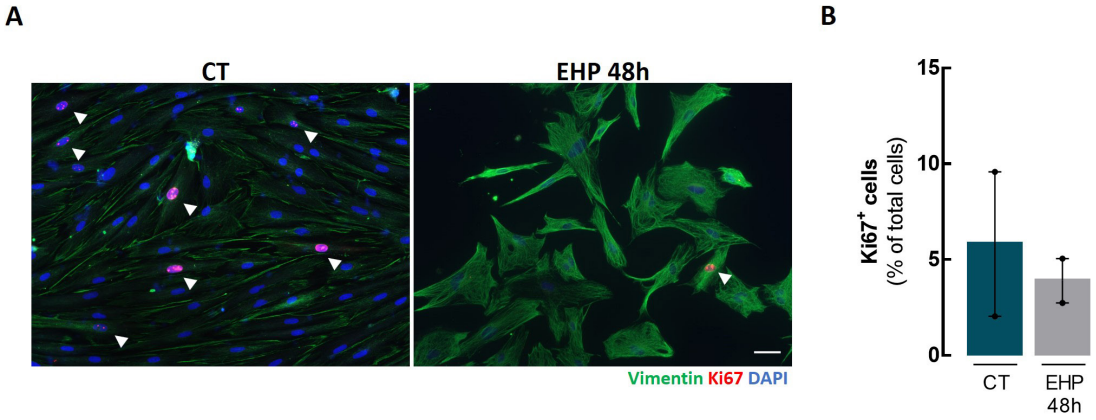

Figure 7: Effect of EHP in the proliferation of rat Müller cells. Müller cells were incubated in control pressure (CT) or EHP for 48h. **A.** Cell proliferation was evaluated after immunolabelling for Ki67 (red) and Müller cells were identified with anti-vimentin antibody (green). Nuclei were stained with DAPI (blue). Representative images are depicted. **B.** The number of proliferating Müller cells (Vimentin+ Ki67+ cells) was expressed in percentage of total cells (DAPI+ cells). Scale bar: 50 μm.

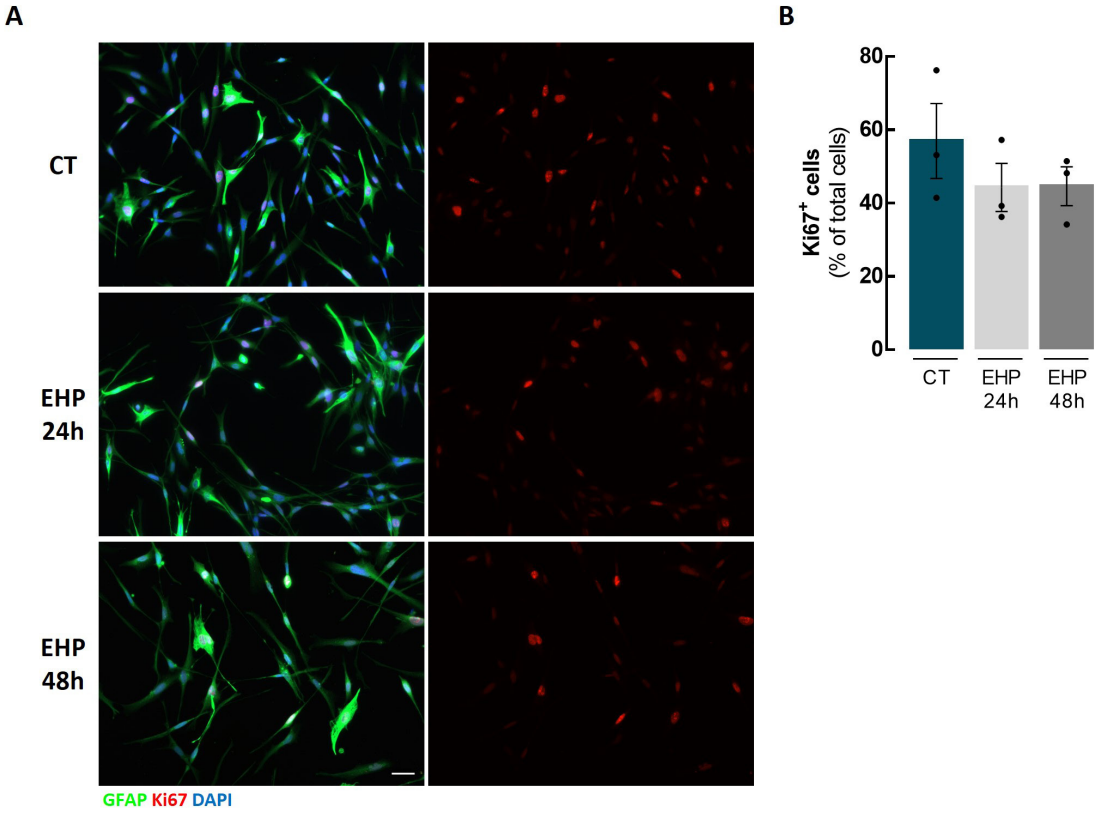

Figure 8: Effect of EHP in the proliferation of MIO-M1 cells. MIO-M1 cells were incubated in control pressure or EHP for 24h or 48h. **A.** Cells were immunolabelled for Ki67 (red) and GFAP (green). Nuclei were stained with DAPI (blue). Representative images are depicted. **B.** The number of proliferative cells (GFAP+ Ki67+ cells) was expressed by the percentage of total cells (DAPI+ cells). Scale bar: 50 μm.

The effect of EHP on death of MIO-M1 cells was determined by the TUNEL assay (Figure 9A). The exposure of MIO-M1 cells to EHP for 24h or 48h did not significantly altered cell death (1.2±0.3 % and 2.2±0.3 % of total cells, for EHP 24h or 48h, respectively), when compared with control (0.8±0.3 % of total cells) (Figure 9B). The total number of cells in culture, as an additional measurement of cell viability or death, was not altered by the exposure to EHP (Figure 9C).

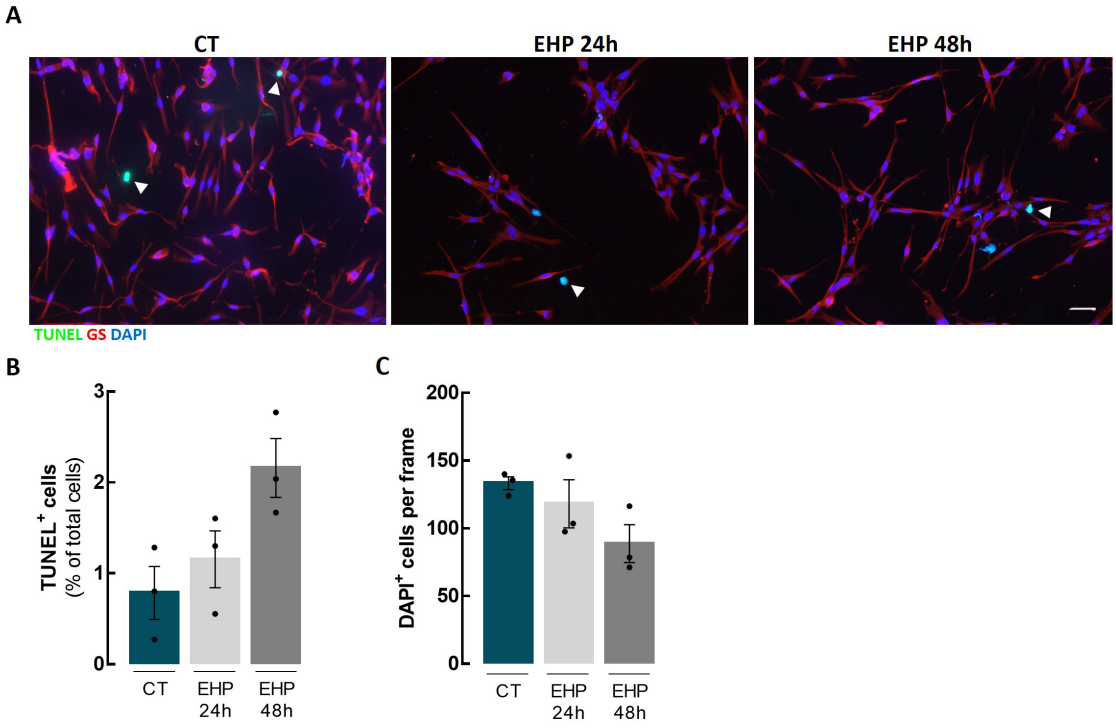

Figure 9: Effect of EHP in the death of MIO-M1 cells. MIO-M1 cells were incubated under control pressure or EHP for 24h or 48h. **A.** Cell death was evaluated by TUNEL assay (green). MIO-M1 cells were stained with anti-GS antibody (red). Nuclei were stained with DAPI (blue). Representative images are depicted. Arrowheads indicate some TUNEL$^+$ cells. **B.** The number of TUNEL$^+$ cells was counted and was expressed in percentage of total cells (DAPI$^+$ cells). C. The total number of cells per image was counted. Scale bar: 50 μm.

3.3. Effect of conditioned medium from Müller cells in RGC survival

To assess the potential protective properties of the secretome of Müller cells in the survival of RGCs, we exposed RGCs to EHP for 24h (the time-point we identified as sufficient to impact RGC survival, see Figure 4) in the presence or absence of CM from primary Müller cells (CM Müller) or from MIO-M1 cells (CM MIO-M1) (Figure 10A). RGCs cultures were immunolabelled with an antibody against vimentin (a marker of Müller cells) to assess the purity of the culture. No cells were immunolabelled for vimentin, indicating the absence of Müller cells. In RGCs cultured in normal pressure, both CM Müller and CM MIO-M1 increased the survival of RGCs to 142.7±15.4 % and 129.0±6.3 % of control, respectively. The exposure of RGCs to EHP, similar to

Figure 4, substantially decreased the survival of RGCs to 27.3±5.2 % of control. This effect was attenuated when RGC were incubated with CM Müller and CM MIO-M1 to 104.4±5.2 % and 109.8±31.2 % of control, respectively (Figure 10B).

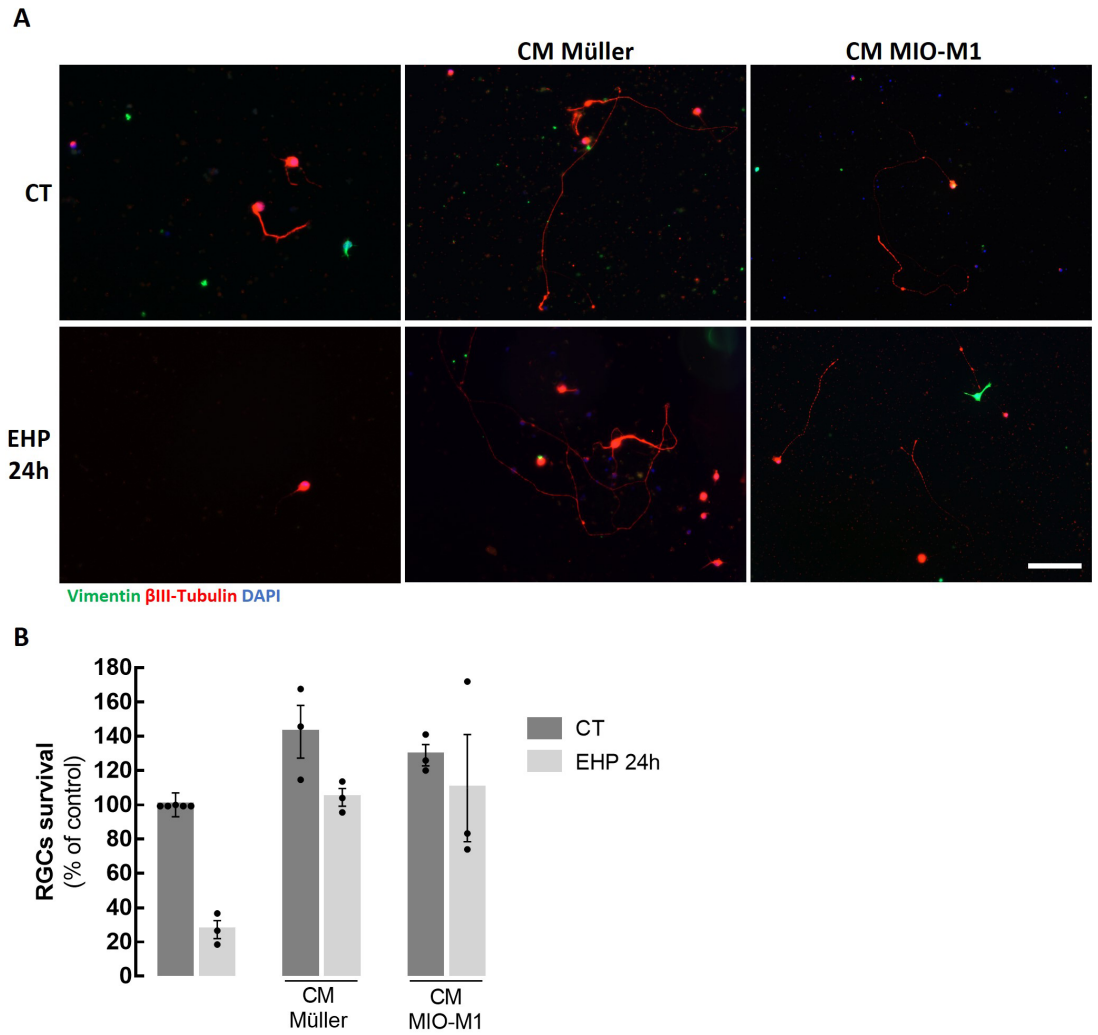

Figure 10: Effect of CM from primary Müller cells and MIO-M1 cells in the survival of RGCs. Primary cultures of RGCs were cultured at control pressure or EHP for 24h in the presence or absence of CM from Müller or from MIO-M1 cells. **A.** RGCs were immunolabelled for βIII-Tubulin (red) and an antibody against vimentin (green) was used to assess the purity of the culture. Nuclei were stained with DAPI (blue) **B.** The number of RGCs was counted and expressed in percentage of control. Scale bar: 50 μm. #p≤0.05, compared with CT, Kruskal-Wallis test followed by Dunn's multiple comparison test.

The effect of CM Müller and CM MIO-M1 in the survival of RGCs and Müller cells was also addressed in co-cultures (Figure 11A). When co-cultures were grown in control pressure both CM Müller and CM MIO-M1 did not significantly change the number of RGCs in culture (101.7±10.4 % and 90.5±8.3 % of control, respectively; Figure 11B) nor the number of Müller cells (79.2±17.1 % and 81.0±19.4 % of control; Figure 11C), comparing with the respective controls. The number of RGCs in co-cultures exposed to

EHP for 72h, significantly decreased to 48.2±4.8 % of control (p≤0.05), as demonstrated previously in Figure 5. The incubation with CM Müller and CM MIO-M1 did not modify the survival of RGC (66.3±8.1 % and 58.1±5.2 % of control, for CM Müller and CM MIO-M1 respectively; Figure 11B). The exposure of EHP for 72h decreased Müller cells survival in co-cultures (50.9±6.3 % of control). When co-cultures were incubated with CM Müller, the survival of Müller cells was 69.1±3.6 % of the control. Incubation with CM MIO-M1 did not significantly modify the effect of EHP (55.0±4.2 % of the control).

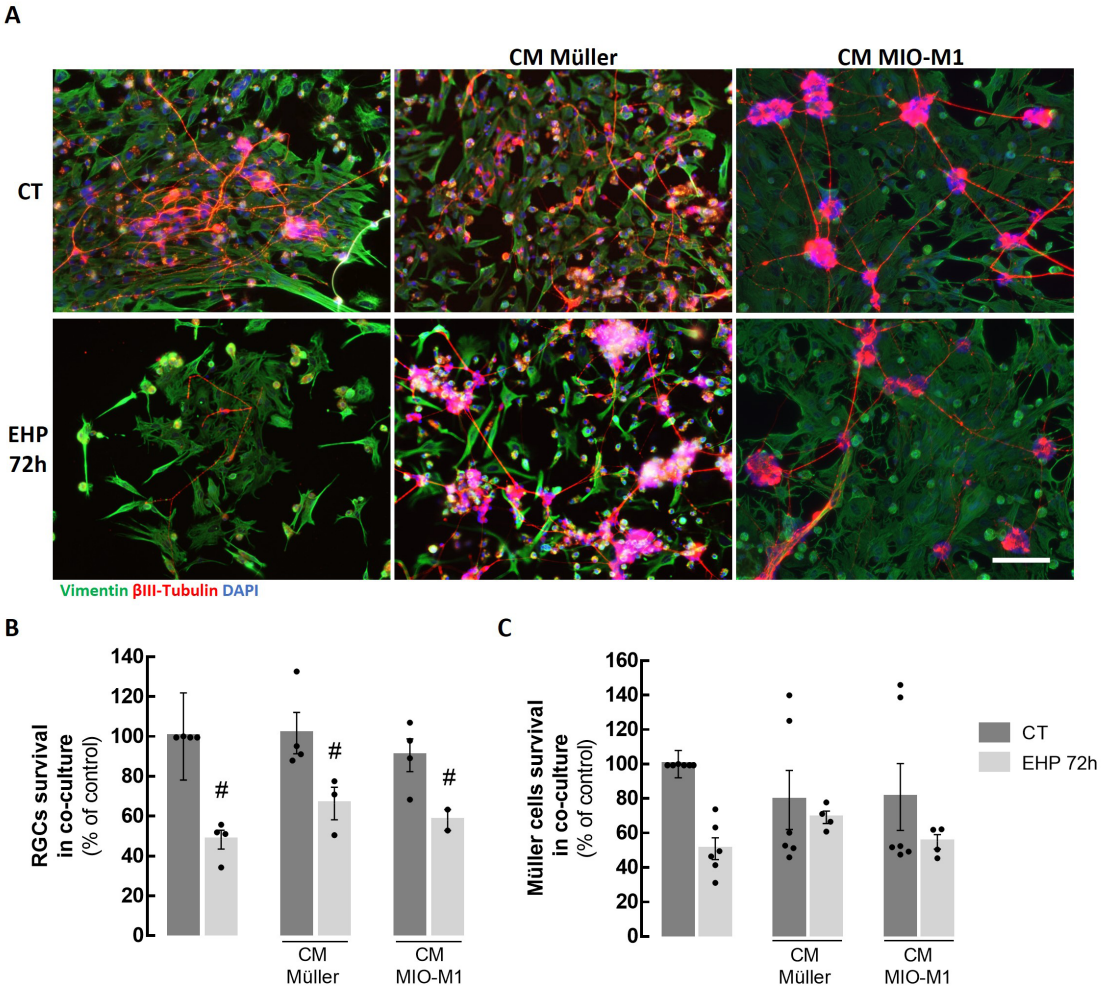

Figure 11: Effect of CM from Müller cells and MIO-M1 cells in the survival of RGCs in co-cultures of RGCs and Müller cells. Co-cultures of RGCs and Müller cells were incubated in control pressure or EHP for 72h in the presence or absence of CM from Müller cells or MIO-M1 cells. **A.** RGCs were immunolabelled for βIII-Tubulin (red) and Müller cells for vimentin (green). Nuclei were stained with DAPI (blue) **B.** The number of RGCs was counted and expressed in percentage of control. **C.** The number of Müller cells was counted and expressed in percentage of control. Scale bar: 50 μm. #p≤0.05, compared with CT, Kruskal-Wallis test followed by Dunn's multiple comparison test.

3.4. Characterization of extracellular vesicles

In order to study whether the extracellular vesicles released by Müller cells contribute to the protective effect observed with the CM, the supernatant of Müller cells (MIO-M1 and primary cells) was collected and EVs were isolated by sequential ultracentrifugation: MVs and EXOs.

MVs and EXOs were characterized by size, number, shape and protein markers (Figure 12). The EXOs from MIO-M1 cells presented a size of 136.9±2.4 nm, and the concentration was 2.5x109±1.1x10^{9} particles/mL (n=3) (Figure 12A). The MVs from MIO-M1 cells (MVs MIO-M1) had an average size of 195.6±8.7 nm and the concentration was 4.0x108±4.1x10^{7} particles/mL (n=4) (Figure 12B).

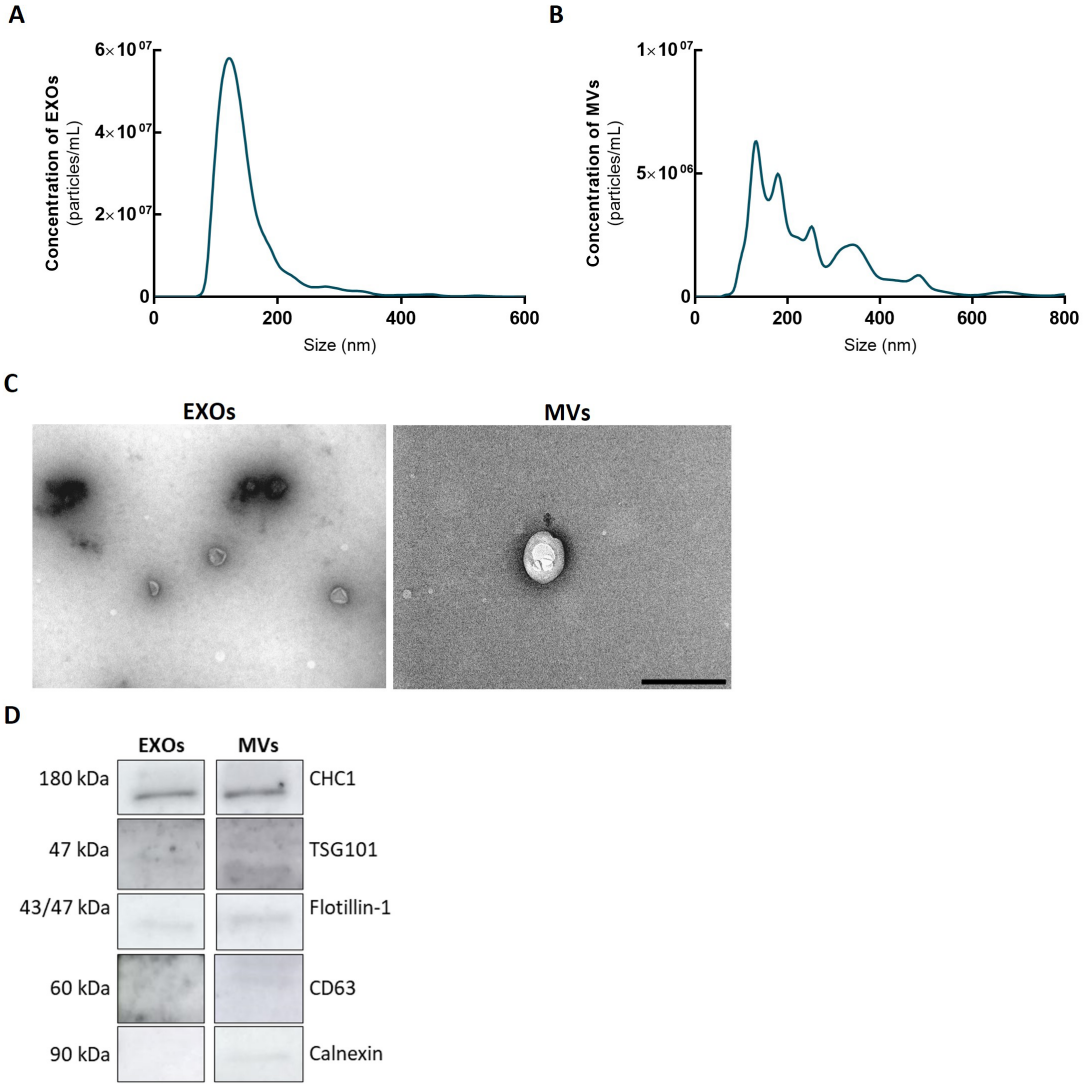

Figure 12: Characterization of extracellular vesicles released by MIO-M1 cells. Extracellular vesicles were isolated from the supernatant of MIO-M1 cells cultured in normal pressure for 48h. The size and concentration of particles were analyzed by NTA **(A-B)** and TEM **(C)**. Graphs represented were averaged from 2-3 independent experiments and images are representative of 2 independent experiments. D. The presence of CHC1, TSG101, Flotillin-1, CD63 and calnexin was analyzed by Western Blot. Scale bar: 500 nm.

The size of both EXO and MVs, as determined by TEM, was similar to the results from NTA and the morphology was consistent with EVs (Figure 12C).

Several proteins have been used as markers for the characterization of MVs or EXOs, although some of these proteins are not exclusive of one type of EVs (Thery et al. 2018). By Western Blot (Figure 12D), clathrin heavy chain (CHC1), tumor susceptibility 101 (TSG101), flotillin-1 and CD63 were detected in both MVs and EXOs. Calnexin was present only in MVs.

The MVs from primary Müller cells (MVs Müller) were also characterized by NTA, TEM and Western Blot. MVs had an average size of 224.7±22.0 nm, and the average concentration was $2.1x10^{8}$±$4.2x10^{7}$ particles/mL (Figure 13A). Size and shape of MVs observed by TEM were similar to MVs from MIO-M1 cells (Figure 13B). MVs from primary Müller cells presented TSG101, glutamate-aspartate receptor (GLAST) and calnexin (Figure 13C).

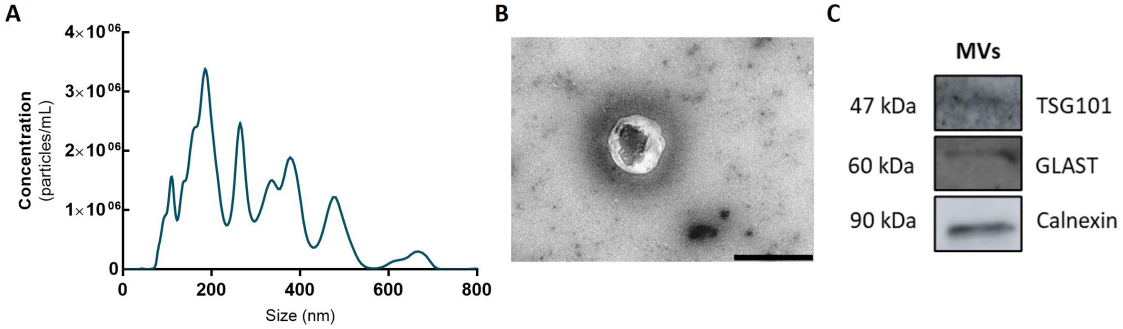

Figure 13: Characterization of MVs released by Müller cells. MVs were isolated from the supernatant of primary Müller cells cultured in normal pressure for 48h. The size and concentration of particles were analyzed by NTA **(A)** and TEM **(B)**. Graph represented was averaged from 2 independent experiments and images are representative of 2 independent experiments. **C.** The presence of TSG101, GLAST and calnexin was analyzed by Western Blot. Scale bar: 500 nm.

3.5. Effect of MVs derived from Müller cells and MIO-M1 cells in the survival of RGCs

RGCs were cultured in normal pressure or exposed to EHP for 24h. In control pressure, incubation with MVs Müller or MVs MIO-M1 did not significantly change RGC survival (103.6±6.1 % and 85.9±11.2 % of control, for MVs Müller and MVs MIO-M1, respectively), when comparing with control (Figure 14). However, MVs Müller and MVs MIO-M1 had a trend to increase the survival of RCGs when the cells were challenged with EHP for 24h (81.4±6.0 % and 61.3±17.6 % of control, for MVs Müller and MVs MIO-M1, respectively), when comparing with RGCs exposed to EHP (19.4±2.2 % of control) (Figure 14B). These results suggest that MVs derived from Müller cells or MIO-M1 cells promote the survival of RGCs.

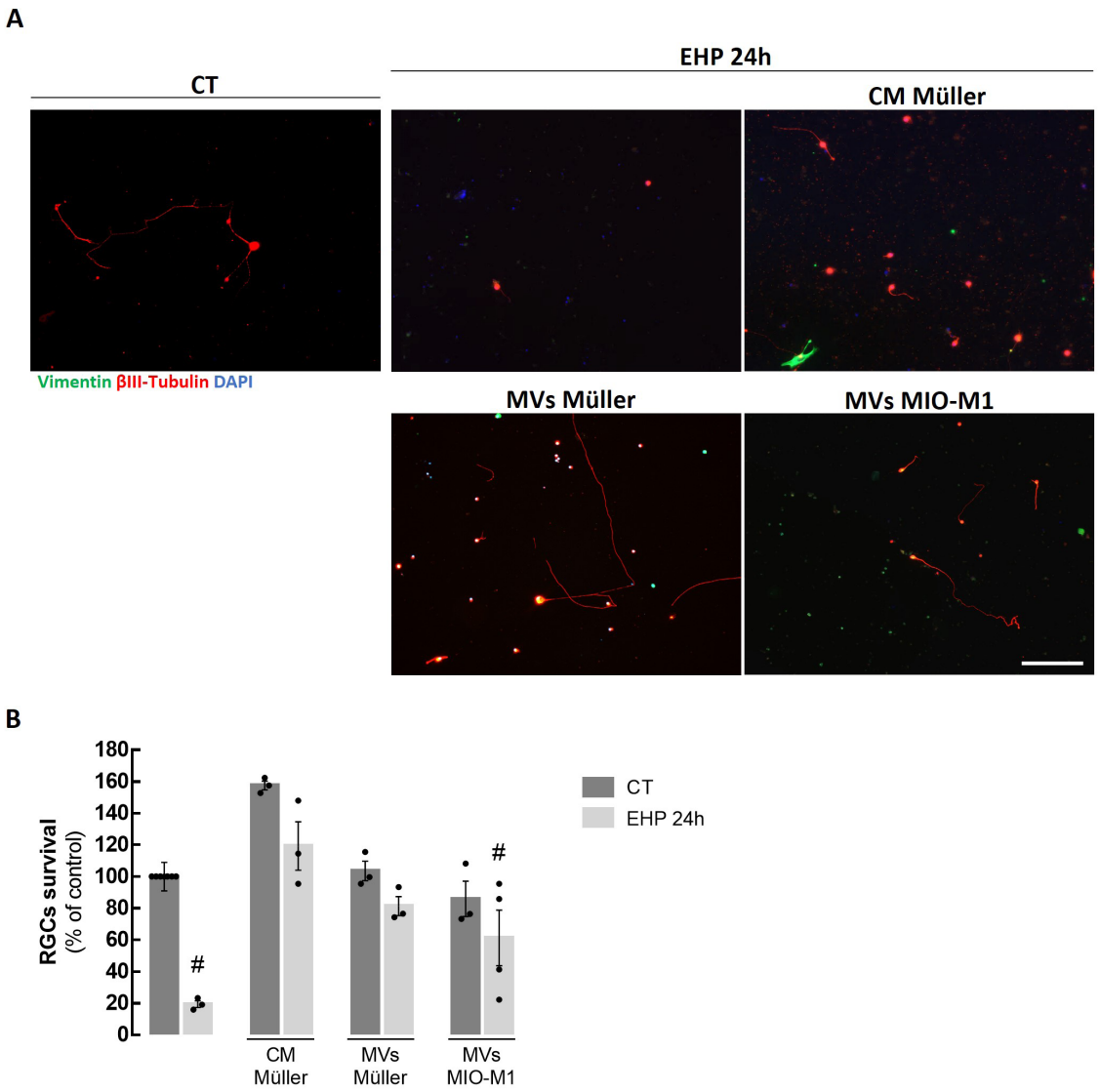

Figure 14: Effect of MVs released by Müller cells or MIO-M1 cells to the survival of RGCs. Primary cultures of RGCs were incubated in control pressure or EHP for 24h in the presence or absence of MVs isolated from Müller cells or MIO-M1 cells. A. RGCs were immunolabelled for βIII-Tubulin (red) and an antibody against vimentin (green) was used to determine the purity of the culture. Nuclei were stained with DAPI (blue). Representative images are depicted. B. The number of RGCs was counted and the results were expressed as percentage of control. Scale bar: 50 μm. #p≤0.05, compared with CT, Kruskal-Wallis test followed by Dunn's multiple comparison test.

3.6. Effect of MVs MIO-M1 in the proliferation of MIO-M1 cells exposed to EHP

MIO-M1 cells cultured in control pressure or exposed to EHP for 24h and 48h were incubated with MVs MIO-M1, and cell proliferation was determined by counting the number of Ki67$^+$ cells (Figure 15). The proliferation of MIO-M1 cells was not significantly altered in the presence of MVs MIO-M1 either in control pressure (CT: 49.9±0.5 %; CT+MVs: 63.4±7.8 % of Ki67$^+$ cells), either in EHP 24h (EHP 24h: 53.9±4.9 %; EHP

24h+MVs: 54.2±6.2 % of Ki67$^+$ cells) and under 48h of EHP (EHP 48h: 41.3±2.4; EHP 48h+MVs: 36.6±3.2 % of Ki67$^+$ cells) as compared with the control (Figure 15B).

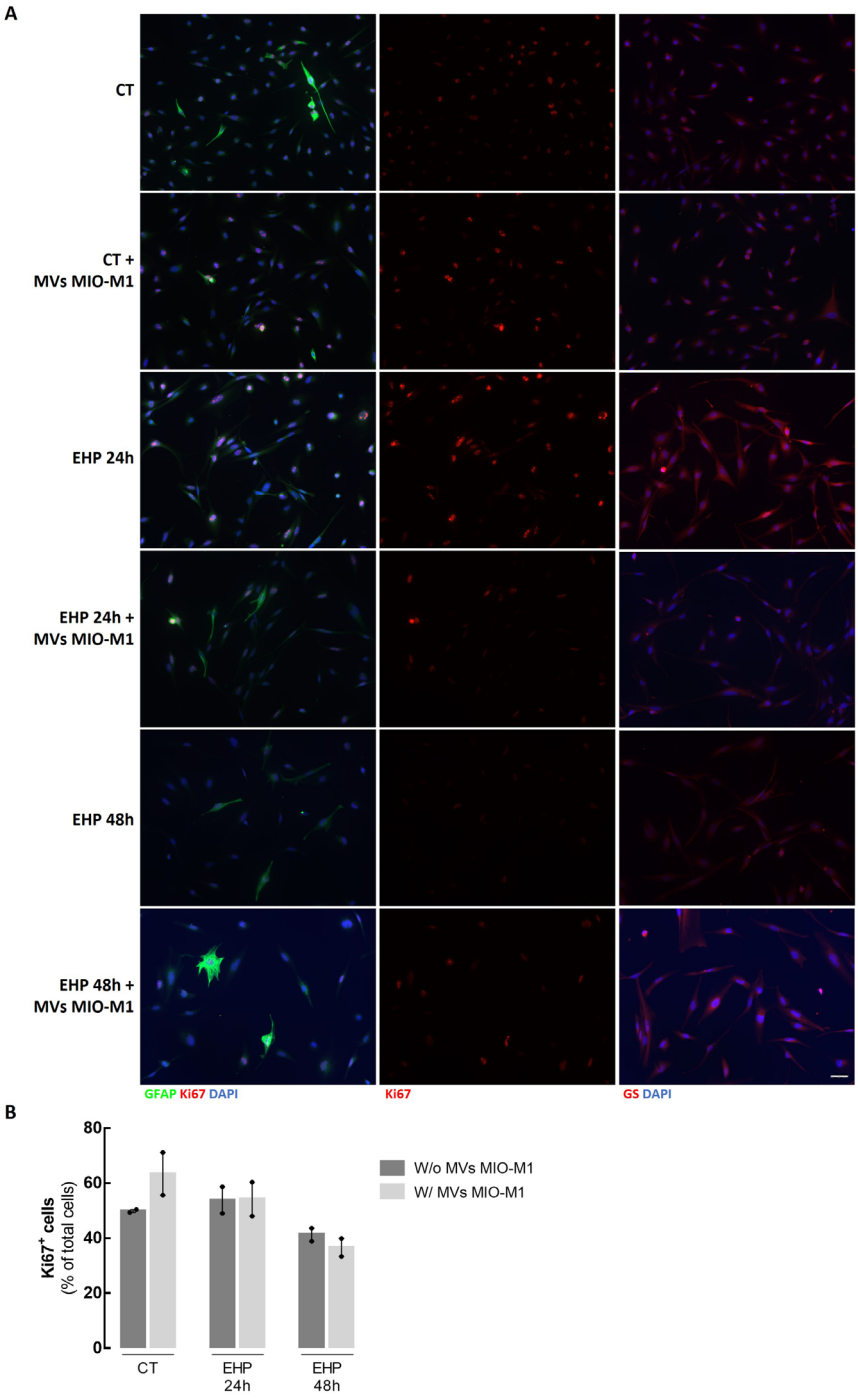

Figure 15: Effect of MVs released by MIO-M1 cells to the proliferation of MIO-M1 cells. MIO-M1 cells were cultured in control pressure or challenged with EHP for 24h or 48h in the presence or absence of MVs isolated from MIO-M1 cells. **A.** MIO-M1 cells were immunolabelled for GFAP (green) and GS (red). Proliferative MIO-M1 cells were immunolabelled for Ki67 (red). Nuclei were stained with DAPI (blue). Representative images are depicted. **B.** The number of proliferative cells (Ki67$^+$ cells) was counted and the results were expressed as the percentage of total cells (DAPI$^+$ cells). Scale bar: 50 μm.

3.7. Effect of intravitreal injection of PBS prior to ischemia-reperfusion injury

The retinal I-R injury animal model has been widely used to study the mechanisms of RGC death and to identify potential therapeutic targets in the field of RGC neuroprotection (Madeira et al. 2016; Boia et al. 2017).

The analysis of the retinal scans obtained by optical coherence tomography (OCT) of eyes that were subjected to I-R (7 days after I-R), showed a decrease in total retinal thickness, especially due to the thinning of the inner layers (NFL, GCL and IPL), as expected (Sho et al. 2005) (Figure 16, above). In order to establish the technique for future experiments assessing the effects of the intravitreal injection of MVs from MIO-M1 cells, in a third group of animals, PBS (the vehicle of MVs) was injected in the vitreous 1h before I-R. We observed that the intravitreal injection of PBS together with I-R caused significant alterations in the retina, with loss of retinal layers (Figure 16). We repeated this experiment with a commercially available PBS and the result was very similar. The contralateral eyes of the I-R eyes injected with PBS did not present changes in retinal structure. Therefore, we proceeded the project, evaluating only the effect of intravitreal injection of MVs MIO-M1 in retinas contralateral to ischemic retinas.

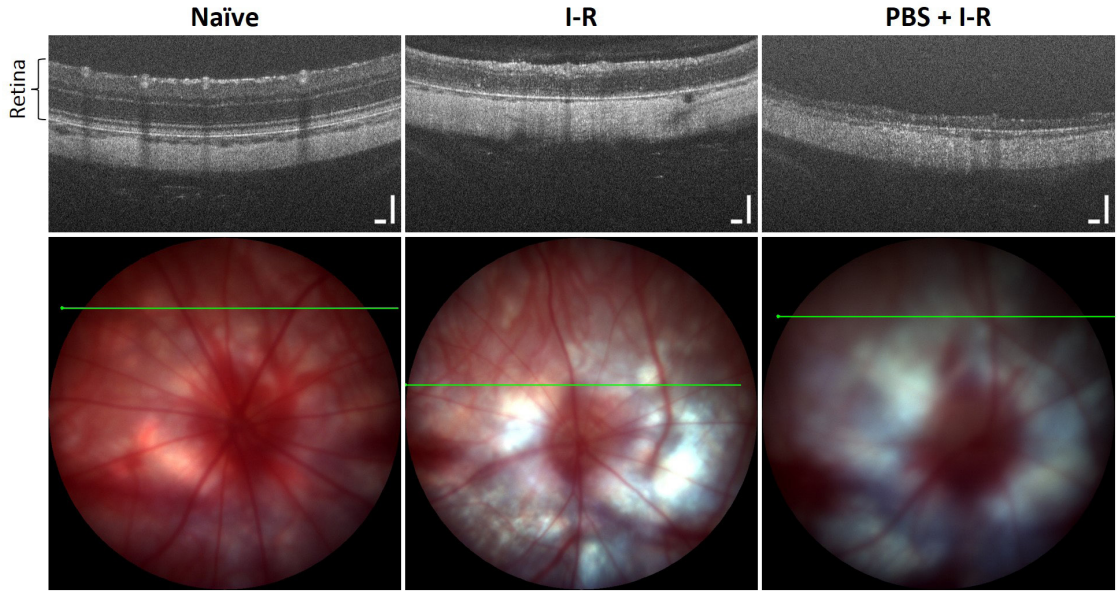

Figure 16: Effect of intravitreal injection of PBS in the retina after ischemia-reperfusion injury in the retina of Wistar Han rats. Three conditions were analysed: naïve (non-treated animals), I-R retinas and PBS (intravitreal injection of PBS followed by I-R). Representative images of the B-scan from OCT (above) and corresponding eye fundus (below). Scale bars: 50 μm.

3.8. Effect of intravitreal injection of MVs in Wistar Han animals

Seven days after the intravitreal injection of MVs MIO-M1 or PBS the retinal function and structure were analysed by ERG and OCT, respectively. ERG revealed that the intravitreal injection of MVs or PBS did not affect the function of RGCs (Figure 17 A-C), bipolar cells (Figure 17 D, F-H) or photoreceptors - cones (Figure 17 I-L) and rods (Figure 17 D, E) - comparing with naïve (Table 4).

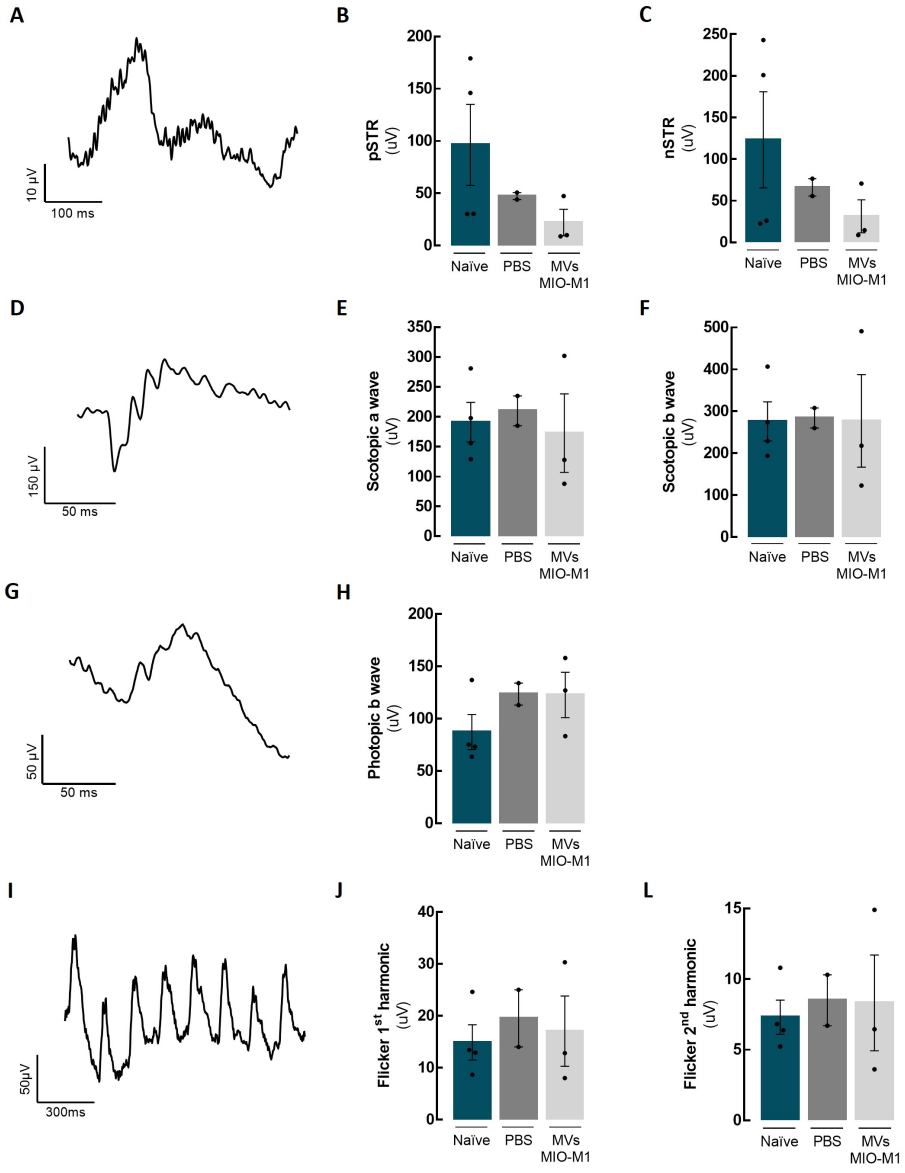

Figure 17: Effect of intravitreal injection of MVs isolated from MIO-M1 cells in the visual function. PBS or MVs (5 μL) were injected in the vitreous of Wistar Han rats and ERG was performed 7 days after the injection. **A**, **D**, **G** and **I**. Representative ERGs of a naïve animal for each test. **B-C**. pSTR and nSTR amplitudes from STR test. **E-F**. a-wave and b-wave amplitudes from scotopic test. **H.** b-wave amplitude from photopic test. **J**, **L**. 1st and 2nd harmonic amplitudes from flicker test.

Table 4: Effect of intravitreal injection of PBS and MVs MIO-M1 in retinal function evaluated by ERG

		Amplitude (μV)		
Test	Component	Naïve	PBS	MVs
STR	**pSTR**	96.4±38.8	47.7±3.4	22.1±12.7
	nSTR	123.2±57.7	66.1±10.4	31.4±19.8
Scotopic	**a-wave**	191.0±33.2	210.0±25.0	176.6±65.7
	b-wave	276.0±46.6	284.0±24.0	277.3±110.3
Photopic	**b-wave**	87.4±16.7	123.5±10.5	122.8±21.6
Flicker	**1st harmonic**	14.9±3.4	19.5±5.5	17.0±6.8
	2nd harmonic	7.3±2.1	8.5±1.8	8.3±3.4

The images obtained by OCT were segmented into retinal layers and their thickness were determined (Figure 18). The analysis revealed that the intravitreal injection of PBS and MVs MIO-M1 did not change retinal layer thickness comparing with naïve retinas (Figure 18B) (Table 5). We could also find some bright spots in the vitreous of animals that received an intravitreal injection of PBS and MVs MIO-M1 (Figure 18A), that may indicate the presence of cell infiltrates.

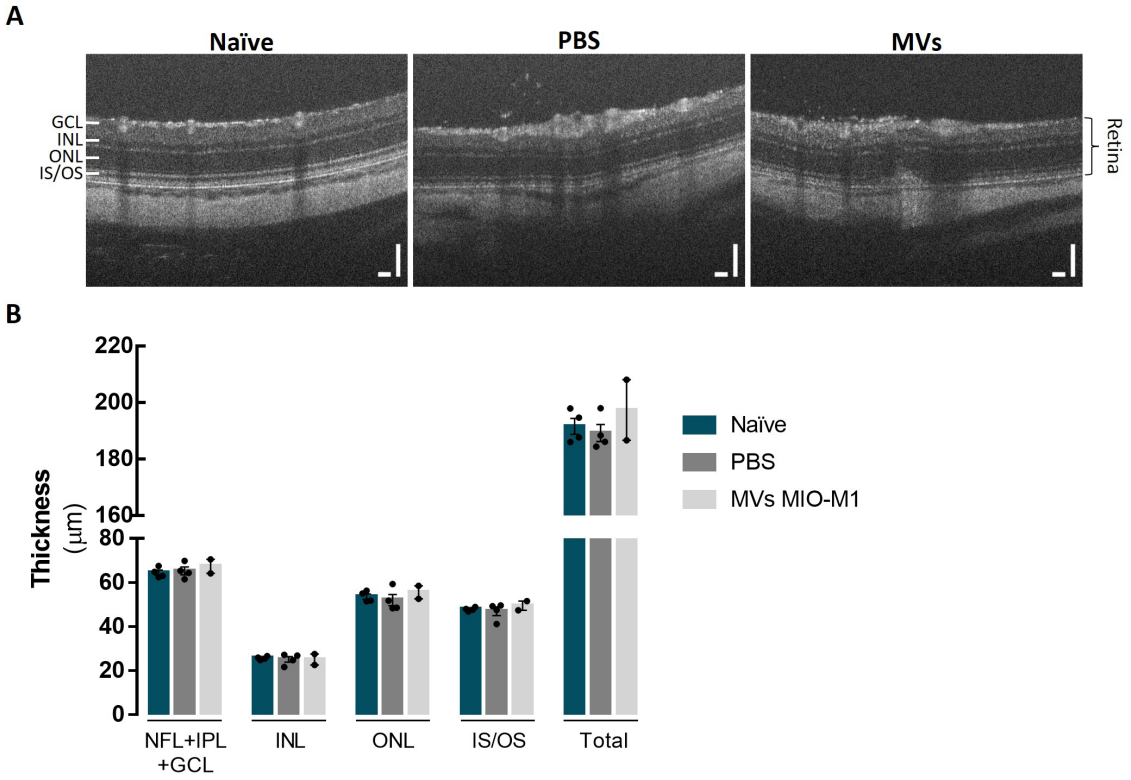

Figure 18: Effect of intravitreal injection of MVs isolated in retinal thickness. PBS or MVs (5 μL) were injected in the vitreous of Wistar rats and 7 days after the injection retinal structure and thickness were evaluated by OCT. **A.** Representative images of OCT images depicting the different retinal layers and the limits considered to measure total retinal thickness of the retinal layers. **B.** Retinal thickness was determined after layer segmentation. Values were obtained from 2 to 3 independent experiments. Scale bars: 50 μm.

Table 5: Effect of intravitreal injection of PBS and MVs MIO-M1 in retinal thickness evaluated by OCT

		Thickness (μm)		
		Naïve	PBS	MVs
Retinal layers	NFL+IPL+GCL	64.4±1.2	65.2±1.7	67.3±3.2
	INL	25.7±0.38	25.1±1.3	25.0±2.5
	ONL	53.62±1.2	52.0±2.6	55.5±3.0
	IS/OS	47.8±0.4	46.9±2.0	49.5±2.1
Total		191.5±2.8	189.2±3.0	197.3±10.7

Animals were sacrificed 7 days after the intravitreal injection and vertical sections were prepared. We started by evaluating if the number of microglial cells (Iba1$^+$ cells) was affected by the MVs MIO-M1 and also if there is a change in microglia reactivity (MHC-II$^+$ Iba1$^+$ cells), since MHC-II is the major histocompatibility complex II mostly expressed by antigen-presenting cells as microglia (Ito et al. 1998; Jurga, Paleczna, and Kuter 2020) (Figure 19).

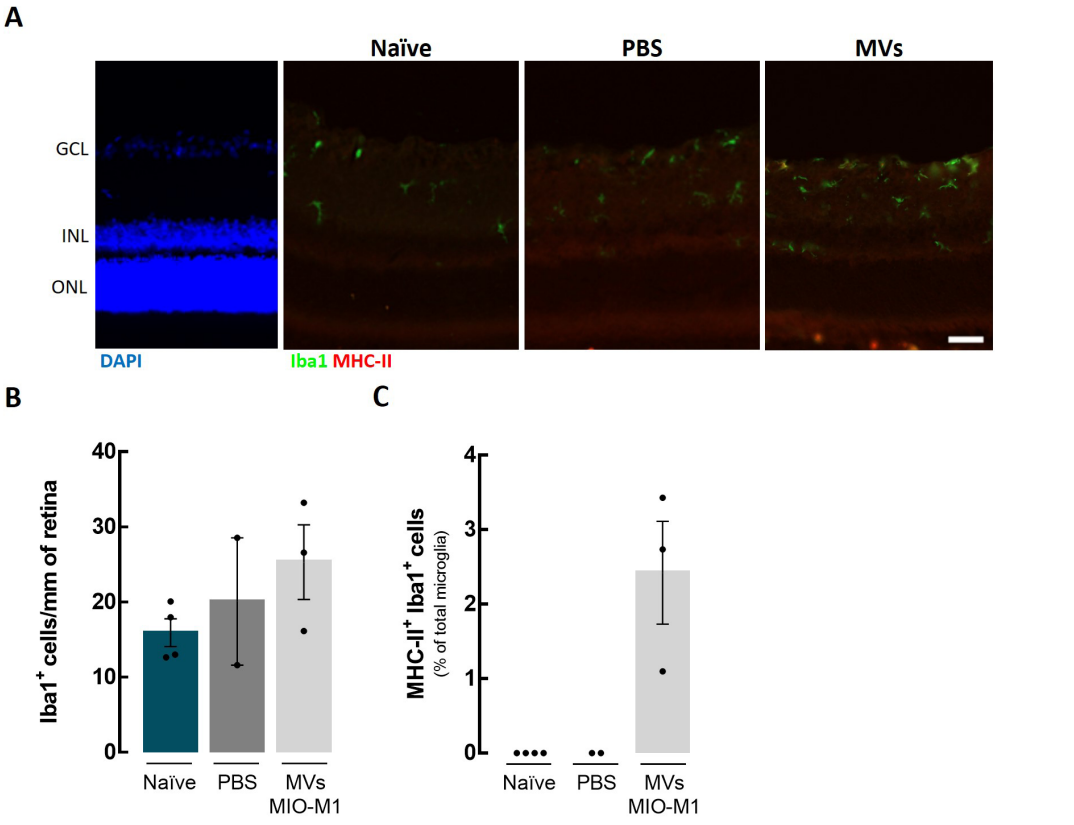

Figure 19: Effect of MVs from MIO-M1 cells in the number and reactivity of retinal microglia. MVs derived from MIO-M1 cells were injected in the vitreous of Wistar rats and the animals were sacrificed 7 days after. **A.** Retinal cryosections were immunostainned for Iba1 (green) and MHC-II (red). Nuclei were stained with DAPI (blue). **B.** The number of microglial cells (Iba1$^+$ cells) was expressed per mm of retinal section. **C.** The number of reactive microglial cells (MHC-II$^+$ Iba1$^+$ cells) was counted, and the results were presented as percentage of total microglia (Iba1$^+$ cells). Scale bar: 50 μm.

There were no differences in the number of Iba1$^+$ cells in retinas that received the intravitreal injection of PBS (20.1±8.5 Iba1$^+$ cells/mm retina) and MVs MIO-M1 (25.3±5.0 Iba1$^+$ cells/mm retina) comparing with naïve retinas (15.9±1.8 Iba1$^+$ cells/mm retina). Reactive microglia cells were only observed in retinas that received the MVs MIO-M1 (2.4±0.7 MHC-II$^+$Iba1$^+$ cells/mm retina) (Figure 19B, C). The presence of GFAP in Müller cells and astrocytes was classified, as follows: as "low" levels if present only in the GCL; "moderated" if detected from GCL until IPL; and "high" if all Müller cell body was observed. Naïve animals had lower GFAP expression, while intravitreal injection with PBS and MVs MIO-M1 increased GFAP immunoreactivity (Figure 20B).

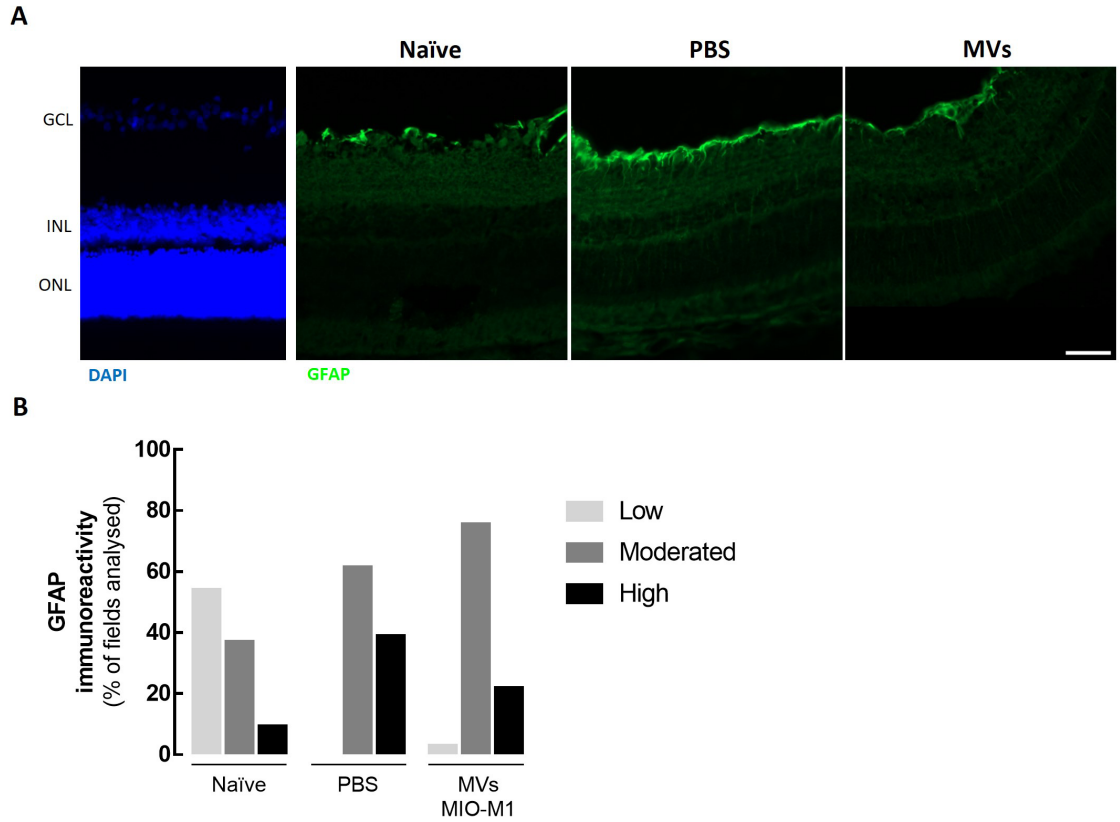

Figure 20: Effect of MVs from MIO-M1 cells in GFAP immunoreactivity. MVs derived from MIO-M1 cells were injected in the vitreous of Wistar rats and the animals were sacrificed 7 days after injection. **A.** Retinal cryosections were immunolabeled for GFAP (green). The nuclei were labelled with DAPI (blue). **B.** Images were classified as low, moderated and high reactivity (as detailed in Materials and Methods) and were represented as the percentage of each category in each condition. Values were obtained from 2 to 3 independent experiments.

Retinal cell death was evaluated by TUNEL assay (Figure 21). The injection of PBS or MVs MIO-M1 did not significantly change the number of TUNEL$^+$ cells (1.0±0.6 TUNEL$^+$ cells/mm and 0.8±0.2 TUNEL$^+$ cells/mm, for PBS and MVs MIO-M1, respectively) when compared with naïve retinas (1.0±0.4 TUNEL$^+$ cells/mm) (Figure 21B). The number of RGCs was assessed by immunolabeling with Brn3a, a selective RGC marker (Nadal-Nicolas et al. 2009). RGCs were not affected by PBS (38.8±2.5

Brn3a⁺ cells/mm of retina) or MVs MIO-M1 (32.3±2.1 Brn3a⁺ cells/mm of retina) injections since the number of cells did not differ from naïve (39.5±2.8 Brn3a⁺ cells/mm of retina) (Figure 22B).

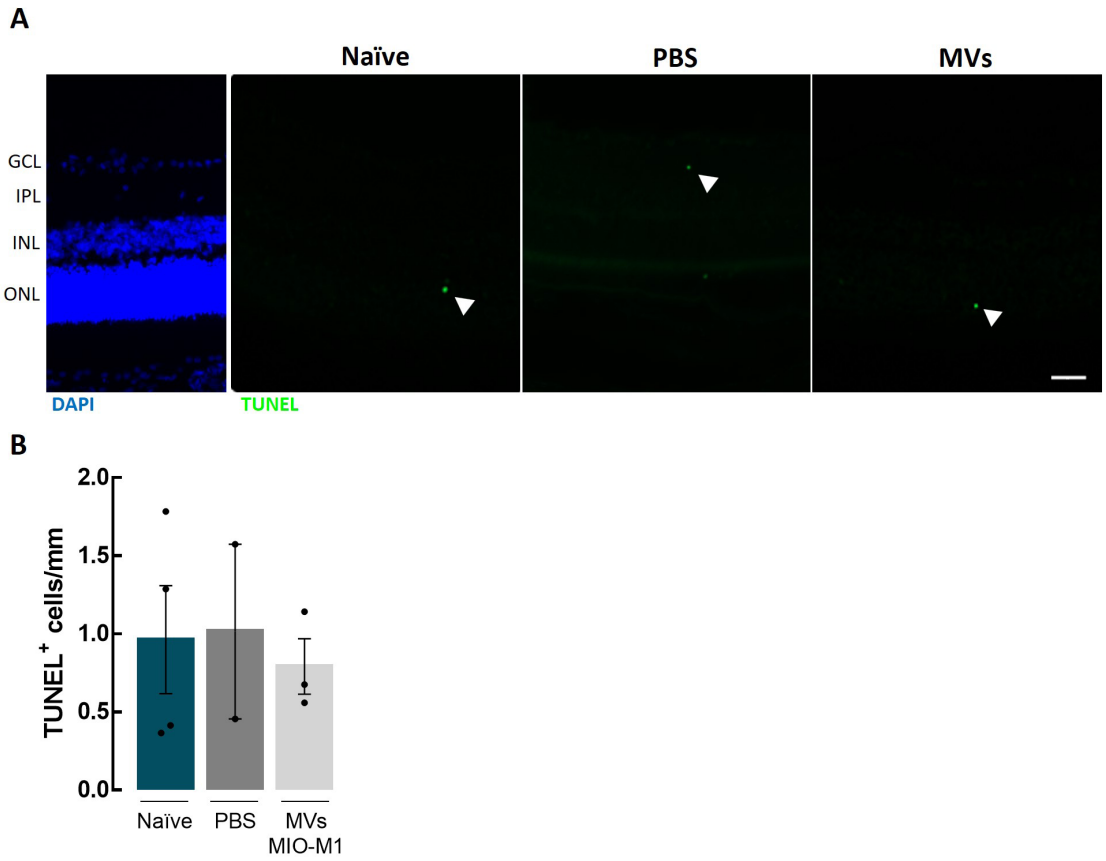

Figure 21: Effect of MVs from MIO-M1 cells in retinal cell death. MVs derived from MIO-M1 cells were injected in the vitreous of Wistar rats and the animals were sacrificed 7 days after injection. **A.** Cell death was assessed by TUNEL assay (white). The nuclei were stained with DAPI (blue). Representative images are depicted. Arrowheads indicate TUNEL⁺ cells. **B.** The number of TUNEL⁺ cells was counted and was expressed per mm of retina. Scale bar: 50 μm.

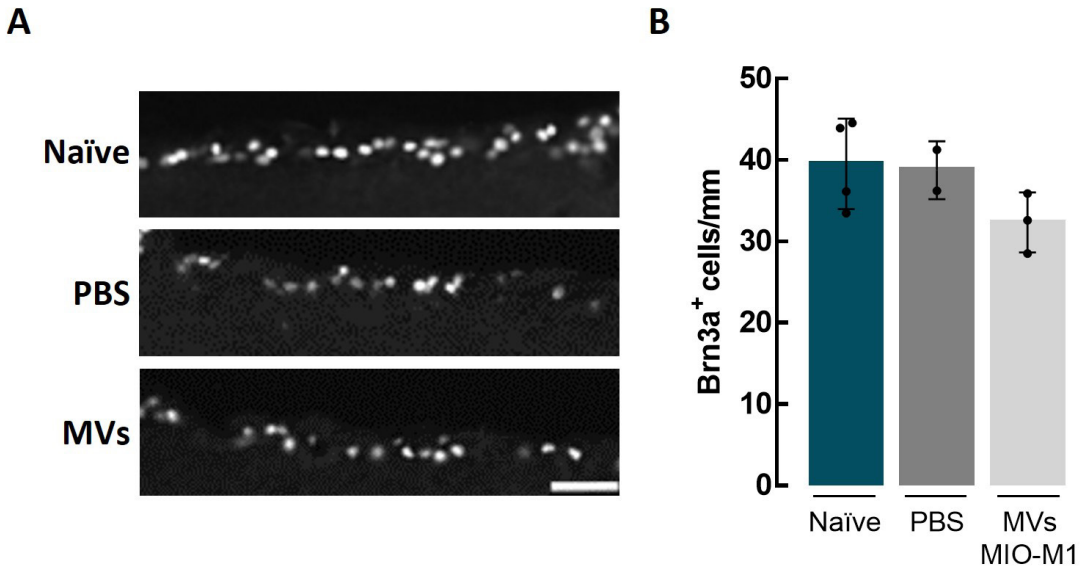

Figure 22: Effect of MVs from MIO-M1 cells in the number of RGCs. MVs derived from MIO-M1 cells were injected in the vitreous of Wistar rats and the animals were sacrificed 7 days after injection. **A.** RGCs were immunolabeled for Brn3a (white). **B.** The number of Brn3a$^+$ cells was expressed per mm of retinal section. Scale bar: 50 μm.

Chapter 4

Discussion

The most common features of glaucoma are loss of RGCs, thinning of the retinal NFL, and optic nerve atrophy.

Müller cells are the principal glial cell type in the retina and are responsible for maintaining homeostasis, providing functional, structural and metabolic support to neurons, protecting the tissue from damage during harmful conditions (Vecino et al. 2016). There is an intimate relationship between Müller cells and RGCs, and this interaction is compromised in glaucoma (Vecino et al. 2016). Elevated IOP is the main risk factor of glaucoma, and *in vitro* experimental models may mimic this condition by increasing the pressure to which cells and tissues are exposed (Aires, Ambrosio, and Santiago 2017). In this work, we studied the effect of EHP on the survival of RGCs and Müller cells and the contribution of MVs derived from Müller cells to the protection of RGCs.

The exposure to EHP impacted the survival of RGCs and Müller cells. Indeed, it was already reported that RGCs are susceptible to pressure elevation in several experimental models, from RGC cultures, retinal organotypic cultures and the animal models with ocular hypertension (Madeira et al. 2015b; Lee et al. 2015; Wu et al. 2019). Although the mechanisms are not fully understood, one possibility is through the activation of the transient receptor potential vanilloid 1 (TRPV1), a non-selective cation channel receptor that is expressed in numerous cell types throughout the entire body, including RGCs (Sappington et al. 2009). TRPV channels have been implicated in optic nerve degeneration (Ryskamp et al. 2014; Sappington et al. 2015) and axonal neuropathies (Echaniz-Laguna et al. 2014). Indeed, TRPV1 antagonism or extracellular Ca^{2+} chelation reduced EHP-induced RGCs apoptosis (Sappington et al. 2009), suggesting that TRPV1 is activated in EHP conditions, and increased intracellular Ca^{2+} concentration which leads to RGC apoptosis.

The survival of Müller cells was also affected by EHP. Interestingly, Müller cells seem less susceptible to pressure increase than RGCs, since in pure cultures, at 24h under EHP RGCs suffered a significative decrease in cell survival which was only observed in Müller cells at least with 48h under EHP. Müller cells were already described to react to EHP changing the expression of several genes and proteins as Kir 2.1, Kir 4.1, glycoprotein nonmetastatic melanoma protein B (GPMNB) and amphiregulin (AREG) for example (Yu et al. 2012; Xue et al. 2011). GPMNB, a protein that may play a role in antigen presentation of astrocytes to control immune responses (Rostami et al. 2020; Neal et al. 2018; Xue et al. 2011), was found to be decreased in Müller cells exposed to EHP (Xue et al. 2011). AREG, a member of the epidermal growth factor family, an autocrine growth factor and a mitogen for astrocytes, Schwann cells, and fibroblasts increases in Müller cells after exposure to EHP (Xue et al. 2011).

Müller cells transport K^+ through their cell bodies to avoid potassium-induced depolarization of neurons, from extracellular regions of high K^+ to those of low K^+ in the retina (Yu et al. 2012). In Müller cells, the most significant mediators of K^+

buffering are the Kir channels localized in the cell membrane, particularly the Kir 2.1 and Kir 4.1 channels (Kofuji et al. 2002; Bringmann et al. 2000). The expression of Kir 2.1 and Kir 4.1 channels increases in Müller cells in EHP conditions (Kofuji et al. 2002). These alterations suggest that Müller cells remain capable of taking up K^+ and mediate the potassium concentration in the retina even under EHP, preventing neuronal hyperexcitation and excessive release of glutamate (Yu et al. 2012).

Taking the crosstalk between Müller cells and RGCs it is possible that the changes occurring in Müller cells gene expression in response to elevated pressure are causally linked with the RGC loss in glaucoma. Interestingly, when in co-culture, both RGCs and Müller cells were less susceptible to the noxious environment caused by EHP, indicating the existence of a communication system that attempts to rescue the dying cells. It is known that Müller cells secrete trophic factors that mediate the survival and regeneration of RGCs. A trophic factor produced by activated Müller cells that enhances RGC axonal regeneration is CNTF but there are other trophic factors produced by reactive Müller cells that may be involved in RGC survival including BDNF, glial cell line-derived neurotrophic factor (GDNF) and the basic fibroblast growth factor (bFGF) (Bonnet et al. 2004; Garcia et al. 2002, 2003; Garcia and Vecino 2003; Kinkl et al. 2003; Ruzafa et al. 2018b). However, RGCs also produce neurotrophins such as nerve growth factor (NGF) (Roberti et al. 2014) and BDNF (Vecino et al. 1999; Pietrucha-Dutczak et al. 2018) that can support Müller cells survival under harmful conditions (Harada et al. 2011). Indeed, the protective effect of the CM from Müller cells in RGCs survival was already demonstrated (Pereiro et al. 2020a), however this is the first time where the protective effect of CM from Müller cells was observed under harmful environment caused by EHP.

In a previous work, our group demonstrated that primary retinal microglial cells proliferate more when exposed to EHP, comparing with cells exposed to atmospheric pressure (Ferreira-Silva et al. 2020). In the present study we also studied whether EHP could affect the proliferation of Müller cells (primary Müller cells and MIO-M1 cells) and we observed that EHP did not change the proliferation of these cells, demonstrating that EHP affects retinal glia proliferation differently. Furthermore, we studied whether EHP could affect death of Müller cells and MIO-M1 cells. EHP did not cause death of MIO-M1 cells, indicating that this cell line is more resistant than primary Müller cells to the same magnitude of pressure at 24h and 48h. This might be explained by the differences between cell line and primary cultures. Primary cultures are known to be more susceptible to noxious conditions, and more difficult to obtain and maintain than cell lines, but cell lines offer several advantages over primary cultures for biochemical and molecular biological studies (Kaur and Dufour 2012). To the best of our knowledge, resistance of MIO-M1 cell have never been reported and indeed this cell line is nowadays used for several studies (Lorenz et al. 2021; Dierschke et al. 2020; Ciavarella et al. 2020).

In the CNS, the crosstalk between glia and neurons is crucial for a variety of biological

functions. Studies have already demonstrated that Müller cells secrete factors to the extracellular space that are beneficial to adult RGCs (Garcia et al. 2002; Ruzafa et al. 2018b). Several factors were identified by proteomic analysis in the secretome of cultured adult Müller cells that might offer RGCs protection against noxious situations in the retina. For example, PDGF, clusterin, basigin and SPP1 were identified as providing neuroprotective effects in RGCs, with SPP1 and basigin with a greater effect in RGC cultures (Ruzafa et al. 2018b). Nevertheless, when adding only one of these proteins or a combination of two the protective effect to RGCs is not equivalent to the CM of Müller cells, indicating that Müller cells secrete a wide range of factors that together promote RGC protection (Ruzafa et al. 2018b). In the present work, we found that CM from primary Müller cells and from MIO-M1 cells increased the survival of RGCs when the cells were cultured in atmospheric pressure or challenged to EHP. This effect was not so pronounced in co-cultures of RGCs and Müller cells, and one hypothesis might be that Müller cells may secrete other soluble factors or even other EVs like EXOs when exposed to EHP that could cover the effect of the CM.

EVs are an important part of the secretome of cells and deliver their cargo (proteins, mRNA/miRNA, lipids, among others) into other cells (Skog et al. 2008). Taking the results using CM from MIO-M1 and Müller cells we also studied whether EVs secreted by these cells could have an impact on the survival of RGCs. MIO-M1 cells are known to release EVs (EXOs and MVs) to the extracellular space (DB Lamb 2018). The nomenclature of the different types of EVs and their characterization is still a matter of debate in the scientific community (Thery et al. 2018). EVs were isolated by ultracentrifugation and two populations were considered: MVs to the fraction isolated at low-speed ultracentrifugation and EXOs to the fraction isolated at high-speed ultracentrifugation. Ultracentrifugation is one of the most used techniques for EVs isolation since it allows isolation from large volumes and there is no need of adding reagents that could damage the integrity of EVs (Konoshenko et al. 2018). However, ultracentrifugation does not allow to obtain a pure population of EVs since it might contain contaminants as cell debris or undesired fractions of EVs (Konoshenko et al. 2018). The size and morphology of the EVs isolated by MIO-M1 and Müller cells were consistent for EXOs and MVs (Colombo, Raposo, and Thery 2014; van Niel, D'Angelo, and Raposo 2018). The proteins CHC1, TSG101, flotillin-1 and CD63, usually used as markers of EXOs (Nabhan et al. 2012; Willms et al. 2016; Lee, El Andaloussi, and Wood 2012), were also present in MVs. These proteins have been previously described in MVs from other cells (Larson et al. 2017; Nabhan et al. 2012; Phuyal et al. 2014; Kowal et al. 2016), further reinforcing that relying only on the presence of some proteins for the characterization of EVs is limited (Thery et al. 2018; Kowal et al. 2016). GLAST, the glutamate-aspartate transporter expressed in Müller cells (Bringmann et al. 2013), was found in MVs derived from primary Müller cells. Since this transporter is localized in the cell membrane, this further supports the concept that proteins found at the plasma

membrane can be detected in MVs, mostly because of their biogenesis (Tricarico, Clancy, and D'Souza-Schorey 2017). To our knowledge it was the first time that GLAST was described in MVs from Müller cells. More experiments are needed but GLAST can be proposed as a marker for MVs derived from Müller cells. Calnexin is a protein from the endoplasmatic reticulum and is usually used as a negative control for EVs isolation (Thery et al. 2018). Calnexin was present in MVs from both types of Müller cells, but this was reported previously (Tucher et al. 2018; Haraszti et al. 2016). We cannot conclude that MVs from these cells are endowed with calnexin, as we cannot exclude the possibility of contamination with cell debris (Tucher et al. 2018). Other experiments would need to be performed to further elucidate this. Herein, we focused on the role of MVs in the survival of RGCs when cells are challenged with EHP.

MVs selectively transfer the content from their origin cells to recipient cells, likely altering cellular response, and ultimately, the fate of the recipient cells. We found that MVs from Müller cells and MIO-M1 cells promoted the survival of RGCs in EHP conditions. This effect was not as robust as CM, suggesting that soluble factors also contribute to the survival of RGCs. Indeed, MVs are only a fraction of what cells release to the extracellular space, together with other EVs subtypes and soluble factors. However, MVs could promote the survival of RGCs likely meaning that their content was not noxious to these cells. MVs inner content is composed of mRNA, miRNA, noncoding RNAs, proteins (e.g., enzymes, signaling components, transcription factors), bioactive lipids (e.g., sphingosine-1-phosphate, prostaglandins, leukotrienes), signaling nucleotides, and metabolites (Ratajczak and Ratajczak 2020). A deep study of the content of the MVs released by Müller cells would be crucial to understand if the effect of MVs was due to the same factors found in CM or if different factors are included in MVs with protective potential. Taking all this into account, our MVs seem to be good candidates for the growing concept of "super MVs", custom-engineered MVs designed to inhibit apoptosis of target cells, stimulate cells that have survived damage to proliferate, and recovering vascularization of damaged tissues, thereby serving as a new class of cell-derived therapeutics in regenerative medicine (Ratajczak and Ratajczak 2020).

In our study, MVs from MIO-M1 cells did not change the proliferation of MIO-M1 cells. Moreover, the protein levels of GFAP and GS were not altered in MIO-M1 cells exposed to MVs. Nevertheless, the expression of GS by Müller cells *in vitro* was already described to be altered depending on the hydrostatic pressure (Yu et al. 2011). There is not much information about the effect of MVs in cell proliferation. MVs isolated from human endothelial progenitor cells originating from cord blood and MVs derived from human immortalized mesenchymal stem cells line HATMSC1 increased the proliferation of human endothelial cells of dermal origin in a dose-dependent manner (Krawczenko et al. 2020). In contrast, MVs had a limited impact on the proliferation of fibroblasts and keratinocytes (Krawczenko et al. 2020). Whether MVs from Müller cells change the proliferation of other cells beside Müller cells we do not know.

Concluding from the *in vitro* studies, Müller cells secrete factors that are able to promote the survival of RGCs, protecting the cells from the damage caused by EHP. Since MIO-M1 cells are easier to culture and to maintain than primary Müller cells and MVs from MIO-M1 cells have also a protective effect on RGCs, we further studied the effects of MVs MIO-M1 in the retina of Wistar Han rats.

One of the objectives of the study was to understand if MVs derived from MIO-M1 cells could afford protection to RGCs in a context of increased IOP using the animal model of I-R injury, well established in our laboratory and known to trigger death of RGCs (Madeira et al. 2016; Boia et al. 2017). The induction of acute retinal ischemia for a period of 30–120 minutes followed by reperfusion causes death within a variety of cell types within the retina since damage occurs throughout the various layers of the retina (Szabo et al. 1991; Madeira et al. 2016; Boia et al. 2017; Johnson and Tomarev 2010). By setting IOP above the ocular perfusion pressure, blood flow through the retinal and uveal vasculature is suppressed. After the ischemic exposure, IOP can be normalized reducing the pressure of the perfusion system (Johnson and Tomarev 2010). Our group already reported that it is possible to prevent the loss of RGCs with several drugs when assessing 7 days after I-R (Madeira et al. 2016; Boia et al. 2017). Therefore, we decided to choose 7 days after intravitreal injection (and I-R) as the time point to analyse the effects of MVs. It was reported that intravitreal administration of EXOs derived from human mesenchymal stem cells was well tolerated without immunosuppression and decreased the severity of retinal ischemia in mice (Moisseiev et al. 2017). Unexpectedly, intravitreal injection of PBS together with the induction of I-R created a severe destruction of the retina making the analysis impossible. This result, as far as we know, was never reported. Moreover, it was previously described that PBS is not toxic to the retina and does not interfere with the physiology of the tissue, and it is considered the preferred vehicle when compared with normal saline (Hombrebueno et al. 2014; Stifter et al. 2017). Due to lack of time to understand this atypical observation, we were forced to abandon the study of the effect of MVs in the I-R animal model, since it was not possible to separate the effects caused by MVs or by the vehicle. The study proceeded only analysing the effect of the intravitreal injection of MVs in the contralateral eyes.

Retinal function was assessed by ERG, a record of electrical responses in the eye obtained by stimulating the retina with light flashes in either dark-adapted (scotopic) or light-adapted (photopic) conditions. Generally, when retinal function deteriorates, the light-induced electrical activity in the retina is reduced (Vidal-Sanz et al. 2015). We found that intravitreal injection of neither PBS or MVs impacted cells response in scotopic and photopic conditions. Also, retinal thickness assessed by OCT revealed no changes in retinal structure and only in PBS injected retinas was observed the presence of retinal infiltrates. Taken together, these results suggest that MVs from MIO-M1 cells do not appear to affect retinal function.

Microglial cells are extremely sensitive to changes in their environment (Rashid,

Akhtar-Schaefer, and Langmann 2019). Under acute conditions, microglial cells become activated for a shorter period of time promoting neuroprotection and regenerative processes through neuroinflammation, facilitating a rapid return to tissue homeostasis (Bellver-Landete et al. 2019; Gupta et al. 2018). Nevertheless, in chronic conditions, such as in retinal degenerative diseases, microglia become pathologically activated and release exaggerated amounts of inflammatory mediators that promote tissue damage and disease exacerbation (Zhao et al. 2015; Gupta, Brown, and Milam 2003). In fact, microglial cells are considered to have a key role in the inflammatory environment in glaucomatous conditions. Nevertheless, in studies in the scope of the glaucoma condition, microglia cells presented alterations in morphology, gene expression, cell proliferation, cell adhesion, and immune response, compatible with a reactive phenotype (Ebneter et al. 2010; Bosco, Steele, and Vetter 2011). Recent studies have reported the critical role of EXOs in regulating microglial phenotype in motor neuron diseases (Silverman et al. 2016). Also, in a previous study our group reported that EXOs derived from retinal microglia have an autocrine function and propagate the inflammatory signal in conditions of elevated pressure, contributing to retinal degeneration in glaucomatous conditions (Aires et al. 2020).

The communication between microglia cells and Müller cells is not new, since microglial cells establish important interactions with Müller cells regulating the microglia-Müller-photoreceptor network that serves as a trophic factor-controlling system during retinal degeneration (Harada et al. 2002). However, how this communication occurs is still not well understood. In the present study we found that MVs MIO-M1 may increase the number of microglia cells and also the number of reactive microglia, meaning that MVs released by MIO-M1 cells could possibly activate them. In fact, recently our group reported that MVs derived from microglia cells could interact with Müller cells, where MVs from microglia cells induced changes in the expression of pro-inflammatory cytokines, chemokines, and trophic factors of Müller cells (Rodrigues 2021). Further experiments need to be performed to access if MVs MIO-M1 injected in the vitreous of Wistar Han rats could directly target microglial cells in the retina.

EVs isolated from C6 glioma cells were intravitreally injected in undamaged zebra fish and induced Müller glia to dedifferentiate and proliferate. In the same study, in mice, injection of EVs could also induce Müller cell proliferation (Balaiya 2019). This last result shows that indeed EVs injected in the vitreous could still target Müller cells in rodents. As already discussed here, GFAP is expressed not only by astrocytes but also by reactive Müller cells, and in our study, PBS and MVs increased the expression of GFAP in Müller cells, which we might speculate MVs could interact with Müller cells, but more experiments would need to be performed to assess how this interaction might occur. However, in GCL and NFL are localized not only the Müller cells endfeet but also astrocytes, making impossible in these layers to distinguish the expression of this protein by each type of cell.

The main characteristic of glaucoma is the chronic death of RGCs and it was already reported that intravitreally injected MSCs-derived EXOs in rats successfully protected RGCs (Mead and Tomarev 2017). Also, EXOs derived from umbilical cord mesenchymal stem cells and human embryonic stem cells have also been found to yield similar neuroprotective effects (Pan et al. 2019; Seyedrazizadeh et al. 2020). In our study, we did not observe changes in retinal cell death in the eyes that received the intravitreal injection of PBS neither of MVs. To be able to count RGCs in the retina, several markers can be employed and of the most used RGCs marker is Brn3a, a transcription factor only expressed in RGCs that intervenes in cells differentiation and survival. Not all RGCs express Brn3a but it is still considered a reliable marker for identifying RGCs (Nadal-Nicolas et al. 2009).

Remarkably, the intravitreal injection of MVs from MIO-M1 cells cultured under atmospheric pressure on adult Wistar Han rats do not cause alterations in retinal function and structure. Also, MVs did not appear to affect retinal cell death, and even the increase in reactive microglia may not be relevant (an increase of 3 %). However, we cannot forget that our potential effects were observed in an eye considered undamaged, but in fact it was a contralateral eye, in an animal model of I-R where the injury was induced unilaterally. In rats in which ocular hypertension was induced unilaterally there was a significant microglia activation in the contralateral eye (Tribble et al. 2021). With this in mind, we need to be careful with the interpretation of our results, understanding the limitations of our animal model.

Chapter 5

Conclusions and Future Remarks

In the present study we found that EHP decreases both RGCs and Müller cells survival in pure cultures and also in co-cultures. However, when in co-culture, both cell types were more resistant to EHP effect, needing a larger period under EHP conditions to be observed a decrease in cell survival. MIO-M1 cells survival, cell death and cell proliferation seemed not to be affected by EHP in the time-points chosen. In primary Müller cells, even decreasing the cell survival under EHP, cell proliferation was also not affected.

The results presented in this thesis showed for the first time that *in vitro* healthy primary Müller cells and MIO-M1 cells release MVs that could promote RGCs survival under a noxious environment caused by EHP. MVs from Müller cells and from MIO-M1 cells afford similar effects in RGCs survival under EHP, but this effect was still not so pronounced as the effect caused by CM. The analysis of the content of MVs would be of great importance. The identification of the proteins, miRNAs, and lipids carried by both MVs would provide important information in the field of RGC neuroprotection.

The intravitreal injection of MVs MIO-M1 in the vitreous of Wistar Han rats allowed us to conclude that MVs from MIO-M1 cells are not noxious to the retina: structure and function were not affected, cell death and RGC survival was not altered. However, there was a slight increase in the reactivity of Müller cells and microglial cells that need to be further explored.

Further experiments must be performed to reveal the role played by MVs derived from Müller cells in the possible protection of RGCs in a context of glaucoma. Understanding the role of MVs from MIO-M1 cells exposed to EHP in naïve retinas would be important as well as understand if MVs from MIO-M1 cells cultured in atmospheric pressure could protect neurons from damaged retinas. In this study we were not able to identify the cells that directly interacted with MVs. This could be done using dyes or transfecting cells with a reporter gene. Lipophilic fluorescent dye molecules, such as PKH dyes, are currently the most widely used fluorescent probes for EVs labelling, though they have some limitations since these dyes tend to aggregate, leading to formation of EV-like nanoparticles that can be taken up by cells (Aires et al. 2020; Shimomura et al. 2021). Another option to label EVs, is by cloning the EV specific markers in reporter vectors that are tagged with green fluorescent protein, for example, followed by their transfection into cells of interest (Mondal et al. 2019). Furthermore, some experiments need to be repeated in order to increase the number of independent experiments.

Chapter 6

References

Aires, I. D., Ambrosio, A. F., and Santiago, A. R. 2017. 'Modeling Human Glaucoma: Lessons from the *in vitro* Models', Ophthalmic Res, 57: 77-86.

Aires, I. D., Boia, R., Rodrigues-Neves, A. C., Madeira, M. H., Marques, C., Ambrosio, A. F., and Santiago, A. R. 2019. 'Blockade of microglial adenosine A2A receptor suppresses elevated pressure-induced inflammation, oxidative stress, and cell death in retinal cells', Glia, 67: 896-914.

Aires, I. D., Ribeiro-Rodrigues, T., Boia, R., Catarino, S., Girao, H., Ambrosio, A. F., and Santiago, A. R. 2020. 'Exosomes derived from microglia exposed to elevated pressure amplify the neuroinflammatory response in retinal cells', Glia, 68: 2705-24.

Aires, I. D., Ribeiro-Rodrigues, T., Boia, R., Ferreira-Rodrigues, M., Girao, H., Ambrosio, A. F., and Santiago, A. R. 2021. 'Microglial Extracellular Vesicles as Vehicles for Neurodegeneration Spreading', Biomolecules, 11.

Allen, S. J., Watson, J. J., Shoemark, D. K., Barua, N. U., and Patel, N. K. 2013. 'GDNF, NGF and BDNF as therapeutic options for neurodegeneration', Pharmacol Ther, 138: 155-75.

Ashwell, K. W., Hollander, H., Streit, W., and Stone, J. 1989. 'The appearance and distribution of microglia in the developing retina of the rat', Vis Neurosci, 2: 437-48.

Azadi, S., Johnson, L. E., Paquet-Durand, F., Perez, M. T., Zhang, Y., Ekstrom, P. A., and van Veen, T. 2007. 'CNTF+BDNF treatment and neuroprotective pathways in the rd1 mouse retina', Brain Res, 1129: 116-29.

Balaiya, S., et al. 2019. 'In vivo screen for extracellular vesicles that promote Müller glia proliferation and neurogenic activity in zebrafish and mice', ARVO Annual Meeting Abstract 60.

Becerra, S. P., Dass, C. R., Yabe, T., and Crawford, S. E. 2012. 'Pigment epithelium-derived factor: chemistry, structure, biology, and applications', J Biomed Biotechnol, 2012: 830975.

Bellver-Landete, V., Bretheau, F., Mailhot, B., Vallieres, N., Lessard, M., Janelle, M. E., Vernoux, N., Tremblay, M. E., Fuehrmann, T., Shoichet, M. S., and Lacroix, S. 2019. 'Microglia are an essential component of the neuroprotective scar that forms after spinal cord injury', Nat Commun, 10: 518.

Bilimoria, P. M., and Stevens, B. 2015. 'Microglia function during brain development: New insights from animal models', Brain Res, 1617: 7-17.

Boia, R., Dias, P. A. N., Martins, J. M., Galindo-Romero, C., Aires, I. D., Vidal-Sanz, M., Agudo-Barriuso, M., de Sousa, H. C., Ambrosio, A. F., Braga, M. E. M., and Santiago, A. R. 2019. 'Porous poly(epsilon-caprolactone) implants: A novel strategy for efficient intraocular drug delivery', J Control Release, 316: 331-48.

Boia, R., Elvas, F., Madeira, M. H., Aires, I. D., Rodrigues-Neves, A. C., Tralhao, P., Szabo, E. C., Baqi, Y., Müller, C. E., Tome, A. R., Cunha, R. A., Ambrosio, A. F., and Santiago, A. R. 2017. 'Treatment with A2A receptor antagonist KW6002 and caffeine intake regulate microglia reactivity and protect retina against transient ischemic damage', Cell Death Dis, 8: e3065.

Boia, R., Ruzafa, N., Aires, I. D., Pereiro, X., Ambrosio, A. F., Vecino, E., and Santiago, A. R. 2020. 'Neuroprotective Strategies for Retinal Ganglion Cell Degeneration: Current Status and Challenges Ahead', Int J Mol Sci, 21.

Bonnet, D., Garcia, M., Vecino, E., Lorentz, J. G., Sahel, J., and Hicks, D. 2004. 'Brain-derived neurotrophic factor signalling in adult pig retinal ganglion cell neurite regeneration *in vitro*', Brain Res, 1007: 142-51.

Bosco, A., Steele, M. R., and Vetter, M. L. 2011. 'Early microglia activation in a mouse model of chronic glaucoma', J Comp Neurol, 519: 599-620.

Bothwell, M. 1995. 'Functional interactions of neurotrophins and neurotrophin receptors', Annu Rev Neurosci, 18: 223-53.

Bringmann, A., Francke, M., Pannicke, T., Biedermann, B., Kodal, H., Faude, F., Reichelt, W., and Reichenbach, A. 2000. 'Role of glial K(+) channels in ontogeny and gliosis: a hypothesis based upon studies on Müller cells', Glia, 29: 35-44.

Bringmann, A., Grosche, A., Pannicke, T., and Reichenbach, A. 2013. 'GABA and Glutamate Uptake and Metabolism in Retinal Glial (Müller) Cells', Front Endocrinol (Lausanne), 4: 48.

Bringmann, A., Iandiev, I., Pannicke, T., Wurm, A., Hollborn, M., Wiedemann, P., Osborne, N. N., and Reichenbach, A. 2009. 'Cellular signaling and factors involved in Müller cell gliosis: neuroprotective and detrimental effects', Prog Retin Eye Res, 28: 423-51.

Bringmann, A., Uckermann, O., Pannicke, T., Iandiev, I., Reichenbach, A., and Wiedemann, P. 2005. 'Neuronal versus glial cell swelling in the ischaemic retina', Acta Ophthalmol Scand, 83: 528-38.

Buschow, S. I., Nolte-'t Hoen, E. N., van Niel, G., Pols, M. S., ten Broeke, T., Lauwen, M., Ossendorp, F., Melief, C. J., Raposo, G., Wubbolts, R., Wauben, M. H., and Stoorvogel, W. 2009. 'MHC II in dendritic cells is targeted to lysosomes or T cell-induced exosomes via distinct multivesicular body pathways', Traffic, 10: 1528-42.

Byzov, A. L. 1977. '[Model for the feedback mechanism between horizontal cells and photoreceptors of vertebrate retinas]', Neirofiziologiia, 9: 86-94.

Campoy, I., Lanau, L., Altadill, T., Sequeiros, T., Cabrera, S., Cubo-Abert, M., Perez-Benavente, A., et al. 2016. 'Exosome-like vesicles in uterine aspirates: a comparison of ultracentrifugation-based isolation protocols', J Transl Med, 14: 180.

Cao, W., Wen, R., Li, F., Lavail, M. M., and Steinberg, R. H. 1997. 'Mechanical injury increases bFGF and CNTF mRNA expression in the mouse retina', Exp Eye Res, 65: 241-8.

Cen, L. P., and Ng, T. K. 2018. 'Stem cell therapy for retinal ganglion cell degeneration', Neural Regen Res, 13: 1352-53.

Chapot, C. A., Euler, T., and Schubert, T. 2017. 'How do horizontal cells 'talk' to cone photoreceptors? Different levels of complexity at the cone-horizontal cell synapse', J Physiol, 595: 5495-506.

Chen, H., and Weber, A. J. 2001. 'BDNF enhances retinal ganglion cell survival in cats with optic nerve damage', Invest Ophthalmol Vis Sci, 42: 966-74.

Chidlow, G., and Osborne, N. N. 2003. 'Rat retinal ganglion cell loss caused by kainate, NMDA and ischemia correlates with a reduction in mRNA and protein of Thy-1 and neurofilament light', Brain Res, 963: 298-306.

Ciavarella, C., Buzzi, M., Bergantin, E., Di Marco, S., Giannaccare, G., Campos, E., Bisti, S., and Versura, P. 2020. 'Effects of Cord Blood Serum (CBS) on viability of retinal Müller glial cells under *in vitro* injury', PLoS One, 15: e0234145.

Cizmar, P., and Yuana, Y. 2017. 'Detection and Characterization of Extracellular Vesicles by Transmission and Cryo-Transmission Electron Microscopy', Methods Mol Biol, 1660: 221-32.

Colombo, M., Raposo, G., and Thery, C. 2014. 'Biogenesis, secretion, and intercellular interactions of exosomes and other extracellular vesicles', Annu Rev Cell Dev Biol, 30: 255-89.

Cunha-Vaz, J., Bernardes, R., and Lobo, C. 2011. 'Blood-retinal barrier', Eur J Ophthalmol, 21 Suppl 6: S3-9.

Curcio, M., and Bradke, F. 2018. 'Axon Regeneration in the Central Nervous System: Facing the Challenges from the Inside', Annu Rev Cell Dev Biol, 34: 495-521.

D'Acunzo, P., Perez-Gonzalez, R., Kim, Y., Hargash, T., Miller, C., Alldred, M. J., Erdjument-Bromage, H., et al. 2021. 'Mitovesicles are a novel population of extracellular vesicles of mitochondrial origin altered in Down syndrome', Sci Adv, 7.

DB Lamb, W. et al. 2018. 'Identification of extracellular vesicles released by Müller glial cells *in vitro*', ARVO journal, 59.

Del Rio, P., Irmler, M., Arango-Gonzalez, B., Favor, J., Bobe, C., Bartsch, U., Vecino, E., Beckers, J., Hauck, S. M., and Ueffing, M. 2011. 'GDNF-induced osteopontin from Müller glial cells promotes photoreceptor survival in the Pde6brd1 mouse model of retinal degeneration', Glia, 59: 821-32.

DelMonte, D. W., and Kim, T. 2011. 'Anatomy and physiology of the cornea', J Cataract Refract Surg, 37: 588-98.

Di Polo, A., Aigner, L. J., Dunn, R. J., Bray, G. M., and Aguayo, A. J. 1998. 'Prolonged delivery of brain-derived neurotrophic factor by adenovirus-infected Müller cells temporarily rescues injured retinal ganglion cells', Proc Natl Acad Sci U S A, 95: 3978-83.

Dierschke, S. K., Toro, A. L., Miller, W. P., Sunilkumar, S., and Dennis, M. D. 2020. 'Diabetes enhances translation of Cd40 mRNA in murine retinal Müller glia via a 4E-BP1/2-dependent mechanism', J Biol Chem, 295: 10831-41.

Doyle, L. M., and Wang, M. Z. 2019. 'Overview of Extracellular Vesicles, Their Origin, Composition, Purpose, and Methods for Exosome Isolation and Analysis', Cells, 8.

Ebneter, A., Casson, R. J., Wood, J. P., and Chidlow, G. 2010. 'Microglial activation in the visual pathway in experimental glaucoma: spatiotemporal characterization and correlation with axonal injury', Invest Ophthalmol Vis Sci, 51: 6448-60.

Echaniz-Laguna, A., Dubourg, O., Carlier, P., Carlier, R. Y., Sabouraud, P., Pereon, Y., Chapon, F., Thauvin-Robinet, C., Laforet, P., Eymard, B., Latour, P., and Stojkovic, T. 2014. 'Phenotypic spectrum and incidence of TRPV4 mutations in patients with inherited axonal neuropathy', Neurology, 82: 1919-26.

Eirin, A., Zhu, X. Y., Puranik, A. S., Woollard, J. R., Tang, H., Dasari, S., Lerman, A., van Wijnen, A. J., and Lerman, L. O. 2016. 'Comparative proteomic analysis of extracellular vesicles isolated from porcine adipose tissue-derived mesenchymal stem/stromal cells', Sci Rep, 6: 36120.

Ellis, E. M., Gauvain, G., Sivyer, B., and Murphy, G. J. 2016. 'Shared and distinct retinal input to the mouse superior colliculus and dorsal lateral geniculate nucleus', J Neurophysiol, 116: 602-10.

Escartin, C., Brouillet, E., Gubellini, P., Trioulier, Y., Jacquard, C., Smadja, C., Knott, G. W., Kerkerian-Le Goff, L., Deglon, N., Hantraye, P., and Bonvento, G. 2006. 'Ciliary neurotrophic factor activates astrocytes, redistributes their glutamate transporters GLAST and GLT-1 to raft microdomains, and improves glutamate handling in vivo', J Neurosci, 26: 5978-89.

Feher, Joseph. 2012. 'Vision.' in, Quantitative Humam Physiology: An Introduction (Academic Press).

Felleman, D. J., and Van Essen, D. C. 1991. 'Distributed hierarchical processing in the primate cerebral cortex', Cereb Cortex, 1: 1-47.

Ferreira-Silva, J., Aires, I. D., Boia, R., Ambrosio, A. F., and Santiago, A. R. 2020. 'Activation of Adenosine A3 Receptor Inhibits Microglia Reactivity Elicited by Elevated Pressure', Int J Mol Sci, 21.

Fischer, A. J., Schmidt, M., Omar, G., and Reh, T. A. 2004. 'BMP4 and CNTF are neuroprotective and suppress damage-induced proliferation of Müller glia in the retina', Mol Cell Neurosci, 27: 531-42.

Fischer, R. A., Roux, A. L., Wareham, L. K., and Sappington, R. M. 2019. 'Pressure-dependent modulation of inward-rectifying K(+) channels: implications for cation homeostasis and K(+) dynamics in glaucoma', Am J Physiol Cell Physiol, 317: C375-C89.

Forrester, J., and Peters, A. 1967. 'Nerve fibres in optic nerve of rat', Nature, 214: 245-7.

Franze, K., Grosche, J., Skatchkov, S. N., Schinkinger, S., Foja, C., Schild, D., Uckermann, O., Travis, K., Reichenbach, A., and Guck, J. 2007. 'Müller cells are living optical fibers in the vertebrate retina', Proc Natl Acad Sci U S A, 104: 8287-92.

Fu, L., Kwok, S. S., Chan, Y. K., Ming Lai, J. S., Pan, W., Nie, L., and Shih, K. C. 2019. 'Therapeutic Strategies for Attenuation of Retinal Ganglion Cell Injury in Optic Neuropathies: Concepts in Translational Research and Therapeutic Implications', Biomed Res Int, 2019: 8397521.

Garcia-Valenzuela, E., Shareef, S., Walsh, J., and Sharma, S. C. 1995. 'Programmed cell death of retinal ganglion cells during experimental glaucoma', Exp Eye Res, 61: 33-44.

Garcia, M., Forster, V., Hicks, D., and Vecino, E. 2002. 'Effects of Müller glia on cell survival and neuritogenesis in adult porcine retina *in vitro*', Invest Ophthalmol Vis Sci, 43: 3735-43.

Garcia, M., Forster, V., Hicks, D., and Vecino, E. 2003. 'In vivo expression of neurotrophins and neurotrophin receptors is conserved in adult porcine retina in vitro', Invest Ophthalmol Vis Sci, 44: 4532-41.

Garcia, M., and Vecino, E. 2003. 'Role of Müller glia in neuroprotection and regeneration in the retina', Histol Histopathol, 18: 1205-18.

Gauthier, S. A., Perez-Gonzalez, R., Sharma, A., Huang, F. K., Alldred, M. J., Pawlik, M., Kaur, G., Ginsberg, S. D., Neubert, T. A., and Levy, E. 2017. 'Enhanced exosome secretion in Down syndrome brain - a protective mechanism to alleviate neuronal endosomal abnormalities', Acta Neuropathol Commun, 5: 65.

Goldberg, J. L., Espinosa, J. S., Xu, Y., Davidson, N., Kovacs, G. T., and Barres, B. A. 2002. 'Retinal ganglion cells do not extend axons by default: promotion by neurotrophic signaling and electrical activity', Neuron, 33: 689-702.

Guescini, M., Genedani, S., Stocchi, V., and Agnati, L. F. 2010. 'Astrocytes and Glioblastoma cells release exosomes carrying mtDNA', J Neural Transm (Vienna), 117: 1-4.

Guo, W., Nagappan, G., and Lu, B. 2018. 'Differential effects of transient and

sustained activation of BDNF-TrkB signaling', Dev Neurobiol, 78: 647-59.

Gupta, N., Brown, K. E., and Milam, A. H. 2003. 'Activated microglia in human retinitis pigmentosa, late-onset retinal degeneration, and age-related macular degeneration', Exp Eye Res, 76: 463-71.

Gupta, N., Shyamasundar, S., Patnala, R., Karthikeyan, A., Arumugam, T. V., Ling, E. A., and Dheen, S. T. 2018. 'Recent progress in therapeutic strategies for microglia-mediated neuroinflammation in neuropathologies', Expert Opin Ther Targets, 22: 765-81.

Harada, C., Guo, X., Namekata, K., Kimura, A., Nakamura, K., Tanaka, K., Parada, L. F., and Harada, T. 2011. 'Glia- and neuron-specific functions of TrkB signalling during retinal degeneration and regeneration', Nat Commun, 2: 189.

Harada, T., Harada, C., Kohsaka, S., Wada, E., Yoshida, K., Ohno, S., Mamada, H., Tanaka, K., Parada, L. F., and Wada, K. 2002. 'Microglia-Müller glia cell interactions control neurotrophic factor production during light-induced retinal degeneration', J Neurosci, 22: 9228-36.

Harada, T., Harada, C., Nakayama, N., Okuyama, S., Yoshida, K., Kohsaka, S., Matsuda, H., and Wada, K. 2000. 'Modification of glial-neuronal cell interactions prevents photoreceptor apoptosis during light-induced retinal degeneration', Neuron, 26: 533-41.

Haraszti, R. A., Didiot, M. C., Sapp, E., Leszyk, J., Shaffer, S. A., Rockwell, H. E., Gao, F., Narain, N. R., DiFiglia, M., Kiebish, M. A., Aronin, N., and Khvorova, A. 2016. 'High-resolution proteomic and lipidomic analysis of exosomes and microvesicles from different cell sources', J Extracell Vesicles, 5: 32570.

Hernandez, M., Pearce-Kelling, S. E., Rodriguez, F. D., Aguirre, G. D., and Vecino, E. 2010. 'Altered expression of retinal molecular markers in the canine RPE65 model of Leber congenital amaurosis', Invest Ophthalmol Vis Sci, 51: 6793-802.

Hirrlinger, P. G., Ulbricht, E., Iandiev, I., Reichenbach, A., and Pannicke, T. 2010. 'Alterations in protein expression and membrane properties during Müller cell gliosis in a murine model of transient retinal ischemia', Neurosci Lett, 472: 73-8.

Hollborn, M., Ulbricht, E., Rillich, K., Dukic-Stefanovic, S., Wurm, A., Wagner, L., Reichenbach, A., Wiedemann, P., Limb, G. A., Bringmann, A., and Kohen, L. 2011. 'The human Müller cell line MIO-M1 expresses opsins', Mol Vis, 17: 2738-50.

Hombrebueno, J. R., Luo, C., Guo, L., Chen, M., and Xu, H. 2014. 'Intravitreal Injection of Normal Saline Induces Retinal Degeneration in the C57BL/6J Mouse', Transl Vis Sci Technol, 3: 3.

Ihara, T., Yamamoto, T., Sugamata, M., Okumura, H., and Ueno, Y. 1998. 'The process of ultrastructural changes from nuclei to apoptotic body', Virchows Arch, 433:

443-7.

Ito, D., Imai, Y., Ohsawa, K., Nakajima, K., Fukuuchi, Y., and Kohsaka, S. 1998. 'Microglia-specific localisation of a novel calcium binding protein, Iba1', Brain Res Mol Brain Res, 57: 1-9.

J.M. Gudbergsson, M. Duroux. 2017. Mesenchymal Stromal Cells as Tumor Stromal Modulators (Elsevier).

Ji, H., Chen, M., Greening, D. W., He, W., Rai, A., Zhang, W., and Simpson, R. J. 2014. 'Deep sequencing of RNA from three different extracellular vesicle (EV) subtypes released from the human LIM1863 colon cancer cell line uncovers distinct miRNA-enrichment signatures', PLoS One, 9: e110314.

Johnson, T. V., and Tomarev, S. I. 2010. 'Rodent models of glaucoma', Brain Res Bull, 81: 349-58.

Johnstone, R. M., Adam, M., Hammond, J. R., Orr, L., and Turbide, C. 1987. 'Vesicle formation during reticulocyte maturation. Association of plasma membrane activities with released vesicles (exosomes)', J Biol Chem, 262: 9412-20.

Ju, W. K., Lee, M. Y., Hofmann, H. D., Kirsch, M., and Chun, M. H. 1999. 'Expression of CNTF in Müller cells of the rat retina after pressure-induced ischemia', Neuroreport, 10: 419-22.

Jurga, A. M., Paleczna, M., and Kuter, K. Z. 2020. 'Overview of General and Discriminating Markers of Differential Microglia Phenotypes', Front Cell Neurosci, 14: 198.

Kaneko, A., and Tachibana, M. 1987. 'GABA mediates the negative feedback from amacrine to bipolar cells', Neurosci Res Suppl, 6: S239-51.

Katsman, D., Stackpole, E. J., Domin, D. R., and Farber, D. B. 2012. 'Embryonic stem cell-derived microvesicles induce gene expression changes in Müller cells of the retina', PLoS One, 7: e50417.

Kaur, G., and Dufour, J. M. 2012. 'Cell lines: Valuable tools or useless artifacts', Spermatogenesis, 2: 1-5.

Kettenmann, H., Hanisch, U. K., Noda, M., and Verkhratsky, A. 2011. 'Physiology of microglia', Physiol Rev, 91: 461-553.

Kim, B. J., Braun, T. A., Wordinger, R. J., and Clark, A. F. 2013. 'Progressive morphological changes and impaired retinal function associated with temporal regulation of gene expression after retinal ischemia/reperfusion injury in mice', Mol Neurodegener, 8: 21.

Kimura, A., Noro, T., and Harada, T. 2020. 'Role of animal models in glaucoma

research', Neural Regen Res, 15: 1257-58.

Kinkl, N., Ruiz, J., Vecino, E., Frasson, M., Sahel, J., and Hicks, D. 2003. 'Possible involvement of a fibroblast growth factor 9 (FGF9)-FGF receptor-3-mediated pathway in adult pig retinal ganglion cell survival *in vitro*', Mol Cell Neurosci, 23: 39-53.

Kofuji, P., Biedermann, B., Siddharthan, V., Raap, M., Iandiev, I., Milenkovic, I., Thomzig, A., Veh, R. W., Bringmann, A., and Reichenbach, A. 2002. 'Kir potassium channel subunit expression in retinal glial cells: implications for spatial potassium buffering', Glia, 39: 292-303.

Kolb, H. 2003. 'How the retina works', American Scientist, 91: 28-35.

Konoshenko, M. Y., Lekchnov, E. A., Vlassov, A. V., and Laktionov, P. P. 2018. 'Isolation of Extracellular Vesicles: General Methodologies and Latest Trends', Biomed Res Int, 2018: 8545347.

Kowal, J., Arras, G., Colombo, M., Jouve, M., Morath, J. P., Primdal-Bengtson, B., Dingli, F., Loew, D., Tkach, M., and Thery, C. 2016. 'Proteomic comparison defines novel markers to characterize heterogeneous populations of extracellular vesicle subtypes', Proc Natl Acad Sci U S A, 113: E968-77.

Krawczenko, A., Bielawska-Pohl, A., Paprocka, M., Kraskiewicz, H., Szyposzynska, A., Wojdat, E., and Klimczak, A. 2020. 'Microvesicles from Human Immortalized Cell Lines of Endothelial Progenitor Cells and Mesenchymal Stem/Stromal Cells of Adipose Tissue Origin as Carriers of Bioactive Factors Facilitating Angiogenesis', Stem Cells Int, 2020: 1289380.

Kumar, A., Pandey, R. K., Miller, L. J., Singh, P. K., and Kanwar, M. 2013. 'Müller glia in retinal innate immunity: a perspective on their roles in endophthalmitis', Crit Rev Immunol, 33: 119-35.

Kupfer, C., Chumbley, L., and Downer, J. C. 1967. 'Quantitative histology of optic nerve, optic tract and lateral geniculate nucleus of man', J Anat, 101: 393-401.

Lagnado, L. 1998. 'Retinal processing: Amacrine cells keep it short and sweet', Current Biology, 8: 598-600.

Lammert, E., Zeeb M. 2014. Metabolism of Human Diseases, Organ Physiology and Pathophysioogy.

Lane, R. E., Korbie, D., Hill, M. M., and Trau, M. 2018. 'Extracellular vesicles as circulating cancer biomarkers: opportunities and challenges', Clin Transl Med, 7: 14.

Larson, E. R., Van Zelm, E., Roux, C., Marion-Poll, A., and Blatt, M. R. 2017. 'Clathrin Heavy Chain Subunits Coordinate Endo- and Exocytic Traffic and Affect Stomatal Movement', Plant Physiol, 175: 708-20.

Lee, J. E., Liang, K. J., Fariss, R. N., and Wong, W. T. 2008. 'Ex vivo dynamic imaging

of retinal microglia using time-lapse confocal microscopy', Invest Ophthalmol Vis Sci, 49: 4169-76.

Lee, S. J., Duncan, D. S., Echevarria, F. D., McLaughlin, W. M., Hatcher, J. B., and Sappington, R. M. 2015. 'Pressure-Induced Alterations in PEDF and PEDF-R Expression: Implications for Neuroprotective Signaling in Glaucoma', J Clin Exp Ophthalmol, 6.

Lee, Y., El Andaloussi, S., and Wood, M. J. 2012. 'Exosomes and microvesicles: extracellular vesicles for genetic information transfer and gene therapy', Hum Mol Genet, 21: R125-34.

Libby, R. T., Anderson, M. G., Pang, I. H., Robinson, Z. H., Savinova, O. V., Cosma, I. M., Snow, A., Wilson, L. A., Smith, R. S., Clark, A. F., and John, S. W. 2005. 'Inherited glaucoma in DBA/2J mice: pertinent disease features for studying the neurodegeneration', Vis Neurosci, 22: 637-48.

Limb, G. A., Salt, T. E., Munro, P. M., Moss, S. E., and Khaw, P. T. 2002. '*In vitro* characterization of a spontaneously immortalized human Müller cell line (MIO-M1)', Invest Ophthalmol Vis Sci, 43: 864-9.

London, A., Benhar, I., and Schwartz, M. 2013. 'The retina as a window to the brain-from eye research to CNS disorders', Nat Rev Neurol, 9: 44-53.

Lorenz, L., Hirmer, S., Schmalen, A., Hauck, S. M., and Deeg, C. A. 2021. 'Cell Surface Profiling of Retinal Müller Glial Cells Reveals Association to Immune Pathways after LPS Stimulation', Cells, 10.

Madeira, M. H., Boia, R., Elvas, F., Martins, T., Cunha, R. A., Ambrosio, A. F., and Santiago, A. R. 2016. 'Selective A2A receptor antagonist prevents microglia-mediated neuroinflammation and protects retinal ganglion cells from high intraocular pressure-induced transient ischemic injury', Transl Res, 169: 112-28.

Madeira, M. H., Boia, R., Santos, P. F., Ambrosio, A. F., and Santiago, A. R. 2015a. 'Contribution of microglia-mediated neuroinflammation to retinal degenerative diseases', Mediators Inflamm, 2015: 673090.

Madeira, M. H., Elvas, F., Boia, R., Goncalves, F. Q., Cunha, R. A., Ambrosio, A. F., and Santiago, A. R. 2015b. 'Adenosine A2AR blockade prevents neuroinflammation-induced death of retinal ganglion cells caused by elevated pressure', J Neuroinflammation, 12: 115.

Martins, J., Castelo-Branco, M., Batista, A., Oliveiros, B., Santiago, A. R., Galvao, J., Fernandes, E., Carvalho, F., Cavadas, C., and Ambrosio, A. F. 2011. 'Effects of 3,4-methylenedioxymethamphetamine administration on retinal physiology in the rat', PLoS One, 6: e29583.

Mead, B., and Tomarev, S. 2017. 'Bone Marrow-Derived Mesenchymal Stem Cells-

Derived Exosomes Promote Survival of Retinal Ganglion Cells Through miRNA-Dependent Mechanisms', Stem Cells Transl Med, 6: 1273-85.

———. 2020. 'Extracellular vesicle therapy for retinal diseases', Prog Retin Eye Res, 79: 100849.

Moisseiev, E., Anderson, J. D., Oltjen, S., Goswami, M., Zawadzki, R. J., Nolta, J. A., and Park, S. S. 2017. 'Protective Effect of Intravitreal Administration of Exosomes Derived from Mesenchymal Stem Cells on Retinal Ischemia', Curr Eye Res, 42: 1358-67.

Mondal, A., Ashiq, K. A., Phulpagar, P., Singh, D. K., and Shiras, A. 2019. 'Effective Visualization and Easy Tracking of Extracellular Vesicles in Glioma Cells', Biol Proced Online, 21: 4.

Morrison, J. C., Cepurna, W. O., and Johnson, E. C. 2015. 'Modeling glaucoma in rats by sclerosing aqueous outflow pathways to elevate intraocular pressure', Exp Eye Res, 141: 23-32.

Muralidharan-Chari, V., Clancy, J., Plou, C., Romao, M., Chavrier, P., Raposo, G., and D'Souza-Schorey, C. 2009. 'ARF6-regulated shedding of tumor cell-derived plasma membrane microvesicles', Curr Biol, 19: 1875-85.

Nabhan, J. F., Hu, R., Oh, R. S., Cohen, S. N., and Lu, Q. 2012. 'Formation and release of arrestin domain-containing protein 1-mediated microvesicles (ARMMs) at plasma membrane by recruitment of TSG101 protein', Proc Natl Acad Sci U S A, 109: 4146-51.

Nadal-Nicolas, F. M., Jimenez-Lopez, M., Sobrado-Calvo, P., Nieto-Lopez, L., Canovas-Martinez, I., Salinas-Navarro, M., Vidal-Sanz, M., and Agudo, M. 2009. 'Brn3a as a marker of retinal ganglion cells: qualitative and quantitative time course studies in naive and optic nerve-injured retinas', Invest Ophthalmol Vis Sci, 50: 3860-8.

NationalCancerInstituteUS. 2021. Retinoblastoma Treatment (PDQ®): Patient Version.

Neal, M. L., Boyle, A. M., Budge, K. M., Safadi, F. F., and Richardson, J. R. 2018. 'The glycoprotein GPNMB attenuates astrocyte inflammatory responses through the CD44 receptor', J Neuroinflammation, 15: 73.

Newman, E., and Reichenbach, A. 1996. 'The Müller cell: a functional element of the retina', Trends Neurosci, 19: 307-12.

Okunuki, Y., Mukai, R., Nakao, T., Tabor, S. J., Butovsky, O., Dana, R., Ksander, B. R., and Connor, K. M. 2019. 'Retinal microglia initiate neuroinflammation in ocular autoimmunity', Proc Natl Acad Sci U S A, 116: 9989-98.

Palmhof, M., Frank, V., Rappard, P., Kortenhorn, E., Demuth, J., Biert, N., Stute, G., Dick, H. B., and Joachim, S. C. 2019. 'From Ganglion Cell to Photoreceptor Layer:

Timeline of Deterioration in a Rat Ischemia/Reperfusion Model', Front Cell Neurosci, 13: 174.

Pan, B. T., Teng, K., Wu, C., Adam, M., and Johnstone, R. M. 1985. 'Electron microscopic evidence for externalization of the transferrin receptor in vesicular form in sheep reticulocytes', J Cell Biol, 101: 942-8.

Pan, D., Chang, X., Xu, M., Zhang, M., Zhang, S., Wang, Y., Luo, X., Xu, J., Yang, X., and Sun, X. 2019. 'UMSC-derived exosomes promote retinal ganglion cells survival in a rat model of optic nerve crush', J Chem Neuroanat, 96: 134-39.

Pardue, M. T., and Allen, R. S. 2018. 'Neuroprotective strategies for retinal disease', Prog Retin Eye Res, 65: 50-76.

Peichl, L. 2005. 'Diversity of mammalian photoreceptor properties: adaptations to habitat and lifestyle?', Anat Rec A Discov Mol Cell Evol Biol, 287: 1001-12.

Peng, Y., Baulier, E., Ke, Y., Young, A., Ahmedli, N. B., Schwartz, S. D., and Farber, D. B. 2018. 'Human embryonic stem cells extracellular vesicles and their effects on immortalized human retinal Müller cells', PLoS One, 13: e0194004.

Pereiro, X., Miltner, A. M., La Torre, A., and Vecino, E. 2020a. 'Effects of Adult Müller Cells and Their Conditioned Media on the Survival of Stem Cell-Derived Retinal Ganglion Cells', Cells, 9.

Pereiro, X., Ruzafa, N., Acera, A., Fonollosa, A., Rodriguez, F. D., and Vecino, E. 2018. 'Dexamethasone protects retinal ganglion cells but not Müller glia against hyperglycemia *in vitro*', PLoS One, 13: e0207913.

Pereiro, X., Ruzafa, N., Acera, A., Urcola, A., and Vecino, E. 2020b. 'Optimization of a Method to Isolate and Culture Adult Porcine, Rats and Mice Müller Glia in Order to Study Retinal Diseases', Front Cell Neurosci, 14: 7.

Phuyal, S., Hessvik, N. P., Skotland, T., Sandvig, K., and Llorente, A. 2014. 'Regulation of exosome release by glycosphingolipids and flotillins', FEBS J, 281: 2214-27.

Pietrucha-Dutczak, M., Amadio, M., Govoni, S., Lewin-Kowalik, J., and Smedowski, A. 2018. 'The Role of Endogenous Neuroprotective Mechanisms in the Prevention of Retinal Ganglion Cells Degeneration', Front Neurosci, 12: 834.

Pitt, J. M., Kroemer, G., and Zitvogel, L. 2016. 'Extracellular vesicles: masters of intercellular communication and potential clinical interventions', J Clin Invest, 126: 1139-43.

Poon, I. K., Lucas, C. D., Rossi, A. G., and Ravichandran, K. S. 2014. 'Apoptotic cell clearance: basic biology and therapeutic potential', Nat Rev Immunol, 14: 166-80.

Prasad, S., and Galetta, S. L. 2011. 'Anatomy and physiology of the afferent visual system', Handb Clin Neurol, 102: 3-19.

Purves D, Augustine GJ, Fitzpatrick D, et al. 2001. Neuroscience (Sinauer Associates).

Quigley, H. A., Guy, J., and Anderson, D. R. 1979. 'Blockade of rapid axonal transport. Effect of intraocular pressure elevation in primate optic nerve', Arch Ophthalmol, 97: 525-31.

Quigley, H. A., McKinnon, S. J., Zack, D. J., Pease, M. E., Kerrigan-Baumrind, L. A., Kerrigan, D. F., and Mitchell, R. S. 2000. 'Retrograde axonal transport of BDNF in retinal ganglion cells is blocked by acute IOP elevation in rats', Invest Ophthalmol Vis Sci, 41: 3460-6.

Ramirez, M. I., Amorim, M. G., Gadelha, C., Milic, I., Welsh, J. A., Freitas, V. M., Nawaz, M., et al. 2018. 'Technical challenges of working with extracellular vesicles', Nanoscale, 10: 881-906.

Rashid, K., Akhtar-Schaefer, I., and Langmann, T. 2019. 'Microglia in Retinal Degeneration', Front Immunol, 10: 1975.

Ratajczak, J., Miekus, K., Kucia, M., Zhang, J., Reca, R., Dvorak, P., and Ratajczak, M. Z. 2006. 'Embryonic stem cell-derived microvesicles reprogram hematopoietic progenitors: evidence for horizontal transfer of mRNA and protein delivery', Leukemia, 20: 847-56.

Ratajczak, M. Z., and Ratajczak, J. 2020. 'Extracellular microvesicles/exosomes: discovery, disbelief, acceptance, and the future?', Leukemia, 34: 3126-35.

Ravichandran, K. S. 2010. 'Find-me and eat-me signals in apoptotic cell clearance: progress and conundrums', J Exp Med, 207: 1807-17.

Roberti, G., Mantelli, F., Macchi, I., Massaro-Giordano, M., and Centofanti, M. 2014. 'Nerve growth factor modulation of retinal ganglion cell physiology', J Cell Physiol, 229: 1130-3.

Rodrigues-Neves, A. C., Aires, I. D., Vindeirinho, J., Boia, R., Madeira, M. H., Goncalves, F. Q., Cunha, R. A., Santos, P. F., Ambrosio, A. F., and Santiago, A. R. 2018. 'Elevated Pressure Changes the Purinergic System of Microglial Cells', Front Pharmacol, 9: 16.

Rodrigues, Magda. 2021. 'Influence of elevated hydrostatic pressure on Müller cells phenotype. Do microglia-derived microvesicles play a role?', University of Coimbra.

Roesch, K., Stadler, M. B., and Cepko, C. L. 2012. 'Gene expression changes within Müller glial cells in retinitis pigmentosa', Mol Vis, 18: 1197-214.

Rostami, J., Fotaki, G., Sirois, J., Mzezewa, R., Bergstrom, J., Essand, M., Healy, L., and Erlandsson, A. 2020. 'Astrocytes have the capacity to act as antigen-presenting cells in the Parkinson's disease brain', J Neuroinflammation, 17: 119.

Ruzafa, N., Pereiro, X., Aspichueta, P., Araiz, J., and Vecino, E. 2018a. 'The Retina of

Osteopontin deficient Mice in Aging', Mol Neurobiol, 55: 213-21.

Ruzafa, N., Pereiro, X., Lepper, M. F., Hauck, S. M., and Vecino, E. 2018b. 'A Proteomics Approach to Identify Candidate Proteins Secreted by Müller Glia that Protect Ganglion Cells in the Retina', Proteomics, 18: e1700321.

Ruzafa, N., and Vecino, E. 2015. 'Effect of Müller cells on the survival and neuritogenesis in retinal ganglion cells', Arch Soc Esp Oftalmol, 90: 522-6.

Ryskamp, D. A., Redmon, S., Jo, A. O., and Krizaj, D. 2014. 'TRPV1 and Endocannabinoids: Emerging Molecular Signals that Modulate Mammalian Vision', Cells, 3: 914-38.

Salinas-Navarro, M., Alarcon-Martinez, L., Valiente-Soriano, F. J., Jimenez-Lopez, M., Mayor-Torroglosa, S., Aviles-Trigueros, M., Villegas-Perez, M. P., and Vidal-Sanz, M. 2010. 'Ocular hypertension impairs optic nerve axonal transport leading to progressive retinal ganglion cell degeneration', Exp Eye Res, 90: 168-83.

Salinas-Navarro, M., Mayor-Torroglosa, S., Jimenez-Lopez, M., Aviles-Trigueros, M., Holmes, T. M., Lund, R. D., Villegas-Perez, M. P., and Vidal-Sanz, M. 2009. 'A computerized analysis of the entire retinal ganglion cell population and its spatial distribution in adult rats', Vision Res, 49: 115-26.

Sanchez-Migallon, M. C., Valiente-Soriano, F. J., Nadal-Nicolas, F. M., Vidal-Sanz, M., and Agudo-Barriuso, M. 2016. 'Apoptotic Retinal Ganglion Cell Death After Optic Nerve Transection or Crush in Mice: Delayed RGC Loss With BDNF or a Caspase 3 Inhibitor', Invest Ophthalmol Vis Sci, 57: 81-93.

Santiago, A. R., Baptista, F. I., Santos, P. F., Cristovao, G., Ambrosio, A. F., Cunha, R. A., and Gomes, C. A. 2014. 'Role of microglia adenosine A(2A) receptors in retinal and brain neurodegenerative diseases', Mediators Inflamm, 2014: 465694.

Sappington, R. M., Carlson, B. J., Crish, S. D., and Calkins, D. J. 2010. 'The microbead occlusion model: a paradigm for induced ocular hypertension in rats and mice', Invest Ophthalmol Vis Sci, 51: 207-16.

Sappington, R. M., Chan, M., and Calkins, D. J. 2006. 'Interleukin-6 protects retinal ganglion cells from pressure-induced death', Invest Ophthalmol Vis Sci, 47: 2932-42.

Sappington, R. M., Sidorova, T., Long, D. J., and Calkins, D. J. 2009. 'TRPV1: contribution to retinal ganglion cell apoptosis and increased intracellular Ca2+ with exposure to hydrostatic pressure', Invest Ophthalmol Vis Sci, 50: 717-28.

Sappington, R. M., Sidorova, T., Ward, N. J., Chakravarthy, R., Ho, K. W., and Calkins, D. J. 2015. 'Activation of transient receptor potential vanilloid-1 (TRPV1) influences how retinal ganglion cell neurons respond to pressure-related stress', Channels (Austin), 9: 102-13.

Schmidt, T. M., Chen, S. K., and Hattar, S. 2011. 'Intrinsically photosensitive retinal

ganglion cells: many subtypes, diverse functions', Trends Neurosci, 34: 572-80.

Schwartz, M. 2005. 'Lessons for glaucoma from other neurodegenerative diseases: can one treatment suit them all?', J Glaucoma, 14: 321-3.

Seki, M., Tanaka, T., Sakai, Y., Fukuchi, T., Abe, H., Nawa, H., and Takei, N. 2005. 'Müller Cells as a source of brain-derived neurotrophic factor in the retina: noradrenaline upregulates brain-derived neurotrophic factor levels in cultured rat Müller cells', Neurochem Res, 30: 1163-70.

Seyedrazizadeh, S. Z., Poosti, S., Nazari, A., Alikhani, M., Shekari, F., Pakdel, F., Shahpasand, K., Satarian, L., and Baharvand, H. 2020. 'Extracellular vesicles derived from human ES-MSCs protect retinal ganglion cells and preserve retinal function in a rodent model of optic nerve injury', Stem Cell Res Ther, 11: 203.

Shimomura, T., Seino, R., Umezaki, K., Shimoda, A., Ezoe, T., Ishiyama, M., and Akiyoshi, K. 2021. 'New Lipophilic Fluorescent Dyes for Labeling Extracellular Vesicles: Characterization and Monitoring of Cellular Uptake', Bioconjug Chem, 32: 680-84.

Sho, K., Takahashi, K., Fukuchi, T., and Matsumura, M. 2005. 'Quantitative evaluation of ischemia-reperfusion injury by optical coherence tomography in the rat retina', Jpn J Ophthalmol, 49: 109-13.

Shruthi, S., Sumitha, R., Varghese, A. M., Ashok, S., Chandrasekhar Sagar, B. K., Sathyaprabha, T. N., Nalini, A., Kramer, B. W., Raju, T. R., Vijayalakshmi, K., and Alladi, P. A. 2017. 'Brain-Derived Neurotrophic Factor Facilitates Functional Recovery from ALS-Cerebral Spinal Fluid-Induced Neurodegenerative Changes in the NSC-34 Motor Neuron Cell Line', Neurodegener Dis, 17: 44-58.

Silverman, J. M., Fernando, S. M., Grad, L. I., Hill, A. F., Turner, B. J., Yerbury, J. J., and Cashman, N. R. 2016. 'Disease Mechanisms in ALS: Misfolded SOD1 Transferred Through Exosome-Dependent and Exosome-Independent Pathways', Cell Mol Neurobiol, 36: 377-81.

Skog, J., Wurdinger, T., van Rijn, S., Meijer, D. H., Gainche, L., Sena-Esteves, M., Curry, W. T., Jr., Carter, B. S., Krichevsky, A. M., and Breakefield, X. O. 2008. 'Glioblastoma microvesicles transport RNA and proteins that promote tumour growth and provide diagnostic biomarkers', Nat Cell Biol, 10: 1470-6.

Stifter, J., Ulbrich, F., Goebel, U., Bohringer, D., Lagreze, W. A., and Biermann, J. 2017. 'Neuroprotection and neuroregeneration of retinal ganglion cells after intravitreal carbon monoxide release', PLoS One, 12: e0188444.

Stuffers, S., Sem Wegner, C., Stenmark, H., and Brech, A. 2009. 'Multivesicular endosome biogenesis in the absence of ESCRTs', Traffic, 10: 925-37.

Su, Y., Wang, F., Teng, Y., Zhao, S. G., Cui, H., and Pan, S. H. 2009. 'Axonal regeneration of optic nerve after crush in Nogo66 receptor knockout mice', Neurosci

Lett, 460: 223-6.

Sun, X., and Kaufman, P. D. 2018. 'Ki-67: more than a proliferation marker', Chromosoma, 127: 175-86.

Szabo, M. E., Droy-Lefaix, M. T., Doly, M., Carre, C., and Braquet, P. 1991. 'Ischemia and reperfusion-induced histologic changes in the rat retina. Demonstration of a free radical-mediated mechanism', Invest Ophthalmol Vis Sci, 32: 1471-8.

Tachibana, M., and Kaneko, A. 1987. 'gamma-Aminobutyric acid exerts a local inhibitory action on the axon terminal of bipolar cells: evidence for negative feedback from amacrine cells', Proc Natl Acad Sci U S A, 84: 3501-5.

Thery, C., Witwer, K. W., Aikawa, E., Alcaraz, M. J., Anderson, J. D., Andriantsitohaina, R., Antoniou, A., et al. 2018. 'Minimal information for studies of extracellular vesicles 2018 (MISEV2018): a position statement of the International Society for Extracellular Vesicles and update of the MISEV2014 guidelines', J Extracell Vesicles, 7: 1535750.

Tribble, J. R., Kokkali, E., Otmani, A., Plastino, F., Lardner, E., Vohra, R., Kolko, M., Andre, H., Morgan, J. E., and Williams, P. A. 2021. 'When Is a Control Not a Control? Reactive Microglia Occur Throughout the Control Contralateral Pathway of Retinal Ganglion Cell Projections in Experimental Glaucoma', Transl Vis Sci Technol, 10: 22.

Tricarico, C., Clancy, J., and D'Souza-Schorey, C. 2017. 'Biology and biogenesis of shed microvesicles', Small GTPases, 8: 220-32.

Tucher, C., Bode, K., Schiller, P., Classen, L., Birr, C., Souto-Carneiro, M. M., Blank, N., Lorenz, H. M., and Schiller, M. 2018. 'Extracellular Vesicle Subtypes Released From Activated or Apoptotic T-Lymphocytes Carry a Specific and Stimulus-Dependent Protein Cargo', Front Immunol, 9: 534.

Unterlauft, J. D., Claudepierre, T., Schmidt, M., Müller, K., Yafai, Y., Wiedemann, P., Reichenbach, A., and Eichler, W. 2014. 'Enhanced survival of retinal ganglion cells is mediated by Müller glial cell-derived PEDF', Exp Eye Res, 127: 206-14.

Unterlauft, J. D., Eichler, W., Kuhne, K., Yang, X. M., Yafai, Y., Wiedemann, P., Reichenbach, A., and Claudepierre, T. 2012. 'Pigment epithelium-derived factor released by Müller glial cells exerts neuroprotective effects on retinal ganglion cells', Neurochem Res, 37: 1524-33.

van Niel, G., D'Angelo, G., and Raposo, G. 2018. 'Shedding light on the cell biology of extracellular vesicles', Nat Rev Mol Cell Biol, 19: 213-28.

Vecino, E., Rodriguez, F. D., Ruzafa, N., Pereiro, X., and Sharma, S. C. 2016. 'Glia-neuron interactions in the mammalian retina', Prog Retin Eye Res, 51: 1-40.

Vecino, E., Ugarte, M., Nash, M. S., and Osborne, N. N. 1999. 'NMDA induces BDNF expression in the albino rat retina in vivo', Neuroreport, 10: 1103-6.

Vestad, B., Llorente, A., Neurauter, A., Phuyal, S., Kierulf, B., Kierulf, P., Skotland, T., Sandvig, K., Haug, K. B. F., and Ovstebo, R. 2017. 'Size and concentration analyses of extracellular vesicles by nanoparticle tracking analysis: a variation study', J Extracell Vesicles, 6: 1344087.

Vidal-Sanz, M., Valiente-Soriano, F. J., Ortin-Martinez, A., Nadal-Nicolas, F. M., Jimenez-Lopez, M., Salinas-Navarro, M., Alarcon-Martinez, L., Garcia-Ayuso, D., Aviles-Trigueros, M., Agudo-Barriuso, M., and Villegas-Perez, M. P. 2015. 'Retinal neurodegeneration in experimental glaucoma', Prog Brain Res, 220: 1-35.

Walland, M. J., Carassa, R. G., Goldberg, I., Grehn, F., Heuer, D. K., Khaw, P. T., Thomas, R., and Parikh, R. 2006. 'Failure of medical therapy despite normal intraocular pressure', Clin Exp Ophthalmol, 34: 827-36.

Wang, L., Cioffi, G. A., Cull, G., Dong, J., and Fortune, B. 2002. 'Immunohistologic evidence for retinal glial cell changes in human glaucoma', Invest Ophthalmol Vis Sci, 43: 1088-94.

Wassle, H. 2004. 'Parallel processing in the mammalian retina', Nat Rev Neurosci, 5: 747-57.

Wassle, H., and Boycott, B. B. 1991. 'Functional architecture of the mammalian retina', Physiol Rev, 71: 447-80.

Willms, E., Johansson, H. J., Mager, I., Lee, Y., Blomberg, K. E., Sadik, M., Alaarg, A., Smith, C. I., Lehtio, J., El Andaloussi, S., Wood, M. J., and Vader, P. 2016. 'Cells release subpopulations of exosomes with distinct molecular and biological properties', Sci Rep, 6: 22519.

Wolf, P. 1967. 'The nature and significance of platelet products in human plasma', Br J Haematol, 13: 269-88.

Wu, J., Mak, H. K., Chan, Y. K., Lin, C., Kong, C., Leung, C. K. S., and Shum, H. C. 2019. 'An *in vitro* pressure model towards studying the response of primary retinal ganglion cells to elevated hydrostatic pressures', Sci Rep, 9: 9057.

Xue, W., Du, P., Lin, S., Dudley, V. J., Hernandez, M. R., and Sarthy, V. P. 2011. 'Gene expression changes in retinal Müller (glial) cells exposed to elevated pressure', Curr Eye Res, 36: 754-67.

Yamamoto, T., and Kitazawa, Y. 1998. 'Vascular pathogenesis of normal-tension glaucoma: a possible pathogenetic factor, other than intraocular pressure, of glaucomatous optic neuropathy', Prog Retin Eye Res, 17: 127-43.

Yu, J., Chen, C., Wang, J., Cheng, Y., Wu, Q., Zhong, Y., and Shen, X. 2012. '*In vitro* effect of adenosine on the mRNA expression of Kir 2.1 and Kir 4.1 channels in rat retinal Müller cells at elevated hydrostatic pressure', Exp Ther Med, 3: 617-20.

Yu, J., Zhong, Y., Cheng, Y., Shen, X., Wang, J., and Wei, Y. 2011. 'Effect of high hydrostatic pressure on the expression of glutamine synthetase in rat retinal Müller cells cultured *in vitro*', Exp Ther Med, 2: 513-16.

Zack, D. J. 2000. 'Neurotrophic rescue of photoreceptors: are Müller cells the mediators of survival?', Neuron, 26: 285-6.

Zeiss, C. J., Allore, H. G., Towle, V., and Tao, W. 2006. 'CNTF induces dose-dependent alterations in retinal morphology in normal and rcd-1 canine retina', Exp Eye Res, 82: 395-404.

Zhao, L., Zabel, M. K., Wang, X., Ma, W., Shah, P., Fariss, R. N., Qian, H., Parkhurst, C. N., Gan, W. B., and Wong, W. T. 2015. 'Microglial phagocytosis of living photoreceptors contributes to inherited retinal degeneration', EMBO Mol Med, 7: 1179-97.